



University of
Nottingham
UK | CHINA | MALAYSIA

DESIGN AND DEVELOPMENT OF DIALYSATE TEMPERATURE CONTROL MODULE PROTOTYPE FOR HEMODIALYSIS

MOHAMED HAROON ABDUL JABBAR, BEng (Hons)

Thesis submitted to the University of Nottingham
for the Degree of Doctor of Philosophy

July 2019

“To my beloved family”

ABSTRACT

In the last few decades, complications caused during hemodialysis (HD) treatment remain a significant cause of morbidity and mortality in patients. During standard HD, there is a significant tendency for the body temperature to rise slightly, which is sufficient to cause complications. Recent studies show that the controlling of body temperature by altering the dialysate temperature, can reduce the complication episodes. Although the importance of active regulation of dialysate temperature control and its benefits have mentioned in literature, an enhanced design of controller and its comparison with dated commercial controller - Blood Temperature Monitor (BTM) have not been reported yet.

Hence, it is the intention of this work to introduce the development of an effective dialysate temperature control module (DTCM) prototype and its comprehensive analysis in providing stable body temperature during the HD treatment. This study is incorporated with various prototype development stages such as prototype design, implementation, controller optimization, parameter estimation through simulation and in-vitro evaluation. Primarily, an innovative dialysate proportioning method is proposed for the development of the DTCM prototype. The study also involves a simulation of the heat transfer in a dialyzer and optimization of fuzzy logic controller design in real environment for the benefit of the DTCM evaluation. Finally, the DTCM prototype was evaluated and validated through in-vitro experiments.

For the simulation study, a Polyflux 210H dialyzer model was developed using COMSOL Multiphysics software. Results showed the decrease in blood temperature

along the membrane could be one of the consequences of venous line cooling as reported in literature and thus necessitates an effective system to control the dialysate temperature.

Prior to the DTCM controller implementation, the performance of fuzzy logic-based temperature control was optimized from numerous designs. Optimum performance was found in the fuzzy logic design with a symmetrical rule base and the highest number of overlapping triangular membership functions. However, the optimized design shows a significant improvement in accuracy ($\pm 0.125^{\circ}\text{C}$) compared to the accuracy ($\pm 0.5^{\circ}\text{C}$) of published experimental study.

For the in-vitro evaluation of DTCM prototype, an extracorporeal thermal energy model incorporating the heat transfer in dialyzer was proposed to estimate the arterial and venous temperatures. The results showed that the estimated arterial and venous temperature under standard dialysate are in accordance to that of published literature. Then, the working of DTCM prototype was evaluated under real-time environment for pre-defined trend of body temperatures and other various parameters. The results showed a remarkable response in maintaining body temperature with a tolerance of $\pm 0.09^{\circ}\text{C}$ under shorter duration. In fact, the DTCM prototype was then validated and noted to have a slightly better error tolerance in comparison with BTM experimental data ($\pm 0.16^{\circ}\text{C}$).

The results obtained provides a gateway towards the development of dialysate temperature control system for HD machines. The potential of DTCM prototype to control the body temperature during the treatment has been proven through this work.

The prototype design used in the current study can be implemented in HD machines, making it more affordable and accessible, paving the way to reduce HD related mortality.

LIST OF PUBLICATIONS

- **Jabbar M.H.A.**, Anandan Shanmugam S., Khiew P.S., (2018) Design and Implementation of Dialysate Temperature Control System for Hemodialysis: A Pilot Study. In: Thalmann D., Subhashini N., Mohanaprasad K., Murugan M. (eds) Intelligent Embedded Systems. Lecture Notes in Electrical Engineering, vol 492. Springer, Singapore.
- **Mohamed Haroon Abdul Jabbar**, S. Anandan Shanmugam, and Poi Sim Khiew. (2018). Investigation on Heat and Mass transfer in a Dialyzer Membrane Model for the Development of Dialysate Temperature Controller. In Proceedings of the 2018 5th International Conference on Bioinformatics Research and Applications (ICBRA '18). ACM, New York, NY, USA, 22-28. DOI: <https://doi.org/10.1145/3309129.3309135>

ACKNOWLEDGEMENT

First and foremost, I am thankful to Almighty Allah for blessing, protecting and guiding me to complete this Thesis. I could never have finished this work without the faith I have in the Allah.

I would like to express my sincere gratitude to both of my supervisors Prof. Khiew Poi Sim and Dr. Anandan Shanmugam for the continuous support of my PhD study and related research, motivation, and immense knowledge. They have been a tremendous mentor for me and I am thankful to them for all their guidance throughout my study duration.

I will always remember Dr. Anandan's support during my difficult times and for treating me like his close friend. Without his encouragement and kind guidance, I could not have completed my thesis. I could not have imagined having a better supervisor and mentor for my PhD study.

Also, I would like to thank my internal examiner: Dr. Roselina Arelhi for meeting me and giving me some of her valuable time and for her questions which helped me to widen my research from various perspectives. My sincere thanks also goes to E&E Technicians especially Mr.Hashimi, Mr.Saiful, and Mr.Hamdi for sharing me their rich practical experience and providing access to the laboratory facilities.

Most importantly, none of this work would have been possible without my family, to whom this thesis is dedicated. My deepest gratitude goes to my Father, Mr. Abdul Jabbar, Mother, Mrs. Pouja, my beloved brother, Mr. Fakeer Ahamed and my sister in law, Mrs. Fasna for their endless love, constant support, patient and motivation at all times in my life. A very special thanks to my Grandmother for her constant prayers during my research. I would like to thank my wife, Dr. Ramsheela for her love, patience, and support during these years. Without your understanding and devotion, this work presented will not be possible.

I would like to thank all my friends who made research life in the University very meaningful. It was because of them that I enjoyed going to the office even when I underwent hardships with research. There are numerous people I want to remember always and thank (just to name a few): Abhay, Afra, Kalai, Piravin, Harshini, Anand, Sharshad, Renu, Denesh, and Ayoub.

Special thanks to my friends, Mr.Mohan, Mrs.Celine, Mr.Rahul and Mr.Vipin for their unconditional love and care that felt like a 'second home' in Malaysia. I will miss them so much.

Finally, I would like to acknowledge Faculty of Engineering, UNMC for awarding me Dean's Scholarship for sponsoring my study. Moreover, I had the privilege to travel to India and Hong Kong for conferences. I would like to thank Faculty of Engineering, UNMC for the funding provided.

TABLE OF CONTENTS

ABSTRACT	III
LIST OF PUBLICATIONS	VI
ACKNOWLEDGEMENT	VII
TABLE OF CONTENTS	IX
LIST OF FIGURES	XII
LIST OF TABLES	XVI
LIST OF ABBREVIATIONS	XVII
CHAPTER 1	1
INTRODUCTION	1
1.1 BACKGROUND	1
1.2 PROBLEM STATEMENT.....	4
1.3 RESEARCH OBJECTIVES	5
1.4 RESEARCH SCOPES	6
1.4.1 <i>Design of a novel dialysate proportioning method</i>	6
1.4.2 <i>Effect of heat transfer in a dialyzer</i>	6
1.4.3 <i>Implementation of fuzzy logic control in Raspberry Pi</i>	6
1.4.4 <i>In-vitro analysis of dialysate temperature control module</i>	7
1.5 CONTRIBUTION OF RESEARCH	7
1.6 THESIS OUTLINE.....	7
CHAPTER - 2	9
LITERATURE REVIEW	9
2.1 SIGNIFICANCE OF HEAT ACCUMULATION IN HEMODIALYSIS.....	9
2.2 TOWARDS AN OPTIMAL DIALYSATE TEMPERATURE	12
2.3 TECHNOLOGICAL ADVANCEMENTS IN HEMODIALYSIS MACHINES TO PREVENT COMPLICATIONS.....	17
2.4 TEMPERATURE CONTROL SYSTEM	22
2.5 IMPLEMENTATION OF FUZZY LOGIC CONTROLLERS IN MEDICAL APPLICATIONS	28
CHAPTER -3	32
DESIGN AND METHODOLOGY	32
3.1 PROBLEM STATEMENT & HYPOTHESIS	33
3.2 INVESTIGATION OF DIALYZER HEAT TRANSFER THROUGH SIMULATION	34
3.3 SIMULATION ANALYSIS	35
3.4 MODELLING THERMAL ENERGY BALANCE OF EXTRACORPOREAL CIRCULATION	36
3.5 DESIGN CONCEPT.....	37
3.6 PROTOTYPE DEVELOPMENT.....	38
3.6.1 <i>Hardware</i>	41
3.6.2 <i>Software</i>	49
3.7 SUBSYSTEM PERFORMANCE AND INTERFACING.....	55
3.7.1 <i>Phase 1</i>	55
3.7.2 <i>Phase 2</i>	56
3.8 PROTOTYPE CONSTRUCTION AND ASSEMBLY	57

3.9	TESTING & VALIDATION	59
3.10	EVALUATION	59
CHAPTER - 4		60
INVESTIGATION ON HEAT TRANSFER IN A DIALYZER MEMBRANE MODEL FOR THE DEVELOPMENT OF DIALYSATE TEMPERATURE CONTROLLER MODULE		60
4.1	INTRODUCTION	60
4.2	SIMULATION METHODOLOGY	62
4.3	RESULTS AND DISCUSSION	68
4.3.1	<i>Heat transfer in a dialyzer.....</i>	<i>68</i>
4.3.2	<i>Effect of heat transfer by varying dialysate temperature.....</i>	<i>70</i>
4.3.3	<i>Effect of heat transfer by varying blood and dialysate flow rate.....</i>	<i>71</i>
4.3.4	<i>Relationship between inlet and outlet blood temperature.....</i>	<i>72</i>
4.4	CONCLUSION.....	76
CHAPTER - 5		77
IMPLEMENTATION AND PERFORMANCE EVALUATION OF FUZZY LOGIC CONTROL WITH RASPBERRY PI		77
5.1	INTRODUCTION	77
5.2	DESIGN AND METHODOLOGY	79
5.2.1	<i>Experimental design</i>	<i>79</i>
5.2.2	<i>Fuzzy logic control design</i>	<i>81</i>
5.2.3	<i>Implementation design.....</i>	<i>90</i>
5.2.4	<i>Evaluation factors.....</i>	<i>91</i>
5.3	RESULTS AND DISCUSSION	92
5.3.1	<i>Design-1</i>	<i>92</i>
5.3.2	<i>Design-2</i>	<i>94</i>
5.3.3	<i>Design-3</i>	<i>96</i>
5.3.4	<i>Design-4</i>	<i>97</i>
5.3.5	<i>Summary of results.....</i>	<i>99</i>
5.3.6	<i>Multiple setpoint of optimized design</i>	<i>102</i>
5.4	CONCLUSION.....	106
CHAPTER - 6		107
IMPLEMENTATION OF DIALYSATE TEMPERATURE CONTROL MODULE PROTOTYPE AND ITS IN-VITRO EVALUATION		107
6.1	INTRODUCTION	107
6.2	EXTRACORPOREAL THERMAL ENERGY BALANCE MODEL	109
6.3	DESIGN AND METHODOLOGY	113
6.3.1	<i>Experimental design</i>	<i>113</i>
6.3.2	<i>Phase 1 design.....</i>	<i>114</i>
6.3.3	<i>Phase 2 design.....</i>	<i>115</i>
6.3.4	<i>Implementation design.....</i>	<i>117</i>
6.4	RESULTS AND DISCUSSION	119
6.4.1	<i>PID temperature control system.....</i>	<i>119</i>
6.4.2	<i>Effect of body temperature with DTCM.....</i>	<i>121</i>
6.4.3	<i>Effect of body temperature for various trends of arterial temperature</i>	<i>126</i>
6.4.4	<i>Effect of body temperature for various blood and dialysate flow rates.....</i>	<i>129</i>

6.4.5	<i>Effect of body temperature for various external factors</i>	131
6.5	CONCLUSION.....	135
CHAPTER - 7		137
CONCLUSION AND FUTURE WORKS		137
7.1	GENERAL CONCLUSION	137
7.2	FUTURE WORKS.....	139
8	BIBLIOGRAPHY	141
9	APPENDICES	160
9.1	APPENDIX A - DTCM SIMULINK MODEL.....	160
9.2	APPENDIX B - TEMPERATURE AND OUTPUT RESPONSE OF DTCM UNDER VARIOUS CONDITIONS....	162
9.3	APPENDIX C - CALIBRATION OF PERISTALTIC PUMP	168

LIST OF FIGURES

Figure 1.1 – Schematic of HD circuit [3].	2
Figure 1.2 - Flow chart representing the overall thesis outline.	8
Figure 2.1 – Vascular events due to heat accumulation during HD [26].	10
Figure 2.2 - Average weekly body temperatures prior to death in patients whose body temperatures (a) declined and (b) increased [15].	12
Figure 2.3 – Common biofeedback control systems for HD machine.	18
Figure 2.4 – Block representation of Hemocontrol biofeedback control system [52].	19
Figure 2.5 – Block representation of arterial pressure biofeedback system [62].	20
Figure 2.6 –BTM module with temperature sensor heads [65].	22
Figure 2.7 – Structure of closed loop BTM in T-control mode [19].	23
Figure 2.8 – Basic structure of FLC with four basic components [81].	29
Figure 3.1 - Iterative design phases of dialysate temperature control module (DTCM).	33
Figure 3.2 - (a) An overall structure of Polyflux™ 210H dialyzer and (b) cross sectional view of bundled hollow fibers inside the housing.	35
Figure 3.3 – Thermal energy transfer between patient and HD system	37
Figure 3.4 - Proposed design concept of DTCM.	38
Figure 3.5 - Overview of a Baxter’s dialysate circuit including proposed DTCM.	40
Figure 3.6 – Hardware architecture of prototype for phase 1.	41
Figure 3.7 – Image of DC pump used.	42
Figure 3.8 – Image of flow through heater with connecting terminals.	43
Figure 3.9 – Image of DS18B20 temperature sensor used.	44
Figure 3.10 – Image of float switch used.	45
Figure 3.11 – Hardware architecture of prototype for phase 2.	45
Figure 3.12 – Image of DM422C stepper driver used.	47
Figure 3.13 – Side view of peristaltic pump consisting of (1) pump head, (2) coupler and (3) stepper motor.	48
Figure 3.14 – Front view of peristaltic pump with (a) pump head open position and (b) pump head close position.	48
Figure 3.15 – Y-shaped connector used.	49
Figure 3.16 - Block diagram of the PID controller feedback loop	50

Figure 3.17 – Software flow chart of Phase 1 development.	51
Figure 3.18 – Graphical User interface for Phase 1 PID temperature controller using Megunolink Pro.	52
Figure 3.19 – Software flow chart for Phase 2 development.	54
Figure 3.20 – Illustration of DTCM prototype design comprising of PID and fuzzy control.	58
Figure 4.1 - Evolution of Polyflux 210H dialyzer membrane from actual dialyzer to a simulation model comprising of (a) overview of actual dialyzer, (b) bundle of hollow fibers packed inside the housing, (c) cross sectional view of hollow fiber in a dialyzer and (d) 2D geometrical model of single fiber membrane.	63
Figure 4.2 – Dialyzer membrane model showing blood, membrane and dialysate domain and other boundaries.	64
Figure 4.3 - (a) 3D representation and (b) 2D representation of Temperature surface when inlet temperature of blood and dialysate at 37°C and 35°C respectively flows through dialyzer at $Q_b = 300 \text{ ml min}^{-1}$ and $Q_d = 450 \text{ ml min}^{-1}$	69
Figure 4.4 - The graph of (a) blood and (b) dialysate temperature at the inlet and outlet of this model.	69
Figure 4.5 - The outlet (a) blood temperature and (b) dialysate temperature for various dialysate temperatures under normal body temperature.	70
Figure 4.6 - Comparison of change in blood and dialysate temperature along the membrane for various blood flow rate, Q_b , and dialysate flow rate, Q_d	72
Figure 4.7 – Graph of relation between outlet blood temperature in terms of inlet blood and dialysate temperature for $Q_b 300 \text{ ml min}^{-1}$; $Q_d 450 \text{ ml min}^{-1}$	73
Figure 5.1 - Simplified temperature controller schematic for fuzzy logic optimization.	80
Figure 5.2 – Experimental setup for a simplified temperature controller.	80
Figure 5.3 - Schematic diagram of FLC used for the proposed model.	81
Figure 5.4 – Design-1 membership function of inputs (a) error and (b) change in error, while (c) and (d) shows the output membership function in Mamdani and Sugeno FIS respectively.	83
Figure 5.5 - Control surface of (a) Mamdani FIS and (b) Sugeno FIS for Design-1.	85
Figure 5.6 - Design-2 membership function of inputs (a) error and (b) change in error, while (c) and (d) shows the output membership function in Mamdani and Sugeno FIS respectively.	86
Figure 5.7 - Control surface of (a) Mamdani FIS and (b) Sugeno FIS for Design-2.	87
Figure 5.8 - Design-3 membership function of inputs (a) error and (b) change in error, while (c) and (d) shows the output membership function in Mamdani and Sugeno FIS respectively.	88
Figure 5.9- Control surface of (a) Mamdani FIS and (b) Sugeno FIS for Design-3.	88

Figure 5.10 - Design-4 membership function of inputs (a) error and (b) change in error, while (c) and (d) shows the output membership function in Mamdani and Sugeno FIS respectively.	89
Figure 5.11 - Control surface of (a) Mamdani FIS and (b) Sugeno FIS for Design-4.....	90
Figure 5.12 – Simulink model for the proposed temperature control system.....	91
Figure 5.13 – Controller response for Design-1.....	93
Figure 5.14 – Pump output response for Design-1	94
Figure 5.15 - Controller response for Design-2.....	95
Figure 5.16 - Pump output response for Design-2.....	96
Figure 5.17 - Controller response for Design-3.....	97
Figure 5.18 - Pump output response for Design-3.....	97
Figure 5.19 - Controller response for Design-4.....	98
Figure 5.20 - Pump output response for Design-4.....	99
Figure 5.21 – Bar graph showing the comparison of performance indices among the proposed designs.....	100
Figure 5.22 – Controller response for multiple setpoint of optimized design	102
Figure 5.23 – Comparison of (a) optimized fuzzy logic design temperature setpoint response with (b) published fuzzy logic temperature control response [109].	104
Figure 6.1 - Block representation of extracorporeal circuit.	109
Figure 6.2 – Experimental setup for in-vitro evaluation of DTCM prototype.....	114
Figure 6.3 – Circuit diagram for phase 1 of DTCM prototype.	115
Figure 6.4 – Optimized fuzzy logic design for DTCM prototype consisting of (a) error input MFs, (b) change in error input MFs, (c) pump output MFs and (d) output surface for the Mamdani FIS output.....	116
Figure 6.5 – Circuit diagram for phase-2 of DTCM prototype.	117
Figure 6.6 – Flow chart of implementation design of DTCM prototype.	119
Figure 6.7 – The (a) temperature response and (b) output response for 36°C storage tank.....	120
Figure 6.8 - The (a) temperature response and (b) output response for 38°C storage tank.....	120
Figure 6.9 – Temperature response of DTCM prototype at BT = 36.5°C.	122
Figure 6.10 – Temperature response of standard dialysate temperature control at BT = 36.5°C.	122
Figure 6.11 –Graphs shows (a) Output response and (b) Arteriovenous temperature gradient of DTCM prototype at body temperature = 36.5°C.	124
Figure 6.12 – Mean arterial (solid line) and venous (dotted line) temperature changes in BTM during HD [66].....	126

Figure 6.13 – Dialysate temperature changes in BTM during HD [66].....	126
Figure 6.14 – Graph of body temperature error fluctuations for various trends of arterial temperature.	127
Figure 6.15 – Graph of arteriovenous temperature gradient for various trends of arterial temperature.	128
Figure 6.16 - Graph of body temperature error fluctuations for various blood and dialysate flow rates.	130
Figure 6.17 - Graph of arteriovenous temperature gradient for various blood and dialysate blood flow rates.....	131
Figure 6.18 - Graph of body temperature error fluctuations for various external factors.	132
Figure 6.19 - Graph of arteriovenous temperature gradient for various external factors.....	133
Figure A 1 – Overall Simulink model of DTCM prototype.	160
Figure A 2 - Estimation of venous temperature model of DTCM prototype.....	161
Figure A 3 - Estimation of arterial temperature model of DTCM prototype.....	161
Figure B 1 – Temperature response of DTCM under various patient’s temperature.....	162
Figure B 2 - Output response of DTCM under various patient’s temperature.....	162
Figure B 3- Temperature response of DTCM under various trend of patient’s temperature. ...	163
Figure B 4 – Output response of DTCM under various trend of patient’s temperature.....	163
Figure B 5 - Temperature response of DTCM under various dialysate flow rates.....	164
Figure B 6 - Output response of DTCM under various dialysate flow rates.....	164
Figure B 7 - Temperature response of DTCM under various blood flow rates.....	165
Figure B 8 – Output response of DTCM under various blood flow rates.	165
Figure B 9 - Temperature response of DTCM under various recirculation factor.	166
Figure B 10 - Output response of DTCM under various recirculation factor.....	166
Figure B 11 - Temperature response of DTCM under various ambient temperature.	167
Figure B 12 - Output response of DTCM under various ambient temperature.....	167
Figure C 1 – Graph of peristaltic pump calibration with duty cycle via Simulink.	168
Figure C 2 - Rotameter readings for Qd450, Qd400 and Qd350 showing the flow rate in ml min ⁻¹	168

LIST OF TABLES

Table 2.1 – Summary of HD outcomes with the utilization of BTM.....	25
Table 3.1 – Kanthal A1 wire specification for heaters	43
Table 4.1 – Material parameters of blood, dialysate and membrane used in this model	65
Table 4.2 – Coefficients of inlet blood and dialysate temperature for various Q_b and Q_d	74
Table 5.1 – Rule base for Design-1.....	84
Table 5.2 - Rule base for Design-2.	87
Table 5.3 - Rule base for Design-4	90
Table 5.4 – Comparison of transient response among the proposed designs	101
Table 5.5 – Performance indices for the multiple setpoints	103

LIST OF ABBREVIATIONS

ABPS	Arterial Blood Pressure Stabilization
AI	Artificial Intelligence
ANN	Artificial Neural Network
BP	Blood Pressure
BTM	Blood Temperature Monitor
BVM	Blood Volume Monitor
CKD	Chronic Kidney Disease
DTCM	Dialysate Temperature Control Module
FGPA	Field-programmable gate array
FIS	Fuzzy Inference System
FLC	Fuzzy Logic Control
GA	Genetic Algorithm
GUI	Graphical User Interface
IAE	Integral Absolute Error
IDE	Integrated Design Environment
IDH	Intradialytic Hypotension
IoT	Internet of Things
ISE	Integral Squared Error
ITAE	Integral of Time-weighted Absolute Error
MIMO	Multiple Input Multiple Output
MISO	Multiple Input Single Output
PC	Plasma Conductivity
PSO	Particle Swarm Optimization
PWM	Pulse Width Modulation
RRT	Renal Replacement Therapies
UF	Ultrafiltration

1.1 Background

When blood flows through the body, surplus water and toxins can accumulate within the blood from the ongoing metabolic processes of the body. The level of surplus toxins must be removed to sustain the physiological functions of various organs and cells in our body. To retain this balance, the kidney plays a vital role of removing water and wastes from the blood. Other than removing excess water and toxins, the kidneys also provide many other regulatory mechanisms concerned with the maintenance of the body function. These include maintenance of electrolyte balance in body fluids, maintenance of acid-base balance in body fluids and tissues, reabsorption of glucose and amino acids, regulation of blood pressure as well as the production of hormones [1]. Once kidneys fail to function normally, excess fluid is retained, and several solutes and ions accumulate in the body. The consequence of this may become life threatening. The potential ways for patients with kidney failure to survive is either by kidney transplantation or attending a regular hemodialysis (HD) treatment. However, there are many potential benefits of an effective kidney transplant, but the entire numbers of transplants are very low [2]. This is mainly due to the lack of donors, and if they found a donor, sometimes the body fails to accept the new kidney. Hence, the alternative for these patients is to undergo regular HD treatment.

In HD, the patient's blood is passed through tubing system to a semipermeable membrane, which has dialysis fluid (dialysate) running on the other side as shown in Figure 1.1. Diffusion of dissolved substances from one stream to the other removes molecules that are in excess in the blood and replaces those for which there is a deficiency. During HD, the maintenance of body fluid levels is accomplished by the transport of solutes such as urea from the blood into dialysate by diffusion and by the transport of solutes such as bicarbonate from dialysate into the blood by back diffusion. The renal failure patient may have excess water, which is removed by the process of ultrafiltration. Through HD, the cleansed blood is then returned through the system back to the body. HD patients undergo dialysis, usually two or three times a week, about four hours each time, after which patients often feel exhausted or ill. The alternate-day schedule of HD presents a significant barrier to patients seeking to maintain employment or school enrolment. It has been estimated that less than 10% of dialysis patients maintain employment [2].

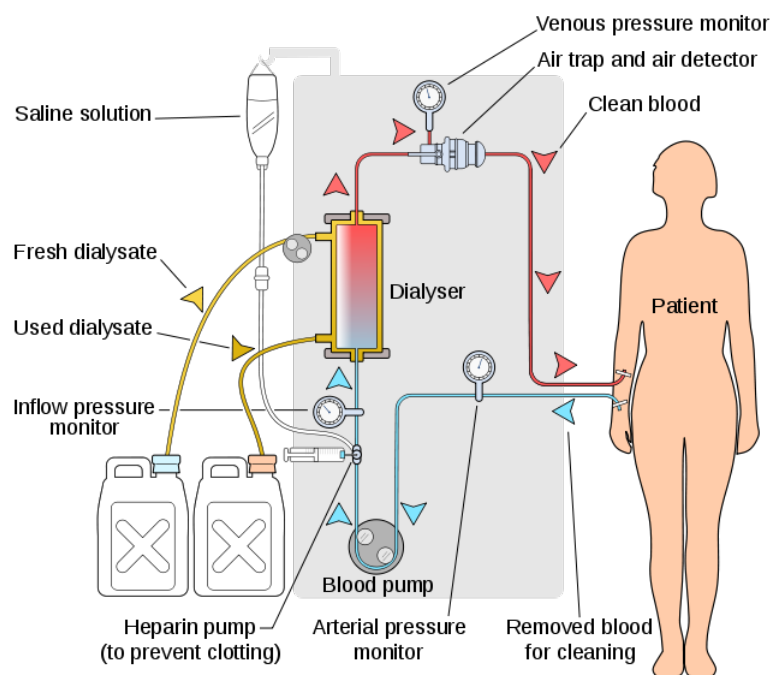


Figure 1.1 – Schematic of HD circuit [3].

HD has been associated with frequent intradialytic complications (hypotension, sickness, cramps, etc.) and post-dialysis complaints of headache, fatigue, inability to concentrate and other functions, which may significantly weaken the quality of life. During early days of the introduction of HD, complications were common due to the technical drawbacks associated with the HD machine. With the help of technological development, particularly in the last 20 years, complications have reduced to a great extent. Yet, intradialytic hypotension (IDH) remains the most common complication in HD which endure as a significant cause of morbidity and mortality [4].

HD machine controls the circulation of blood from patient through dialyzer and back to patient. It continuously monitors and controls all important parameters such as blood flow rate, dialysate temperature, dialysate conductivity etc. and automatically halting treatment in the event of parameters going out of any pre-defined limits. In addition, there are several biofeedback control systems such as blood volume, blood pressure, heart rate, temperature, and dialysate conductivity etc., employed in HD machines, which are responsible for reduction in complications. Studies on temperature biofeedback system in the recent years are quite sparse. The motivation of developing temperature controller is to prevent heat accumulation which normally increases the body temperature in the HD patients. It was also evident that the control of body temperature can improve cardiovascular stability during HD. In addition to this, maintaining the dialysate temperature within the physiological range is vital for patients' safety [5].

1.2 Problem statement

Nowadays, 10% of the population worldwide is affected by chronic kidney disease (CKD) and millions die each year because they do not have access to affordable treatment. CKD is a common health crisis and the incidence of CKD shows an alarming increase especially in developing countries [6]–[8]. The number of patients receiving dialysis is estimated to be more than 1.4 million, with incidence growing by approximately 8% annually all around the world [9]. In Malaysia, there was an exponential growth in the incidence of CKD and the number of those patients on dialysis treatment. According to the 11th & 24th report of the Malaysian Dialysis and Transplant Registry, the dialysis prevalence rate has increased dramatically from 391 per million populations in 2003 to 1159 per million in 2016 [10], [11]. This rapid rise is mainly due to the increase in the incidence of lifestyle diseases like diabetes and hypertension. Moreover, the number of people without access to unaffordable renal replacement therapies (RRT) remain significant in many developing countries [12]. Recent study also shows that the number of people undergoing RRT will be doubled by 2030, mostly in developing regions such as Asia and Africa [13].

IDH is the most adverse effect of HD, occurring up to 20 to 30% of dialysis sessions, which is responsible for various symptoms such as vomiting, dizziness, fatigue, etc. [14]. Such episodes predispose the patients to leave the dialysis unit and if repetitive occurrence can lead to inadequate clearance. IDH is one of the independent risk factors affecting mortality in HD patients. However, body temperature plays a vital role in the onset of IDH. In fact, the highest mortality was observed among the patients whose body temperature fluctuates during the treatment [15]. In the current practice, the constant

dialysate temperature would not be sufficient to keep the body temperature stable. Moreover, it is quite impractical through a manual adjustment in dialysate temperature as it requires significant staff intervention during the treatment. Even though, a commercially available body temperature control is available namely Blood Temperature Monitor (BTM) for HD machine, it is not well-renowned due to its high cost and limited interface with other HD machines. Therefore, the development of an active control module of dialysate temperature is much needed for our society.

1.3 Research objectives

Overall objective of this research was to develop a novel dialysate proportioning prototype and an optimum control method to provide a stable body temperature with certain qualities such as improved efficiency, individualized, modularity and easy-interface with other HD machines. The main drive to develop such dialysate temperature control module (DTCM) prototype was to explore the potential of maintaining body temperature during the treatment which can be implemented in any current HD machines. Specific objectives of this research were as follows:

- To develop a novel design of dialysate proportioning method for the benefit of temperature control.
- To evaluate the effect of heat transfer in a dialyzer under various hemodynamic conditions.
- To evaluate the implementation of fuzzy logic control (FLC) in Raspberry Pi microcontroller for temperature control application.
- To evaluate the in-vitro analysis of the DTCM prototype under various conditions.

1.4 Research scopes

1.4.1 Design of a novel dialysate proportioning method

The design of a novel dialysate proportioning method was proposed for the development of an efficient dialysate temperature controller. The main intention for such development was to introduce an effective temperature control through varying flow rates rather than conventional heaters. This chapter emphasizes on the evolution of prototype development including hardware and software to illustrate the overview of DTCM.

1.4.2 Effect of heat transfer in a dialyzer

The heat transfer in a dialyzer membrane namely Polyflux 210H was investigated using COMSOL Multiphysics software. The effect of temperature trend in blood and dialysate side were analysed under various hemodynamic parameters (dialysate temperature, blood temperature, blood flow rate and dialysate flow rate) in order to deduce the generalized expression of heat transfer in dialyzer.

1.4.3 Implementation of fuzzy logic control in Raspberry Pi

FLC was implemented in a low-cost microcontroller Raspberry Pi for the optimization of temperature controller. The temperature outputs were analysed for various fuzzy logic designs in terms of certain performance indices (IAE, ITAE and ISE) and settling time. The optimized fuzzy logic design was then compared with the published fuzzy logic based temperature control results.

1.4.4 In-vitro analysis of dialysate temperature control module

An extracorporeal thermal energy balance model incorporating the heat transfer in dialyzer was proposed and validated for the in-vitro analysis of DTCM prototype. The effect of body temperature and controller performance using DTCM was then compared against commercially available Blood Temperature Monitor (BTM) clinical results. Moreover, the effect of temperatures such as arterial, venous and dialysate were monitored under various conditions.

1.5 Contribution of Research

The technological advancements in HD machine over the years have solely focussed on biofeedback control systems (arterial pressure, body temperature, relative blood volume and dialysate conductivity). The proposed method adopted in current research will provide an alternate technique for temperature controller module of HD machine in resulting a stable body temperature during the treatment. The individualized body temperature control would have high potential not only to reduce the intradialytic complications but also improves the patient's quality of life. This will also help in bridging the gap between temperature control and avoidable intradialytic complications that will benefit the kidney patients all over the world.

1.6 Thesis outline

The thesis is divided into seven chapters and the following flow chart (Figure 1.2) provides information on the thesis outline.

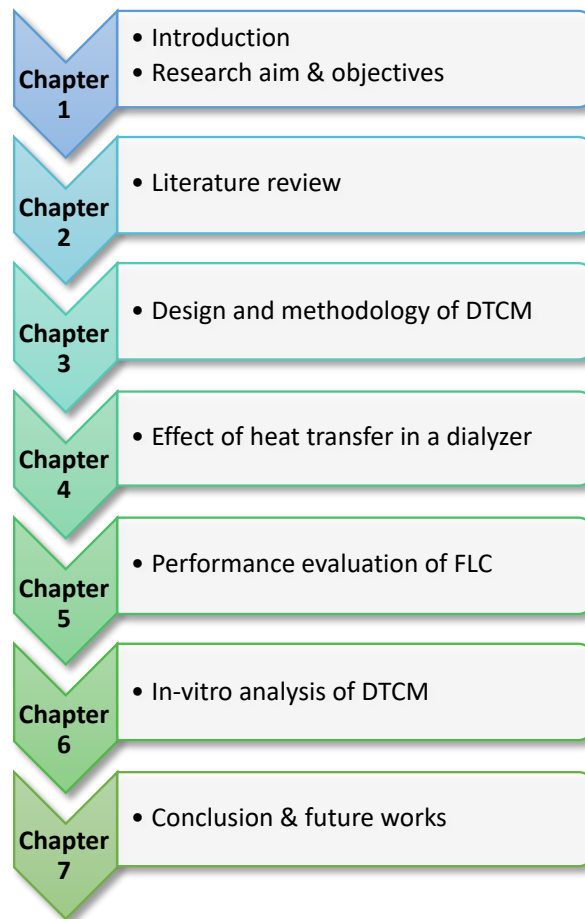


Figure 1.2 - Flow chart representing the overall thesis outline.

In Chapter 1, the prologue of this research which includes background information, objectives and scope of research are clearly portrayed. Chapter 2 provides the review of literatures about the effects of body temperature during HD and recent technological advancements in temperature controller. Design and methodology of this research is explained in Chapter 3, where the proposed prototype is designed and constructed in order to solve the problem at hand. Chapter 4 explains the simulation study on the effect of heat transfer in a dialyzer. Likewise, Chapter 5 has dealt with the performance evaluation and optimization of FLC prior to implementation in DTCM. Then, Chapter 6 illustrates the overall in-vitro analysis of DTCM through various experiments. Finally, Chapter 7 portrays the conclusion of this research. It also states some important summarized facts regarding this research and future work to be done.

2.1 Significance of heat accumulation in Hemodialysis

Normally, a living organism feels most comfortable when it is in a state known as thermal equilibrium, which means the amount of heat lost through the skin equals the amount of heat that enters through the skin. This infers that the body temperature has been kept stable within narrow limits, which is achieved by the thermoregulatory mechanism [16]. However, HD could extremely interrupt the patient's pre-dialysis thermal equilibrium due to the heat exchange taking place in extracorporeal circuit [17]. In contrast to the accumulation of uremic solutes, there is also a potential for thermal energy to accumulate during HD. The accumulated heat results in an increase of body core temperature even with net thermal energy loss from patient to extracorporeal circuit [18]. One of the major possibility for the heat accumulation in HD is due to the decreased dissipation of heat from the body surface during HD [19]. Other possible causes mentioned in the literatures are due to increased metabolic rate and delivery of thermal energy by the extracorporeal circuit [17], [20], [21]. Additional cause includes the exposure of blood to the extracorporeal circulation. In detail, contact of blood with dialyzer and lines, particularly if the materials are of poor quality and not biocompatible, induces an inflammatory response that causes abnormal reactions [22]–[24]. This in turn causes an increase in heat generation, which could result in an increase of body temperature.

The reduced transfer of metabolic heat from the body core to body shell is essentially caused by cutaneous vasoconstriction as a compensation of reduction in blood volume. However, if the heat accumulation increases beyond a critical threshold, the increase in the thermoregulatory mechanism will lead to an increase in cutaneous blood flow and effective blood volume which will reduce peripheral resistances, leading to intradialytic hypotension (IDH) and an increased risk of intradialytic morbidity [25], [26]. This process is shown in Figure 2.1. This can contribute to hemodynamic instability, the threshold for which differs in individual patients. In contrary, an unique subsequent study has reported on insignificant relation in body temperature with a change of cutaneous blood flow and skin temperature [18]. However, the body temperature has changed significantly related to the timing of dialysis shift, in phase with the circadian rhythm [27]. Still, the body temperature plays a vital role in the onset of hypotension [26], [28]. Even slight variations in body temperature might be sufficient to cause complications. Additionally, IDH is a frequent complication of HD, and is associated with under-dialysis and increased mortality and cardiovascular events [29]. So, the prevention of accidents due to IDH is an important challenge for the researchers in this field.

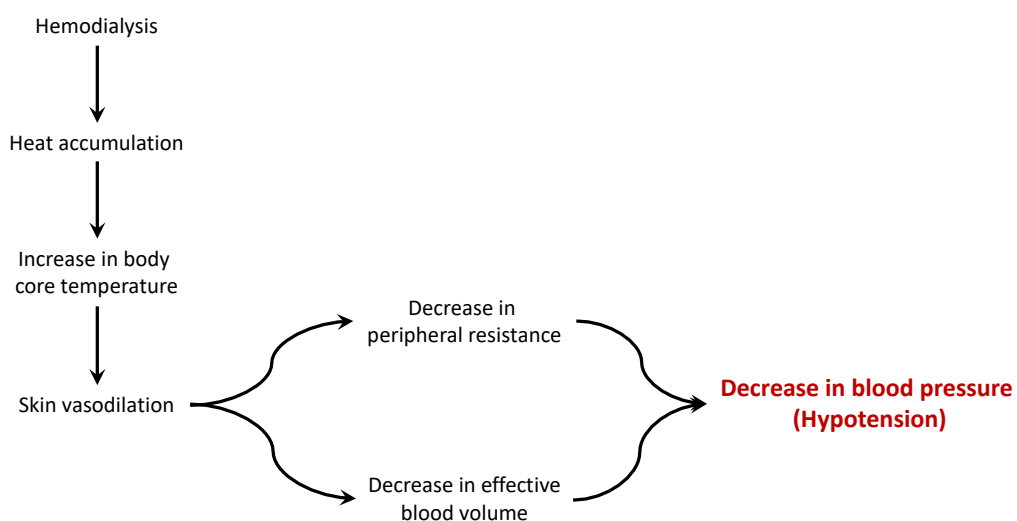


Figure 2.1 – Vascular events due to heat accumulation during HD [26].

There are several literatures in regard to the relation between the intra-dialytic temperature changes and the hemodynamic response during dialysis. But, there is a lack of data regarding the body temperature in HD patients and its long-term course. A recent study has analysed the relationship between trends in body temperature and outcome in HD patients [15]. A total of 12695 incident HD patients have taken part in this study, which took over 1 year of duration. To the best of our knowledge, this is the first study to relate the trend in body temperature with the mortality of HD patients incorporating a large number of patients from around 51 dialysis centres. The result shows that the highest mortality was observed in patients whose body temperature increased or decreased during the period, irrespective of baseline body temperature. Whereas, the lowest mortality was found in the group with the highest body temperature at baseline and with stable temperature during the treatment. A most fascinating fact appeared out of this study; the patients with a decreasing temperature had an increased risk of mortality as compared to the groups with stable temperature.

In an analysis of trends in body temperature before death (*as shown in Figure 2.2*), we observed that declines and increases in blood temperature appear to be long-term phenomena, rather than acute drop preceding death. This reduction of body temperature might be an adaptive response of body to inflammation when the body cannot cope with the increasing demands of fever. Another factor that occur might due to a decrease in body temperature is cardiac failure. The highest mortality in dialysis patients during this study was found to be in the winter period, which shows the effect of ambient temperature in patients' body temperature.

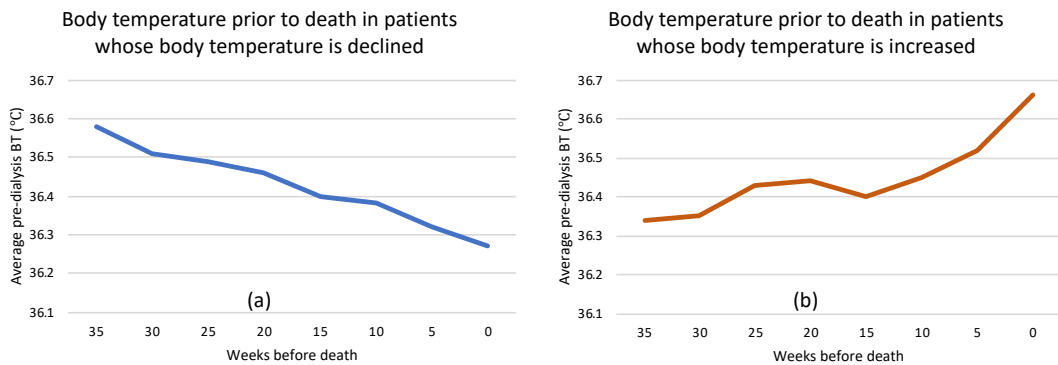


Figure 2.2 - Average weekly body temperatures prior to death in patients whose body temperatures (a) declined and (b) increased [15].

This study serves as a strong evidence in mortality due to fluctuations in body temperature during HD. However, more detailed analysis of body temperature changes is needed to obtain a clear vision into physiological mechanisms behind the mortality in HD patients. The control of body temperature is much needed to overcome this depressing mortality trend. One of the simplest ways to control body temperature is to reduce the dialysate temperature in extracorporeal circuit, first described by Maggiore *et al.* in the 1980s [30]. The primary aim was to compensate the temperature change in HD patients. In addition to this, maintaining the dialysate temperature within the physiological range is vital for patients' safety. As dialysate temperature plays a crucial role in hemodynamic stability, knowledge of an optimal dialysate temperature is important.

2.2 Towards an optimal dialysate temperature

Nowadays, almost all HD machines are equipped with a system to control for a constant dialysate temperature. Traditionally, dialysate temperature of 37°C was considered as standard temperature for everyday HD [31], [32]. It was considered with the intention to keep the core temperature stable within the narrow limits. In reality, the

standard dialysate was somewhat higher than the average physiologic core temperature. However, the body temperature of long-term HD patients were less than 36.5°C, which is lower than healthy individuals [20], [33]. This could lead to an increase in core temperature of about 0.3 to 0.8°C, which could result in high chance of IDH [30], [32], [33]. Early studies confirmed that the body was sensitive to even slight change in temperature. Even a slight increase in temperature would lead to an excessive drop in blood pressure, which in turn increases the frequency of staff interventions [34]. The excess body heat can be eliminated not only via skin but also by means of extracorporeal blood circulation. This depends on the temperature difference between blood and dialysate fluid.

Numerous studies have confirmed that the mild cool dialysate improves the hemodynamic stability when compared to standard dialysate temperature. The idea of cool dialysate postulated to be beneficial by avoiding the heat accumulation and hence reducing the IDH episodes during the treatment. Over the last 10 years, majority of studies have dealt with cool dialysate to prevent IDH as primary investigation. From the reported literatures, the cool dialysate at temperature of 35°C showed a very promising approach in preventing IDH episodes with improvements in hemodynamic stability including stroke volume, heart rate, baroreflex sensitivity and cardiac output [23], [35]–[38]. In a systemic review with a total of 42 studies on cool dialysis have reported that IDH occurred 7.1% times less frequently, while post-dialysis mean arterial pressure was higher than standard dialysate by 11.3 mmHg [23]. However, the recent study has suggested the reduction in sodium concentration with cool dialysate improves the lower fluctuations in blood pressure [37]. In a short study consisting of 5 patients, the cool dialysate improved the tolerance for HD in hypotension prone patients while maintaining

the hemodynamic stability during and after dialysis [39]. In another study, Ghasemi *et al.*, observed that, especially patients with diabetes had lesser episodes of IDH for cool dialysis [31]. Unlike other studies, Korkor *et al.*, have performed a study with a few patients with a decrease in dialysate temperature by a little of 0.5°C – 1.0°C, which resulted in lesser episodes of IDH [40]. Subsequently, the cool dialysate resulted in lesser staff intervention during HD, which has a positive impact on the functionality of HD machine. In addition to study based on IDH episodes, the cool dialysate have substantial improvement in terms of quality of life, insignificance in biocompatibility, improves nocturnal sleep compared to standard dialysate [22], [39], [41]. In a most recent study, the cool dialysate at 36°C have reduced the sensory symptoms (such as numbness) by 10% and motor symptoms (such as muscle weakness) by 36 – 54% [42]. In contrary, the cool dialysate at 36°C did not show any significant benefit compared to standard dialysate at 37°C [43].

Likewise, a study with the utilization of dialysate temperature at 35.5°C have reported that core temperature remained stable, but even increased in some patients despite significant thermal energy loss from the patient to extracorporeal circuit [44]. This could be due to the individual threshold of thermoregulatory mechanism. By considering the HD adequacy, urea based dialysis adequacy is largely unaffected by dialysate temperature as reported in the literatures [25]. However, it is suggested that prolonged utilization of cool dialysate might lead to comorbidities associated with excess toxin accumulation. With the best of our knowledge, a clinical trial for removal of both small and large sized toxins through dialysate temperature manipulation has never been conducted so far.

The data suggests that cool dialysis is simple, inexpensive, and reduces intradialytic events during HD. However, the use of extremely low dialysate temperature in the range of 35°C – 35.5°C, has shown unpleasant effects in some patients such as shivering and cold sensation [23], [39], [40]. It has been reported that up to 70% of patients feel cold sensation during the treatment and shivering was observed in some patients [5], [32]. Even though, this is not a serious disadvantage, yet it would eventually affect the patients in long-term. This could be the reason that cool dialysate is not recommended as standard dialysate prescription even though it was reported over 38 years back with a significant reduction in IDH episodes. It is also expected that individual patients have a different temperature threshold at which a benefit to hemodynamic stability is conferred [34]. It can be seen that there is a lack of long-term studies with limited sample sizes that would help to generalize the effect of cool dialysate to a larger HD patient population worldwide.

This cold symptom tolerability can be optimized by an individualized approach to dialysate temperature prescription. Recently, a recent review study has recommended for an effective treatment by considering the individualized dialysate temperature especially for the patients who suffer from persistent IDH [45]. Majority of recent studies have utilized 0.5°C less than body core temperature (BT-5°C) as individualized dialysate temperature [46]–[50]. These studies have reported a significant improvement in hemodynamic stability compared to fixed dialysate temperature. In a recent study with larger sample and longer duration, the individualized dialysate temperature has reported on the reduction of IDH frequency with no substantial effect in dialysis adequacy in order to implement in real-world HD population [46]. But, almost all patients have felt cold symptoms with a 5% drop out rate. Moreover, Eldehni et al., and Jefferies et al., have

demonstrated that the individualized dialysate temperature improves the preservation of brain white matter and abrogates complications with effective hemodynamic stabilization method [47], [50]. Moreover, a study with hypertension prone patients with improved stability in terms of blood pressure and heart rate were observed with $BT-5^{\circ}C$ compared to $37^{\circ}C$ (standard) and $BT+0.5^{\circ}C$ as dialysate temperatures [48]. In contrary, there was no effect in cardiac structure and functions during individualized dialysate temperature control dialysis compared to standard dialysis [49]. In fact, these studies have improved the stability without any additional cost for therapy. However, more research is required to define the precise temperature at which maximum benefit is achieved without an increase in symptoms. It is also necessary to examine the effect of optimal dialysate temperature on long-term patient outcomes, as improving dialysis stability and reducing IDH episodes.

From these studies, hemodynamic stability can be improved when body temperature is prevented from rising during treatment and when a large fraction of thermal energy produced in the patients should be removed from the body through extracorporeal circulation. When concerned about optimal dialysate temperature, it is probably best to prevent an increase in body temperature during HD allowing increased patient's comfort and reduced complications [5], [17]. In another perspective, the maintenance of stable body temperature could be possible through a continuous manual adjustment in dialysate temperature and monitoring the effect of arterial and venous temperature during HD treatment. Although this can be achieved, it is impractical because it would require significant staff intervention for accurate and fast control of the dialysate temperature [33]. Therefore, an automated control of dialysate temperature

could be achieved using biofeedback control system through HD machine technical development.

2.3 Technological advancements in Hemodialysis machines to prevent complications

Technology developed over many years enabled HD machines to meet the needs of patients and minimize the amount of complications, especially IDH [51]. Mainly, early recognition and rectification of life-threatening complications save lives. Even though some complications may not threaten the patients' life but eventually weaken the quality of life of the patients. Traditionally, HD treatment follows the same prescription with the assumption of clinical and laboratory outcomes unless any adverse events such as IDH occurs during treatment [52]. As a result, these actions would discomfort the patients by interrupting the treatment, which eventually affects the dialysis consequences. To counteract, the technological developments have made possible the detection of subclinical predictors of hemodynamic instability, for example relative blood volume variations, in order to prevent hypotension. With instantaneous measurement of these specific parameters during HD, actions can be implemented to correct the monitored parameters towards a desired target, with the aim of preventing hypotension. These actions are automated and regulated by a closed feedback loop, known by biofeedback control system. At the present time, most common biofeedback control systems for different parameters are: relative blood volume, arterial pressure, blood temperature, and plasma conductivity as shown in Figure 2.3.

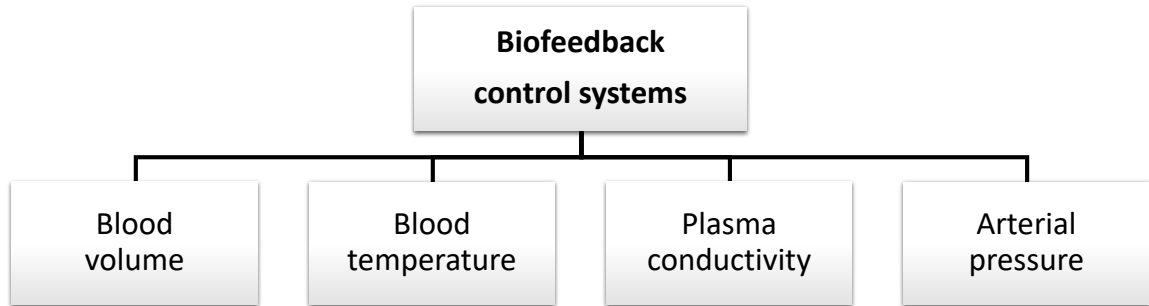


Figure 2.3 – Common biofeedback control systems for HD machine.

Currently, only two commercially blood volume biofeedback devices are available: Hemocontrol (Gambro Lundia, Sweden) and the Blood Volume Monitor (BVM) (Fresenius, Germany) systems. Hemocontrol blood volume management system is based on an automatic multiple input multiple output (MIMO) controller to force the blood volume reduction along a pre-defined trajectory towards a pre-defined target (ideal curve) of blood reduction as shown in Figure 2.4 [53]. The instantaneous control employing PID control technique has resulted in a smoother relative blood volume reduction by avoiding the irregularities in blood volume reduction. The main aim of the Hemocontrol system is to achieve the same sodium and water balance according to traditional approach, while enhancing the hemodynamic tolerability by profiling the ultrafiltration (UF) rate and dialysate conductivity. In fact, when the blood volume approaches the lower acceptable value for a given patient, UF is reduced or stopped as the dialysis conductivity increases [52]. Several studies have reported on the improvement in hemodynamic stability and myocardial episodes with improved efficiency during HD compared to standard dialysis [54]–[56].

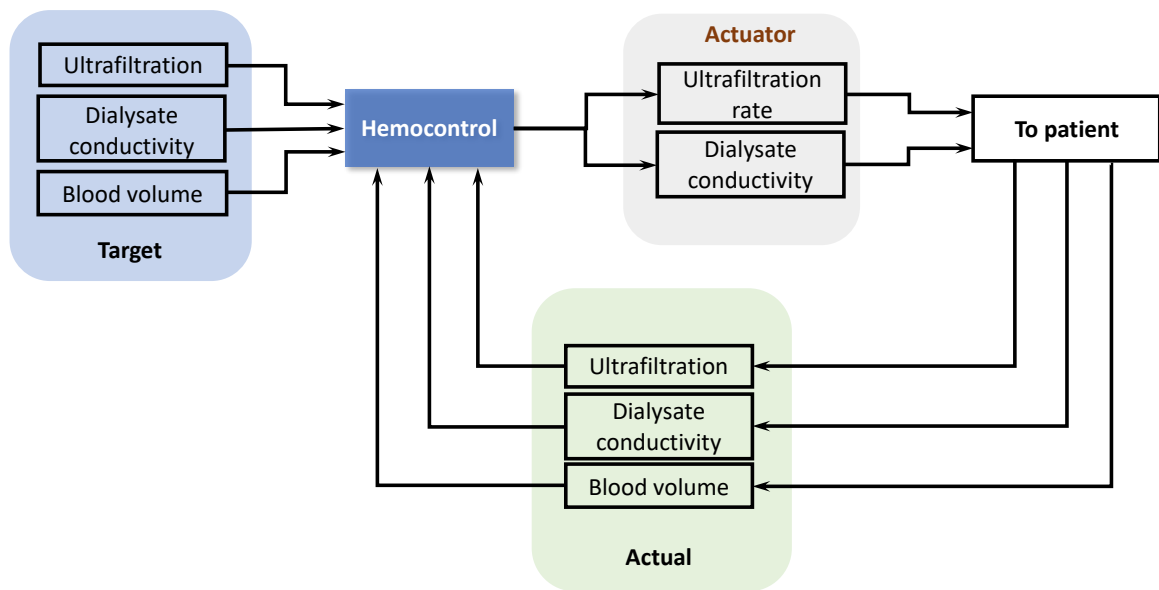


Figure 2.4 – Block representation of Hemocontrol biofeedback control system [52].

Another physiological biofeedback control, BVM deals with the critical relative blood volume instead of tracking an optimal curve to reach a final blood volume [57]. This system works with the pre-defined algorithm that changes UF with respect to the critical relative blood volume. However, the effectivity of BVM is due to the non-invasive ultrasonic blood volume sensor with an accuracy of better than 2%, which works by the principle of speed of protein concentration [58]. Whereas, the Hemocontrol utilizes an optical sensor for the measurement of blood volume [52]. Unlike Hemocontrol, the system does not include control of dialysate conductivity. In a review study, BVM have improved the treatment to prevent IDH and other severe events especially for hypotension-prone patients compared with conventional HD [59], [60].

Many researchers have been designing an optimum control system to reduce the hypotension complication during dialysis. In recent study, a MIMO system-based linear parameter varying model was proposed with dialysate conductivity and UF rate as control input to dialysis machine while keeping blood pressure as well as control inputs within bounds [61]. This system was tested on a small number of patients and future

studies based on implementing the designed control system in a larger population with repeated measure would be needed to better explain the performance of the system in maintaining the hemodynamic stability of patients undergoing HD. These simulation result shows with high accuracy and the implementation of this design could be a positive step toward developing new technologies capable of preventing dialysis-induced complications.

Even though, blood volume biofeedback control system employed to avoid the risk of IDH, it is not extensively used as a direct control of blood pressure. To account for this, an arterial blood pressure biofeedback system was proposed with blood pressure as input parameter [62]. The arterial blood pressure stabilization (ABPS) measures the blood pressure and its trend using an automated cuff inflating pressure by oscillometric manometer at every 5 minutes. The proposed fuzzy logic control (FLC) allows the modulation of UF rate according to the blood pressure as input as shown in Figure 2.5. However, the system is effective in reducing IDH episodes in about 40% for hypotension prone patients, which could be linked to prevention of large reduction in blood volume [21], [62].

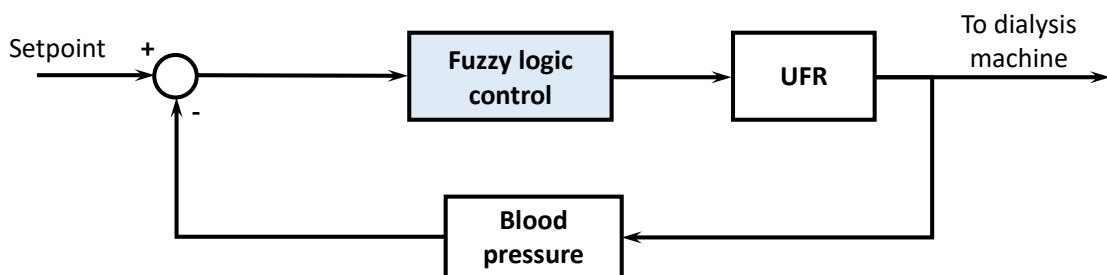


Figure 2.5 – Block representation of arterial pressure biofeedback system [62].

The plasma conductivity (PC) biofeedback control system was designed to control the dialysate sodium concentration to account for the changes in plasma concentration

of patients during the treatment [53]. The system was aimed to reduce the morbidity related to sodium balance impairment of patients. The study reported an insignificant difference between blood volume or PC controlled in the effect of sodium homeostasis [63]. An automatic model was then developed which allows computation of the amount of sodium removed during HD and makes it possible to predict the PC changes and plasma osmolality changes induced by the sodium concentration profile in the dialysate and given UF profile [64]. This model was tested in a non-controlled multi-centre study on 55 patients with intradialytic hypotension. The results of this study showed that adaptive-profiled dialysis treatment significantly improved intradialytic blood pressure, decreased the incidence of hypotensive events and disequilibrium symptoms compared with standard treatment. Also, it did not induce symptoms of sodium/water overload.

These biofeedback control systems were designed with the intention to reduce the occurrence of hypotensive episodes during HD. Monitoring tools can only help in the early detection of complication, which can warn the dialysis staff to take necessary actions to stabilize the patients. However, it would be more beneficial to develop control systems that use these monitoring tools to automatically implement these preventive actions. Hence, advances in dialysis technology can help to minimize the problem of intradialytic hypotension to a great extent. And this strengthens the possibility of an effective temperature biofeedback control system to account for the problem stated. Furthermore, an in-depth research on technical side of HD machine and modules would be beneficial for improving the dialysis efficiency.

2.4 Temperature control system

Until now, there has been only one commercially available device built into a HD machine that was able to measure and control the body temperature and thermal balance of the extracorporeal circuit - Blood Temperature Monitor (BTM) by Fresenius, Germany [38], [57]. This control module is equipped with sensors to measure the venous and arterial temperature as shown in Figure 2.6. Then, the required dialysate temperature is calculated on the basis of results from temperature measurements, actual blood flow and several other constraints in order to change the temperature in the patient effectively. Even if the actual body temperature is disturbed by external disturbances not accounted for by the control system such as vasoconstriction, increased metabolic rate, the information provided by the actual output allows to compensate for such effects [19]. Thus, the control of BTM regulates the temperature of the dialysate using the existing heater to compensate for increase or decrease in body temperature. The BTM can be operated in two control modes - T-control and E-control [65].



Figure 2.6 –BTM module with temperature sensor heads [65].

In E-control (thermoneutral) mode, it is possible to control the thermal energy supply to and from the extracorporeal circulation. If a neutral temperature balance is required, thermal energy is neither supplied nor removed. This means that the measured temperatures of arterial and venous end of the extracorporeal circulation should be identical. In order to realize this, the dialysis machine unceasingly regulates the temperature of dialysate to the temperature recorded by the sensors. As the arterial temperature increases during dialysis, it is not possible to control body temperature using this method.

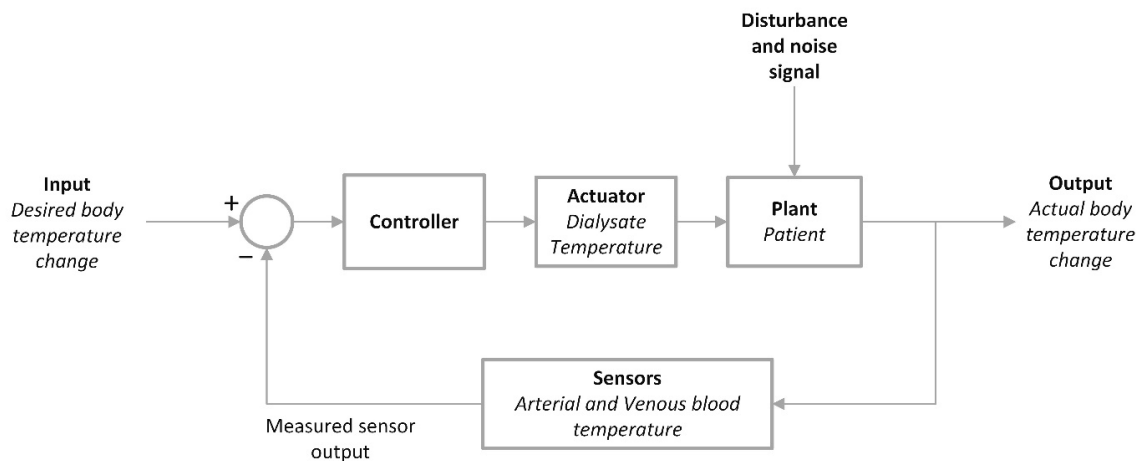


Figure 2.7 – Structure of closed loop BTM in T-control mode [19].

In clinical practice, thermoneutral (E-control) is generally less important than isothermal (T-control) with the BTM [65]. The structure of closed loop temperature control using T-control mode is shown in Figure 2.7. This control mode measures arterial line temperature continuously using sensor heads and adjusts body temperature to the level set by the user. Normally, the body temperature is set at the value measured at the beginning of dialysis. This controller uses the error signal between the desired and actual change in body temperature to actuate a change in dialysate temperature which changes the venous blood temperature returning to the patient. In addition, T-control mode

requires the prescription of an hourly change in body temperature (in °C/hr). This means that the control of constant body temperature needs to be set as $\pm 0.00^{\circ}\text{C/hr}$. This is why T-control mode is considered as a physiologic feedback control system since the body temperature is a physiologic variable.

A number of studies have confirmed that BTM improves the hemodynamic stability and Table 2.1 shows a summary of studies done on this phenomenon. It can be seen that several studies have shown the importance of active control of body temperature in terms of hemodynamic stability during the treatment. In a European randomized trial, 95 hypotension prone patients have reported about 50% reduction in recurrence of hypotension episodes during HD, whereas the adequacy of HD was not affected [66]. Apart from reduction of complications, a recent study have reported none of the patients suffered from IDH with the combination of BVM and BTM control modules [67]. It must be emphasized that there were no cold symptoms or shivering with the isothermal (T-control) dialysis compared to cool dialysate settings [28]. In accordance with other studies, the mean thermal energy of -220kJ has been removed from the extracorporeal circuit in order to maintain a stable body temperature [18], [28], [68], [69]. While, the thermoneutral dialysis (E-control) resulted in lesser energy removal, which resulted in an increase in body temperature during the treatment [18], [28], [66], [68]. It can be seen that the active control of body temperature has the high potential to reduce the IDH episodes for hypotension prone patients without causing cold discomfort or morbidity. However, long-term and large sample size with follow up perspective validation are still lacking.

Table 2.1 – Summary of HD outcomes with the utilization of BTM.

Study	Number of patients	Intervention	Outcome
Maggoire et al., 2002 [66]	95	T-control E-control	T-control almost halved frequency of IDH compared to E-control without affecting dialysis efficiency. However, active control of body temperature significantly improves tolerance in hypotension prone patients.
Schneditz et al., 2002[69]	12	T-control	Stable body temperature maintenance during heat accumulation due to UF induced blood volume reduction.
Van der Sande et al., 2005 [18]	13	T-control E-control	Fluid removal has an effect in thermal variables.
Ramos et al., 2007 [70]	9	Fixed T_d - 36°C BTM - T-control	Active control of body temperature increases the intradialytic tolerance in hypotension prone patients
Horáček et al., 2007 [68]	13	T-control E-control	T-control treatment has maintained stable body temperature compared to E-control.
Van der Sande et al., 2009 [28]	14	Individualized T_d (T-0.5°C) T-control E-control	Individualized cooling reduced IDH episodes compared to T-control, but cooling resulted in cold discomfort for patients.
Dhondt et al., 2010 [71]	10	Constant T_d – 36.3°C and 37.6°C T-control	Blood temperature remained stable during BTM T-control
Cheyron et al., 2013 [72]	74	T_d - 36°C BVM BVM and BTM (T-control)	No significant impact on actively controlled body temperature in ICU patients.
Saxena et al., 2015 [67]	40	BVM and BTM (T-control)	None of the patients suffered from IDH during this study

The crucial part of the body temperature control is the accurate evaluation of pre-dialytic pathophysiological body temperature [73]. The BTM would possibly be unable to set the target temperature in adverse patient's conditions such as fever, hyperthermia, to maintain constant body temperature. However, the dialysate temperature would remain within a physiological range between 35°C - 38°C. In addition, several studies have utilized the arterial and venous temperature sensor heads in BTM in order to monitor the readings for various fixed dialysate temperatures [44], [74]. This shows the importance of temperature sensor in HD machine as it is not currently being monitored during the treatment.

Apart from body temperature control and temperature measurement, BTM allows to estimate the recirculation. The recirculation is caused when the purified venous blood passes through the fistula and re-enters the extracorporeal circulation, which would affect the adequacy and reducing the survival rates [75]. The recirculation is measured by a temperature bolus produced by the temperature change in dialysate [65]. With the help of bolus magnitudes of arterial and venous temperature, recirculation ratio was calculated. Interestingly, measurement of BTM validated the results with another ultrasound dilution technique with regard to recirculation [76].

From these literatures, it can be deduced that the control of dialysate temperature is vital for hemodynamic stability of HD patients. Moreover, BTM utilizes the instantaneous control with existing heater in the dialysate proportioning system. Even with superior performance, it is not well-renowned in today's society, especially in developing countries. This could be due to its price and interface with other brands of HD machine. To account for this, studies have been emerging recently on several design of

dialysate proportioning methods and control methods for the benefit of body temperature control. A preliminary design of a dialysate proportioning system based on balance chamber model was proposed [77]. Through simulation, model based predictive control have been used to control the dialysate temperature for the proposed model and in-depth work is progressing. In addition, another dialysate proportioning system with three chambers comprises of input water collector, heater and output water collector was proposed for the benefit of temperature control [78]. The dialysate temperature is controlled with multiple sensors and actuators to result in effective dialysate temperature. In comparison with these two studies, dialysate proportioning methods have been modified, but the detailed design and processes have not been published. Yet, the results on the performance of this controller was lacking and could not be compared with BTM. In another aspect, a thermal energy model of extracorporeal circuit was proposed with the intention to simulate the venous and arterial temperature measurements by estimating thermal energy transfer [79]. The model was aimed to guarantee a constant core temperature during the treatment.

From the above studies, it can be seen that the idea of active regulation of dialysate temperature according to the patient's body temperature is much needed for our current society. Consequently, the improved design in dialysate proportioning system would enable the machine to actively regulate the dialysate temperature according to the target temperature even if there are any external disturbances during the treatment. Therefore, future research in the field of instantaneous dialysate temperature controller need to show a reduction in morbidity and mortality at the same time with a reduced treatment cost.

2.5 Implementation of fuzzy logic controllers in medical applications

Conventional controller will not perform well due to incomplete and imprecise knowledge of the system. Human brain has an imprecise way of reasoning and thus has a high adaptive control approach. It does not reason as computers do. Computers reason in a clear statement that uses true or false (0 or 1). Thus, a controller with human like reasoning is desired for increasing the probability of success. This leads to the selection of FLC. The idea of fuzzy logic was invented by Professor L.A. Zadeh in 1965 [80]. Also, fuzzy logic techniques have been widely applied in all aspects in today's society.

A FLC is based on fuzzy logic and constitutes a way of converting a linguistic control strategy to an automatic one, by generating a rule base that controls the behaviour of the system. A basic FLC can be decomposed into four basic components: the fuzzification unit, knowledge base (rule base), inference engine (decision making unit) and defuzzification unit as shown in Figure 2.8. Fuzzification converts our crisp input (velocity of fluid is 2 m/s) into linguistic data (velocity of fluid is too slow). Then the fuzzy rule base defines some rules in the form of IF-THEN logic on the information provided by fuzzification. It offers flexibility in system design and implementation, since its implementation uses rule base instead of sophisticated differential equations. The inference engine provides us with appropriate coherence and analysis for an output simulation. Defuzzification gives us an output on the basis of defined membership function and rules. The technology provides room for graphical user interface which makes it understandable by people who do not have process control backgrounds. Also, this control system has the ability to automatically and smoothly adjust the priorities of

a number of controlled variables. These facts help to achieve a stable process for a long period of time without a need for intervention.

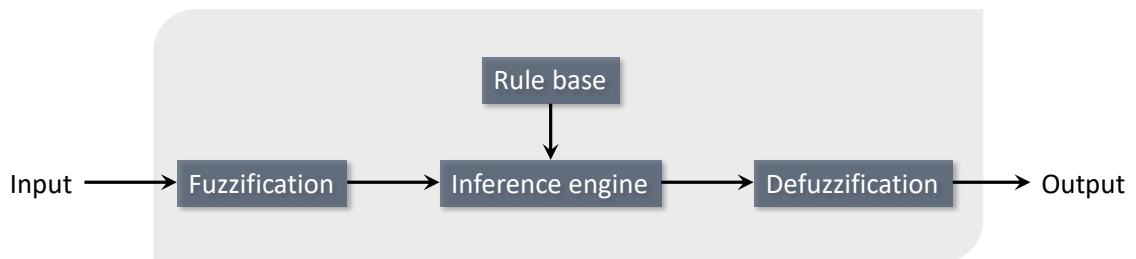


Figure 2.8 – Basic structure of FLC with four basic components [81].

The use of Artificial Intelligence (AI) techniques has now highly increased, especially in the field of medicine [82], [83]. It offers to design such system that allows building intelligent models for both predicting patients' response in treatment and determining prediction of illness risk. The use of AI techniques such as fuzzy logic, artificial neural network, genetic algorithms, artificial immune systems and others has been developed by many researchers. Fuzzy logic approach uses a logic and decision mechanism, which does not have certain boundaries like human logic, and it does not require complete model knowledge as in the other well-known control systems. The number of research contributions in fuzzy logic is rising daily and is growing at an increasing rate [84]. The fuzzy system tries to improve the daily activities of doctors and nurses in a hospital and also helps in diagnosis of various diseases like cancer, heart disease, asthma, diabetes etc. Thus, by making use of medical expert's knowledge and uncertain sensual data, fuzzy systems are being developed currently.

Fuzzy logic plays an important role in some medical areas and its realization is on the rising trend. The use of fuzzy logic in medical field is very diverse, especially in several applications such as diagnosis, surgery and rehabilitation. A review study has shown the application of fuzzy logic in medical image processing and surgery support system [85].

The analysis of the results indicated the controller performance in fuzzy provides more economical, comfortable, reliable and consistent implementation than traditional control systems. Recent studies have reported on the combination of FLC with other control methods such as sliding control and PID control were proposed for the robotic surgery applications [86], [87]. The experimental results of FLC have improved the performance in terms of error and overshoot with a great surgical safety, when compared to conventional control methods. In addition, multiple simulation studies have reported on FLC on robotic surgery models, emphasizing on the potential for medical applications for the future [88], [89]. Apart from robotic surgery application, fuzzy logic designs have been proposed for the control of certain biomedical equipment such as ventilator, controlling of anaesthesia during operation and pacemaker system in order to improve the patient's quality of life [90]–[92]. However, majority of fuzzy logic applications were in the field of disease diagnosis, which provided a solution to enhance the accuracy and precision of medical diagnosis [83], [93], [94]. The results showed a possibility to design more advance diagnosis system to help in the area like drugs prescription, disease diagnosis etc. especially for under-developed countries. Even though fuzzy logic was introduced in 1960s, yet the realization of fuzzy logic is far from over in the current society.

The fuzzy logic shows the possibility to implement a control system in favour for the kidney patients. A fuzzy logic model was proposed for the kidney transplantation patients [95]. This model showed a better accuracy and raised confidence of medical doctors for transplantation. Another fuzzy logic diagnosis system to evaluate the arteriovenous shunt stenosis for HD patents has found a greater efficiency in finding degree of stenosis [96]. Furthermore, recent multiple studies from the same author

published on the development of FLC in peristaltic pump [97]–[99]. Studies have proposed various types of fuzzy logic design with the intention to improve the patient treatment quality. This was achieved by considering the overall system fluid balance through an accurate control of peristaltic pumps. Studies are progressing in order to evaluate and validate the promising controller using a real HD machine [97].

In terms of hemodynamic stability of HD patients, a FLC system utilizing blood pressure and UF rate as control variables was implemented for automatic blood pressure stabilization (ABPS) system [62]. Several tests have been carried out and it showed a remarkable decrease in hypotension episodes nearly by 40%. Another fuzzy controller was proposed for HD machine in order to maintain hemodynamic stability during the treatment [100]. This proposed system uses MIMO fuzzy controller and the results of simulations illustrate that it can improve the stability of a patient's hemodynamic condition. Yet, the realization of this simulation is much needed for this generation. Also, fuzzy control showed us a potential not only for diagnosis but also for controlling the hemodynamic stability of the dialysis patients. Hence, more research on the fuzzy implementation on HD machine would benefit the dialysis patients in many ways.

DESIGN AND METHODOLOGY

This chapter describes the design and methodology of the research study and prototype development. The research design adopted is a combination of descriptive and experimental research design. This means, the research describes the problem of heat transfer during HD rather than focusing on the reason behind the heat transfer. While, the experimental research design was utilized for the development and validation to account to the problem. The study consists of approach to the problem, prototype design and development while a rigor investigation to test the hypothesis were applied. The proposed research consists of sequential process as shown in Figure 3.1. The dotted line denotes the troubleshooting process. The chapter covers the sections explaining the hypothesis, simulation analysis, design concept, prototype development and assembly, modelling, testing and evaluation.

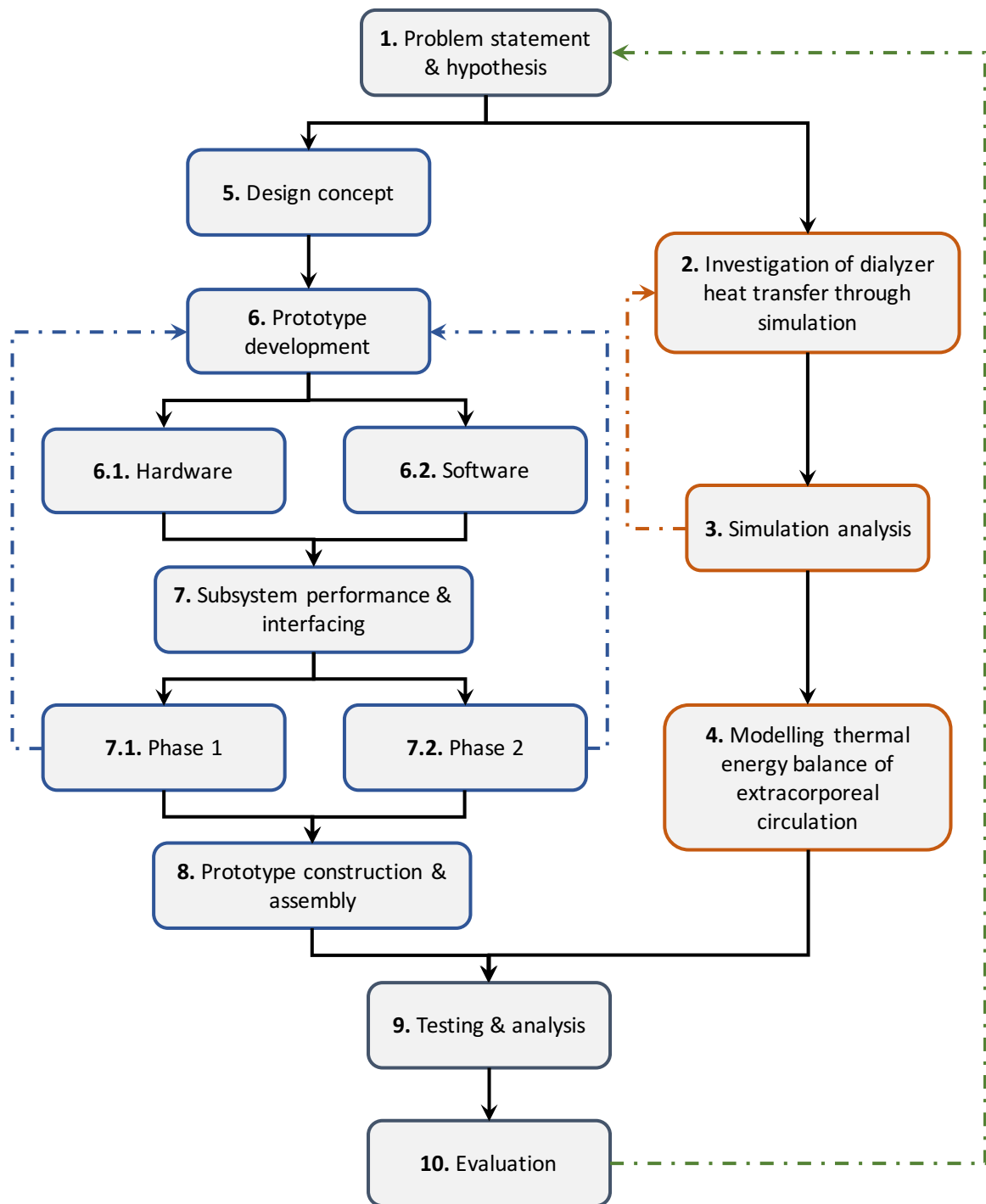


Figure 3.1 - Iterative design phases of dialysate temperature control module (DTCM)

3.1 Problem statement & hypothesis

The initial phase of the research consists of literature reviews and accounts of previous researches to determine the advancements in hemodialysis (HD) machine technology. Precisely, the characteristics of HD machine controllers and identify the key

parameters and techniques to improve its treatment efficiency. A review of control system in medical applications and its implementation were also carried out in order to develop a cost-effective prototype. The important points concerning overall development of a prototype were based on certain parameters such as being cost-effective, modular design, improved efficiency, reduced complication, individualized control. This method employs to clarify the theoretical meaning of the findings and hypothesis development for further studies.

Based on literature review, the ultimate goal of this research is to develop an individualized dialysate temperature control module for HD machine at the appropriate percent contribution of the mentioned qualities of a prototype. This would enable the machine to control the body core temperature efficiently, leading to a better patient's quality of life with negligible complications during the treatment.

3.2 Investigation of dialyzer heat transfer through simulation

In this section, the effect of heat transfer taking place between blood and dialysate in a dialyzer were investigated with an aid of simulation. Even though, there are significant number of simulation studies based on dialyzer design, clearance, flow distribution and other performance parameters, yet a detailed analysis on the heat transfer through dialyzer membrane remains unclear [101]–[103]. Therefore, COMSOL Multiphysics® 5.0 was used for developing and simulating the model of a dialyzer membrane. COMSOL Multiphysics® is a finite element method for the modelling and simulation software for various engineering applications particularly when there are different physical phenomena linked together in a single process.

A high-flux dialyzer membrane namely Polyflux™ 210H (Gambro, Hechingen, Germany) was investigated using COMSOL Multiphysics®. The external housing contains a bundle of approx. 12000 hollow fibers with each fiber measures 270mm in length as shown in Figure 3.2. It has an overall surface area of 2.1m². The inner diameter of the fiber is 200µm with a wall thickness of 45µm. The material of fibers is Polyamix which is a blend of polyarylethersulfone, polyvinylpyrrolidone, and polyamide. Then, the membrane was modelled by following the dimensions of actual Polyflux™ 210H membrane [104], [105]. The detailed modelling technique is mentioned in Chapter 4.

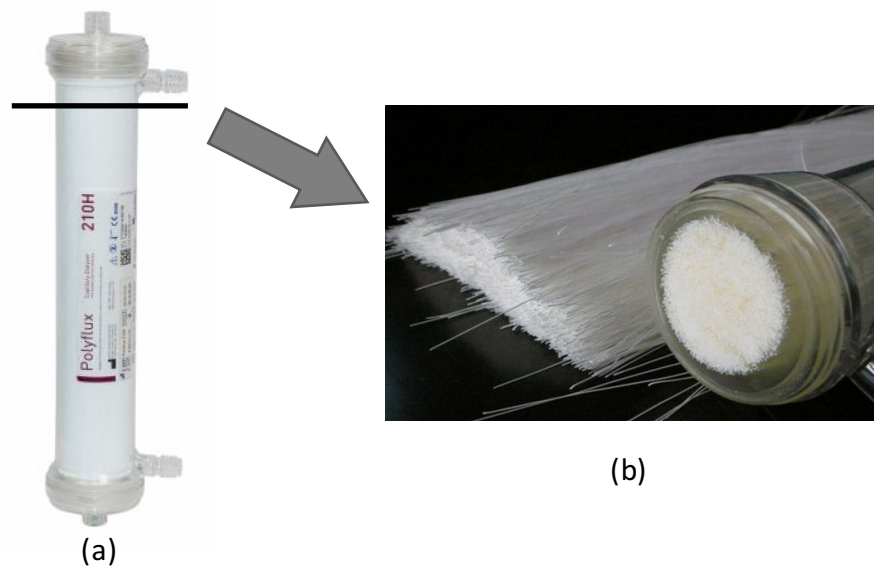


Figure 3.2 - (a) An overall structure of Polyflux™ 210H dialyzer and (b) cross sectional view of bundled hollow fibers inside the housing.

3.3 Simulation analysis

The heat transfer taking place between blood and dialysate through dialyzer membrane was analysed using COMSOL Multiphysics® post-processing tools. In other words, the temperature profile of blood and dialysate at the both ends of dialyzer were examined under various conditions. Primarily, the effect of various physiological dialysate temperatures, blood temperatures, blood flow rates, and dialysate flow rates

were studied. In order to solve this model, a stationary study which implies COMSOL Multiphysics® will use a stationary solver to compute the solution. In certain analysis, the parametric sweep tool was used to repeat simulations for a variety of different values of physiological parameters. Subsequently, the analysis would identify the heat loss/gain during HD and demonstrate the need for body temperature control. In addition, the temperature profile through dialyzer would benefit the thermal energy balance modelling in HD extracorporeal circuit. This method is employed to investigate the heat transfer in dialyzer and the early design concept development.

3.4 Modelling thermal energy balance of extracorporeal circulation

In addition to the heat transfer in dialyzer, the extracorporeal circulation in HD is also expected to affect the thermal energy loss due to certain factors such as ambient temperature, tubing material, length of tubing, and so on. Therefore, it is necessary to consider the extracorporeal thermal energy transfer along with heat transfer in dialyzer to design an overall thermal energy transfer model for extracorporeal circulation. This method allows to estimate the venous and arterial temperature during the process. As this study emphasizes on the in-vitro evaluation of temperature control, the blood side temperatures can be predicted based on various dialysate temperatures.

Figure 3.3 illustrates the mechanism of thermal energy transfer in HD extracorporeal circulation. The thermal energy transfer between the patient and HD system was modelled using energy conservation equation and bio-heat transfer equation as mentioned in a recent study [106]. Subsequently, the energy transfer was analysed in three different sections; that being the arterial side, dialyzer and venous side. The arterial and venous side energy transfer were analysed using the proposed model, while dialyzer

energy transfer was based on COMSOL simulation study. The combination of the three sections determines the overall thermal energy transfer in extracorporeal circuit, which is justified briefly in section 6.2. Thereby, arterial and venous temperature profile can be evaluated for various physiological tests to evaluate the dialysate temperature controller module (DTCM).

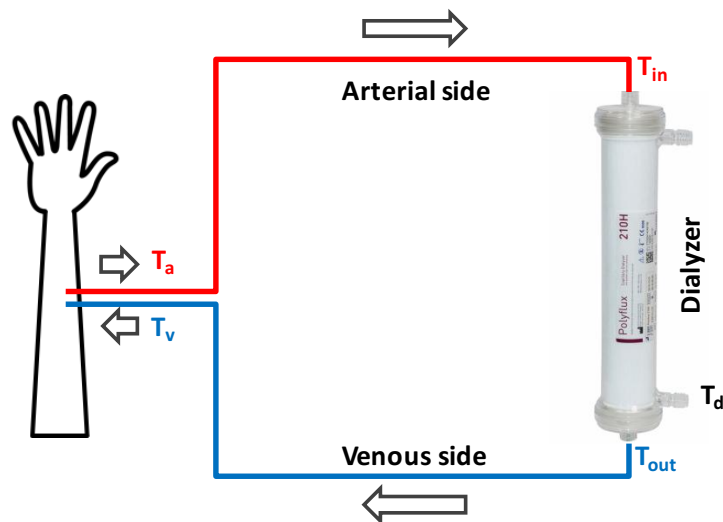


Figure 3.3 – Thermal energy transfer between patient and HD system

3.5 Design concept

The design concept is considered as an initial activity that generates a 'materialised' solution for a 'functional' problem. Thus, evolution of designs was analysed in terms of logic, thinking and reasoning in order to achieve the target, which shows that designing is a non-deterministic process. Decisively, an initial conceptual model of DTCM has been proposed with the intention to develop an effective temperature controller.

The proposed model consists of two dialysate tanks at constant temperature of 35°C and 37°C has been proposed as shown in Figure 3.4. As the dialysate temperature range is narrow (35°C - 37°C), the efficient way to control the temperature is by varying the flow rates using peristaltic pumps. Contrary, the control of temperature can also be

made possible by implementing heating elements through the tubing, which would be ineffective in active regulation. However, the design concept is similar to the concept of heat exchanger with two different inlet temperatures, response time and accuracy of fluid temperature was found to be superior compared to control using heating elements [107]–[109]. Hence, the control of peristaltic pumps by varying flow rates would be superior to conventional heaters for this application. Additionally, the proposed model was designed as an external module that can interface in existing HD machines. Therefore, the required dialysate temperature can be achieved using a robust controller, which controls body temperature in HD by actively regulating the two dialysate flow rates effectively.

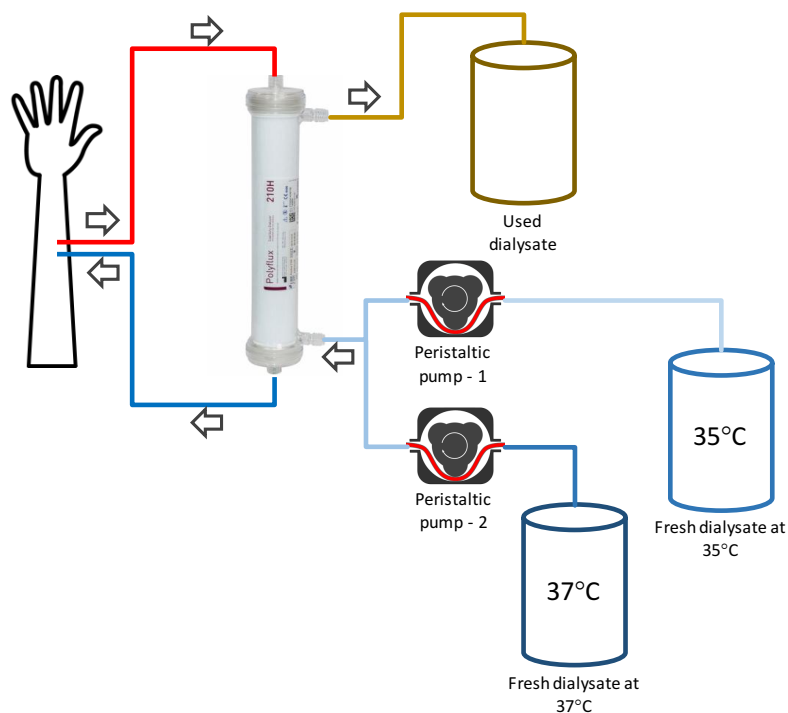


Figure 3.4 - Proposed design concept of DTCM

3.6 Prototype development

In this section, the proposed design concept has been applied for the development of DTCM prototype. Later, prototype would help to get an “actual feel” of

the system and a better understanding of desired system requirements. This method involves the expert knowledge from the dialysis industry for essential understanding on existing dialysis machine technology. The necessary information about dialysate proportioning method and the technical aspects of existing hemodialysis machines were provided by the leading healthcare industry – Baxter Healthcare (Malaysia) Sdn Bhd. Such training influences on the modification of dialysate proportioning methods for the benefit of individualized temperature control as shown in Figure 3.5. However, this is to develop an initial prototype with a novel temperature control method in a dialysate proportioning system without considering certain processes such as mixing of salts, dialysate conductivity, pH value of dialysate, water deaeration etc. In contrary, the inclusion of certain processes in the DTCM module increases the complexity as it would be difficult to monitor the dialysate parameters such as flow rate, conductivity, pressure, etc., along with the blood side parameters. Therefore, the fresh dialysate fluid will enter to the proposed prototype only after several stages of preparation. This would reduce the dialysate heat loss as it will flow directly to dialyzer without the need for other processes.

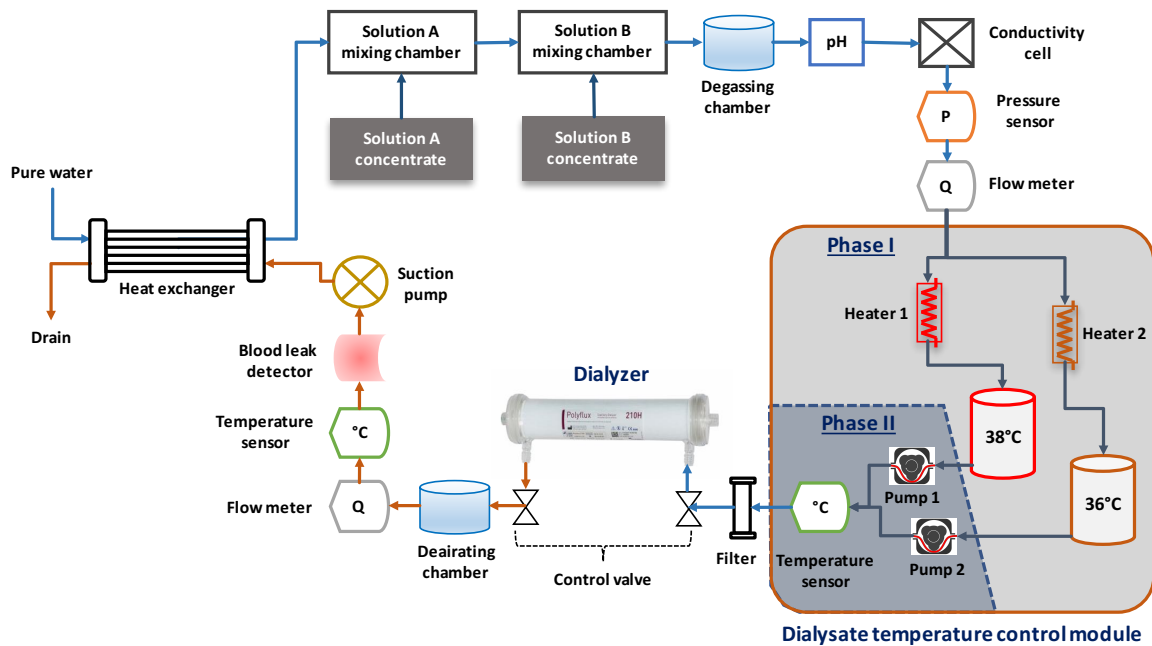


Figure 3.5 - Overview of a Baxter's dialysate circuit including proposed DTCM.

The DTCM prototype comprises of two phases of development as shown in Figure 3.5. The initial temperature of dialysate before heating is approximately 30°C as it passes through a heat exchanger. Although, both temperatures of tank were revised to 36°C and 38°C respectively by considering the heat loss along the tubing. Thus, the development of Phase 1 allows the dialysate to increase its temperature up to 6°C and 8°C using heater and stores in respective tanks. This is followed by Phase 2, that alters the flow rates of two temperatures to achieve the desired temperature.

A prototype development consists of two major elements - hardware and software developments. The hardware development explains the detailed design including component selection and design overview. While, the software development explains the framework that is used to develop a prototype to control the temperature. In the following sections, the hardware and software elements implemented in the development of the prototype will be detailed.

3.6.1 Hardware

This section involves the detailed structure of prototype and hardware elements used in obtaining the optimal performance of dialysate temperature controller according to the HD parameter requirements. The prototype development was based on a number of open source hardware, so that the cost of building the system could be kept low. The hardware elements such as microcontrollers, sensors and actuators for phase 1 and 2 are explained in the following sections.

3.6.1.1 Phase 1

In this section, the structure of this model is composed of five major components, which are Arduino UNO R3, heater, pump, float switch and temperature sensor as shown in Figure 3.6.

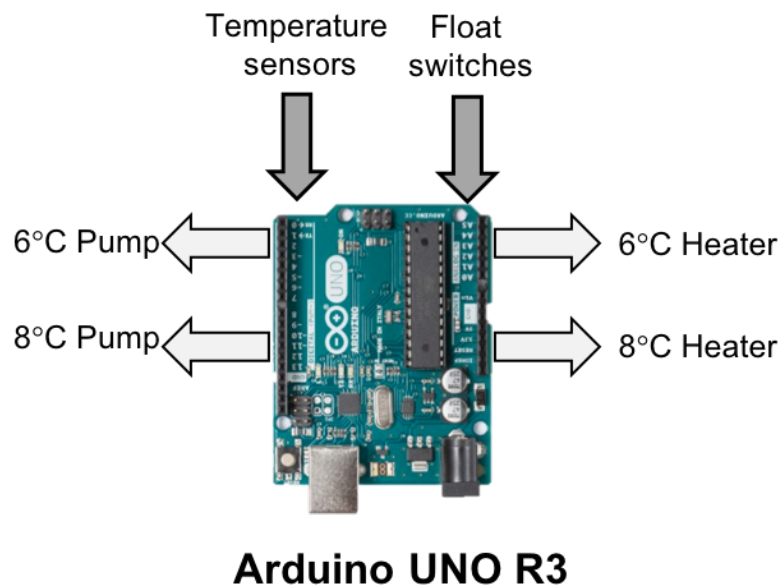


Figure 3.6 – Hardware architecture of prototype for phase 1.

Arduino UNO R3

Arduino UNO plays a major role in controlling sensors and actuators in phase 1 prototype development. This microcontroller is very common for its simplicity, low cost

and open source prototyping platform. The significant features of this microcontroller include six analogue inputs, 14 digital I/O pins, 3.3V and 5V power supply ports. Arduino UNO communicates with the host computer through serial communication with USB. It can be easily programmed using C language using their Arduino IDE programming environment.

Pump

In this phase, two pumps are used to transfer dialysate fluid from its proportioning stages to respective heated storage tanks. The pump has an outlet and inlet with a 6mm diameter which allows the required flow for the system. The fluid flows at constant flow rate of 250 ml/min and then stores in the respective tanks. It requires 5V DC supply and low starting current. Moreover, the pump's motor runs at very low noise. Figure 3.7 shows the image of the pump used in this prototype.



Figure 3.7 – Image of DC pump used.

Heater

Dialysate temperature controller prototype has two heaters to increase the temperatures up to 6°C and 8°C. The flow through heater type was chosen, which heats up the moving fluid through its tubing. This type of heater is prominent in HD machine due to its efficiency in providing heat that regulates the liquid temperature. Thus, flow

through heaters for this prototype were constructed using Kanthal A1 resistance wire and glass tube. Kanthal A1 wire was used to coil around both glass tubes at different resistances to be heated by using DC power supply. The 24 AWG Kanthal A1 wire was chosen, which has resistance of $0.0071 \Omega/\text{mm}$. In addition, the wire was twisted in order to supply more current and thereby more power output. The resistance and power for both heaters were tabulated in Table 3.1.

Table 3.1 – Kanthal A1 wire specification for heaters

Characteristics	Heater 1 (38°C)	Heater 2 (36°C)
Total wire length (mm)	910	735
Total resistance (Ω)	6.46	5.22
Maximum Voltage (V)	31.5	31.7
Maximum Power output (W)	154	192

The heaters were isolated with a layer of polyamide tape and Teflon tape. This would help to withstand temperatures and provides insulation. Figure 3.8 shows the image of flow through heater used in this prototype.

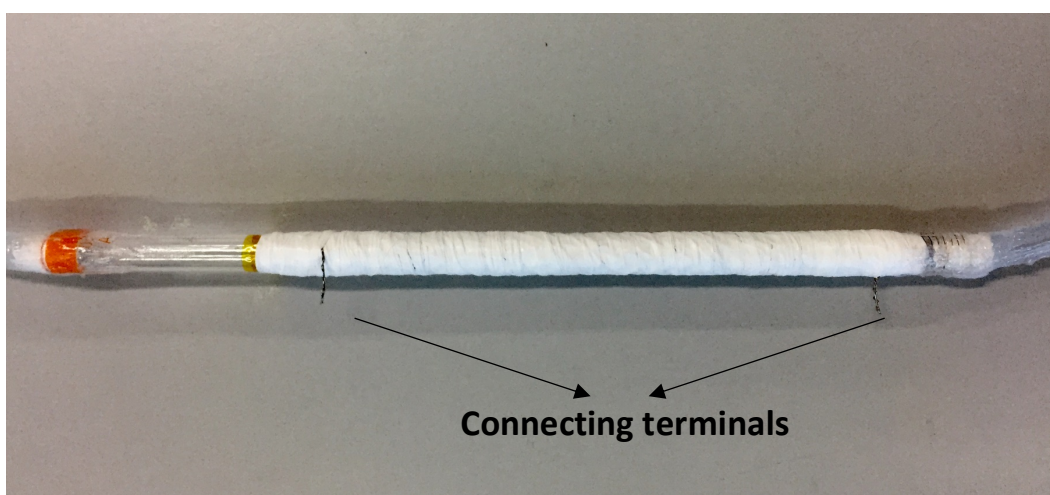


Figure 3.8 – Image of flow through heater with connecting terminals.

Temperature sensor

Temperature sensors were used to sense the temperature of fluid in the storage tanks. The DS18B20 temperature sensor from Maxim integrated was chosen due to its high accuracy and waterproof. It communicates over a 1-wire bus, which requires only data line for communication with a central microcontroller even when there are multiple DS18B20 temperature sensors. In addition, it can able to convert the temperature to 12-bit digital measurements in 750ms, which implies fast response time. Figure 3.9 shows the image of waterproof DS18B20 temperature sensor used in this prototype.



Figure 3.9 – Image of DS18B20 temperature sensor used.

Float switch

In this phase, float switch is used to detect the dialysate fluid level in the storage tank. This is to prevent the overflowing of dialysate fluid by sending a signal to a microcontroller when it reaches a specified level. The float switch contains hermetical sealed reed switch in the stem and a permanent magnet in the float as shown in Figure 3.10. It utilizes a magnetic reed switch to open or close the circuit. Therefore, the signal from float switch can be utilized for control of pumps.



Figure 3.10 – Image of float switch used.

3.6.1.2 Phase 2

In this section, the structure of this model composed of four major components, which are Raspberry Pi 3, stepper driver, peristaltic pump, and temperature sensor as shown in Figure 3.11.

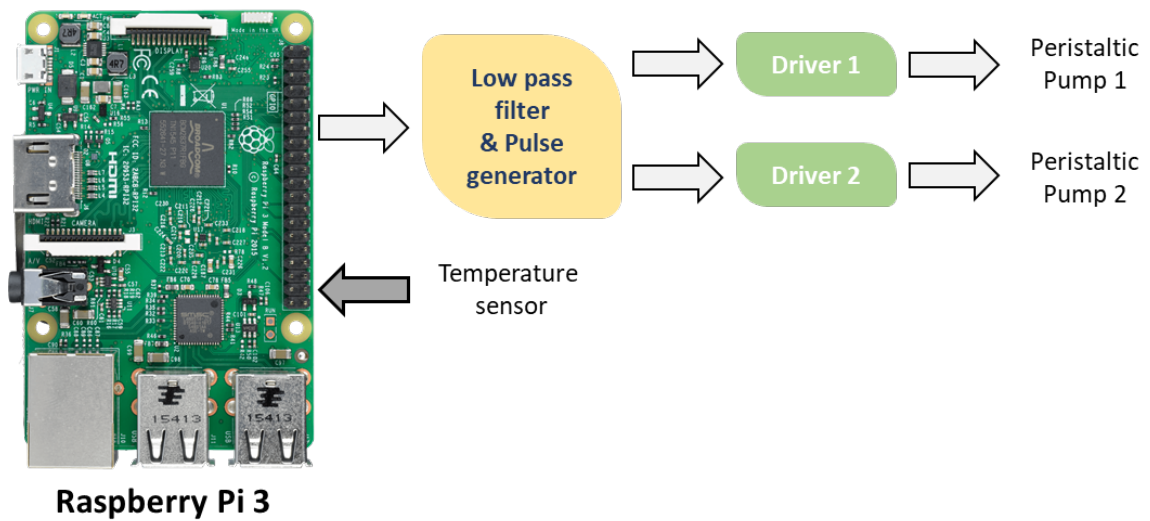


Figure 3.11 – Hardware architecture of prototype for phase 2.

Raspberry Pi 3

Raspberry Pi 3 basically acts as a brain of dialysate temperature controller prototype to regulate the dialysate temperature. Raspberry Pi 3 Model B was chosen as a microcontroller due to its high processing power and peripheral interface. It is a credit card size single board computer with an ARM processor developed by a non-profit

Raspberry Pi Foundation. Raspberry Pi is proven to be exceptionally popular, especially in the field of robotics, Internet of Things (IoT) etc [110], [111]. It includes 40 GPIO (General Purpose Input / Output) pins for attaching peripherals, USB, HDMI video, stereo audio output, wireless LAN, Bluetooth, micro USB (for powering up) etc., connectors in the board. In addition, it provides Ethernet connectivity, which is able to communicate with the host computer effectively.

Low pass filter and Pulse generator

The low pass filter and pulse generator helps to interface the stepper driver and Raspberry Pi effectively. However, Raspberry Pi 3 does not generate high frequency pulses and it does not provide 5V logic level as required by stepper driver. So, due to the hardware limitations of Raspberry Pi, a low pass filter was used to convert the Pulse width modulation (PWM) signal into an analogue DC signal. Thereby, DC signal was then converted into high frequency pulses, which is sufficient for the stepper driver. An Arduino Mega 2560 was used for this purpose, which means acquiring the DC signal and then converts the appropriate frequency pulse for the driver.

Stepper driver

Stepper driver plays a major role in the stepper motor performance. It helps to energize the motor phases in a timely sequence to make the motor run. The DM422C stepper driver from Leadshine Technology Co., Ltd, China was chosen to drive the peristaltic pump as shown in Figure 3.12. It offers an excellent system smoothness, providing optimum torque and nulls mid-range instability. In this case, the driver supplies constant 1.9A to the motor with micro stepping resolution of 1600 pulse/revolution. As

the temperature controller prototype depends on pump's flow rate, the unique features of the driver provide an ideal solution for low-speed smoothness of stepper motor.



Figure 3.12 – Image of DM422C stepper driver used.

Peristaltic pump

In HD machine, blood, dialysate and other fluids flow are maintained by Peristaltic pump [98], [112]. Thus, peristaltic pump from Nanjing Runze Fluid Control Equipment Co Ltd., China was used to transfer the dialysate from storage tanks to dialyzer in the prototype. It utilizes 2 phase bipolar stepper motor to drive the pump. The stepper motor was chosen due to its excellent speed control and accuracy. The NEMA 23 size stepper motor has 1.8° step angle, while each phase draws 2.35A at 4V allowing for a holding torque of 2.244Nm. The shaft of stepper motor attaches to the pump head, where they revolve the rotor with 6 rollers. These rollers press the flexible tube to the manifold where the pump is placed; hence it creates pressure inside the tube. The pressure will push the fluid further in the tube system, when one of rollers leaves the manifold. In this way, the dialysate doesn't get in contact with the pump, which denotes lowers the chance of contamination. Figure 3.13 and 3.14 shows the image of peristaltic pump used in this prototype.

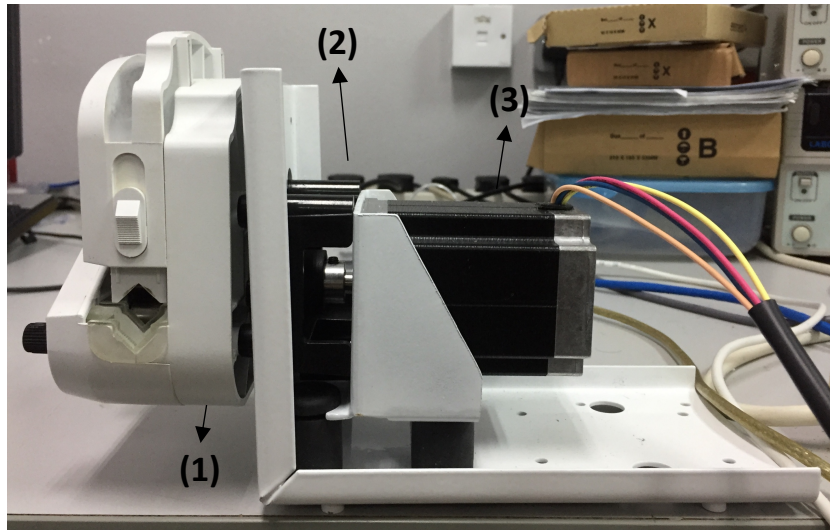


Figure 3.13 – Side view of peristaltic pump consisting of (1) pump head, (2) coupler and (3) stepper motor.

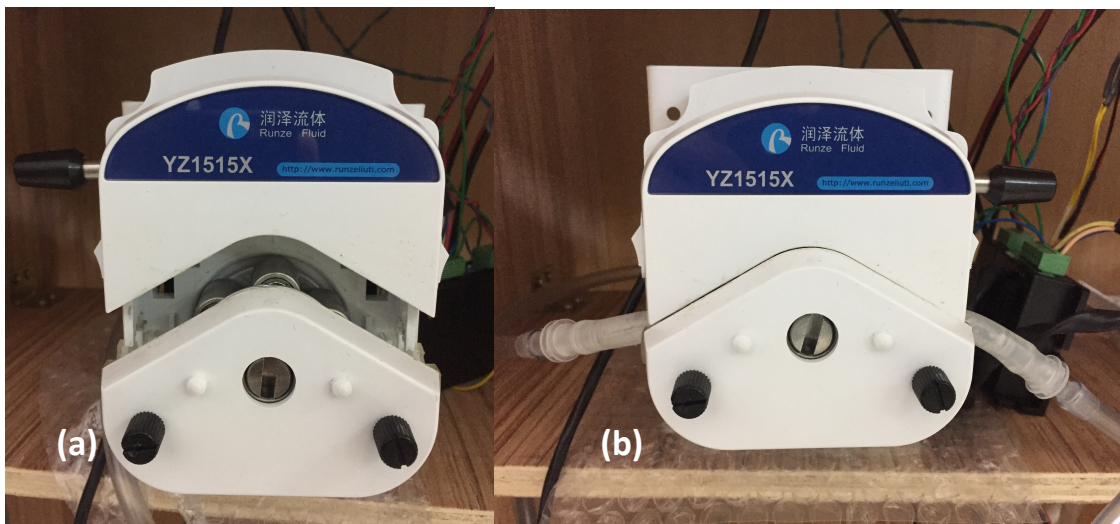


Figure 3.14 – Front view of peristaltic pump with (a) pump head open position and (b) pump head close position.

Temperature sensor

In this phase, the temperature sensor was used to sense the final dialysate temperature before entering to dialyzer. The DS18B20 temperature was chosen as described in section 3.6.1.1.

Tubing and connectors

In this prototype, fluids were transported to several stages using flexible PVC tubing. The flexible PVC tubing were designed to meet properties like UV Stability, cold flexing up to -40°C, heat stability up to 105°C service temperature, Abrasion Resistance, etc. However, the tube dimension of 6mm ID x 8mm OD were chosen to provide uniform flow of fluid. In the final section of prototype, the two temperature dialysate fluids were mixed and joined using a Y-shape connector as shown in Figure 3.15.



Figure 3.15 – Y-shaped connector used.

3.6.2 Software

In this section, a detailed software architecture and its methods used to interface the hardware components are detailed. The software development is also divided into two phases – Phase 1 and Phase 2.

3.6.2.1 Phase 1

This section provides the interfacing of hardware components with Arduino UNO microcontroller to regulate the constant temperature fluids in storage tanks. As

mentioned in section 3.6, two separate heaters need to be controlled to set the temperatures at 36°C and 38°C respectively. Accordingly, two concurrent process design approach chosen to perform this task. In other words, both heater circuits perform tasks separately at the same time. Therefore, PID controller was implemented on the Arduino UNO microcontroller in order to control the fluid temperature at the specified setpoints as shown in Figure 3.16. It gathers the temperature values of both storage tanks to properly drive the flow through heaters respectively. The microcontroller initializes the value of the PID parameters (K_p , K_i , K_d) and the desired temperature setpoints. After computing the error between the desired and the actual temperature, the controller modulates the current to the heaters by means of PWM with a suitable duty cycle. Hence, the controller runs through the PID loop every 1 second of time interval, which also implies the controller's performance. In addition, the pump runs at constant flow rate until it has reached the designated level in storage tank. The overall software flow diagram of the Phase 1 process is shown in Figure 3.17.

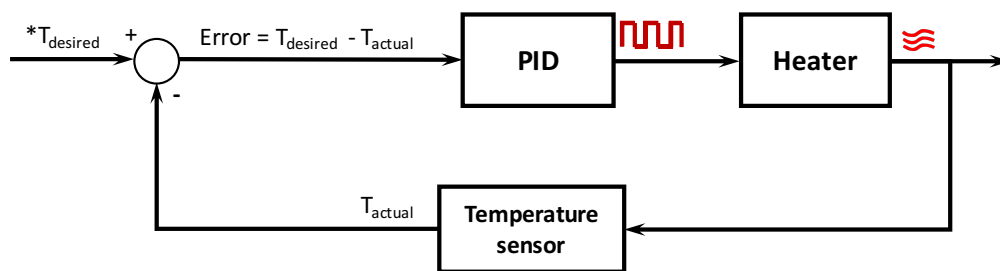


Figure 3.16 - Block diagram of the PID controller feedback loop

As the heater dynamics and setpoints doesn't change over time, the low-level control mechanism is sufficient to achieve optimal control of this system [113]. Whereas, PID controllers are widely used as low-level controllers used today. The PID control parameters have been chosen using a closed-loop tuning method manually adjusted with a trial and error procedure keeping constant two parameters and varying the remaining

one until specification on overshoot and settling time were reached on all range of interest.

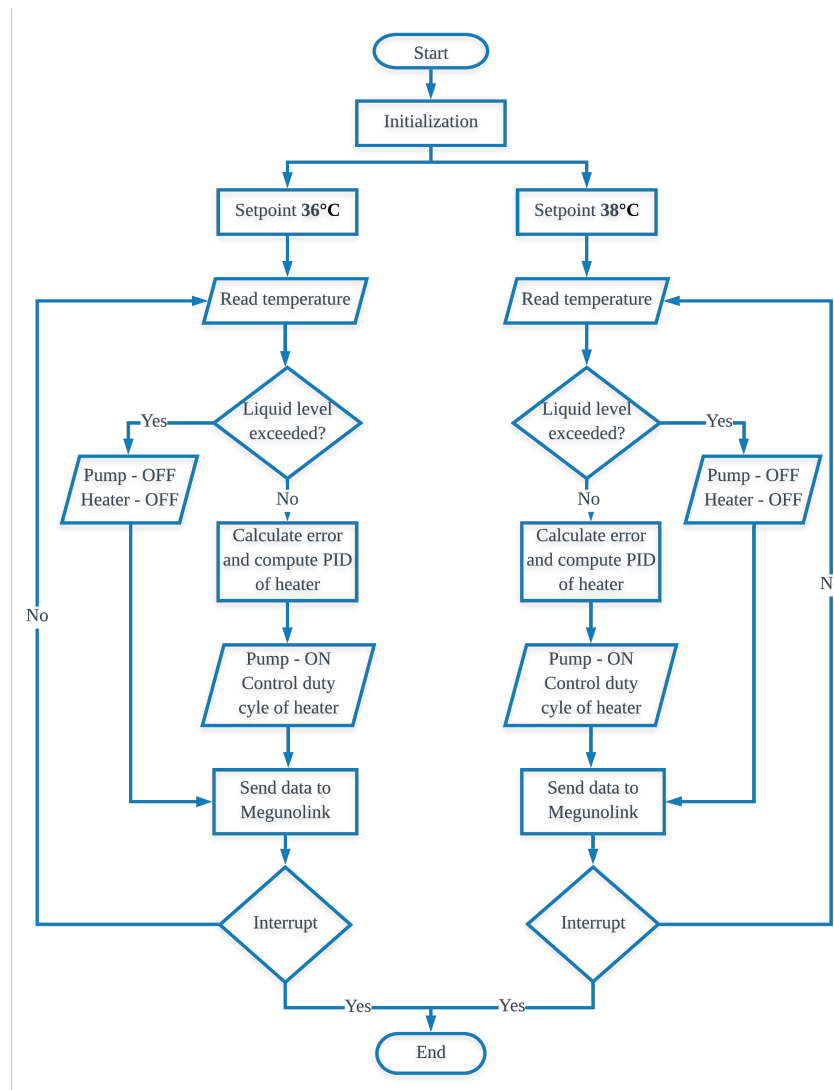


Figure 3.17 – Software flow chart of Phase 1 development.

The Arduino Integrated Design Environment (IDE) is an open-source Arduino environment, which makes it easy to program and upload it to the development boards. It is the most common programming approach for Arduino boards, which utilizes the C programming language. Moreover, it provides an access to an enormous open-source Arduino library, which enables to interface several sensors, control methods, communication easily. Thereby, a PID library was used to compute the PID controller parameters.

The Serial Monitor from Arduino IDE provides limited functions for data acquisition and analysis from the microcontroller. Also, the analysis on different controller parameters in different graphs are lacking during run time. Therefore, a third-party software Megunolink Pro was chosen to interfere with Arduino UNO for more advanced data acquisition and analysis. In addition, it provides customizable interface toolboxes for data plotting, control and monitoring the project parameters [114]. In this phase, the PID parameters (K_p , K_i , K_d) and temperature setpoints were designed as inputs in user-interface, which helps to tune the PID control during run-time. In addition, the monitoring variables such as temperatures, errors and outputs for both heaters were plotted in different graphs simultaneously. The software connects Arduino IDE through Megunolink library, which helps to send or receive data to the Arduino UNO. Figure 3.18 shows the graphical user-interface and graphs layout from Megunolink.

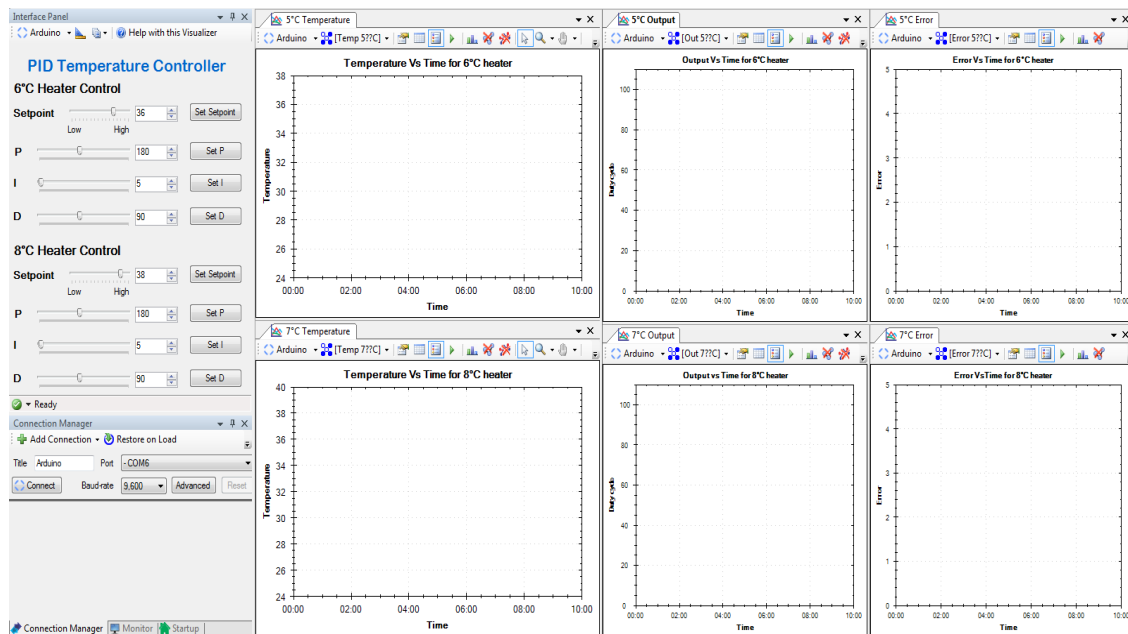


Figure 3.18 – Graphical User interface for Phase 1 PID temperature controller using Megunolink Pro.

3.6.2.2 Phase 2

This section comprises the most vital part in the development of DTCM. It explains the software architecture of interfacing and control mechanism of peristaltic pumps and temperature sensor with Raspberry Pi. In this prototype, the accuracy of dialysate flow rates strongly defines the dialysate and body temperature. Therefore, a high-level control mechanism namely fuzzy logic control (FLC) with feedback was chosen to control the peristaltic pumps. Moreover, this prototype requires controller qualities such as quicker response to disturbances with minimal undershoot and overshoot when the setpoint changes. As a result, FLC was found to be the most suitable controller for this application due to its decision-making capabilities.

In this phase, FLC was designed to control the dialysate temperature according to the target temperature. The FLC modulates the PWM with an appropriate duty cycle for the actuators by calculating the error between the target and the actual temperature and also the change in error. However, the controller runs this cycle at regular intervals in order to maintain the temperature at the setpoint. The evolution of FLC design is explained in Chapter 5. Due to the limitations of the stepper motor to drive using PWM pulses, the signal was converted to DC signal and then to variable frequency pulses. Hence, Arduino IDE was used for this purpose, which acquires analogue DC signals from PWM pulses and then mapped to respective variable square pulses. The in-built timer functions were used to generate variable square pulses to drive the peristaltic pumps. The overall software flow diagram of the Phase 2 process is shown in Figure 3.19.

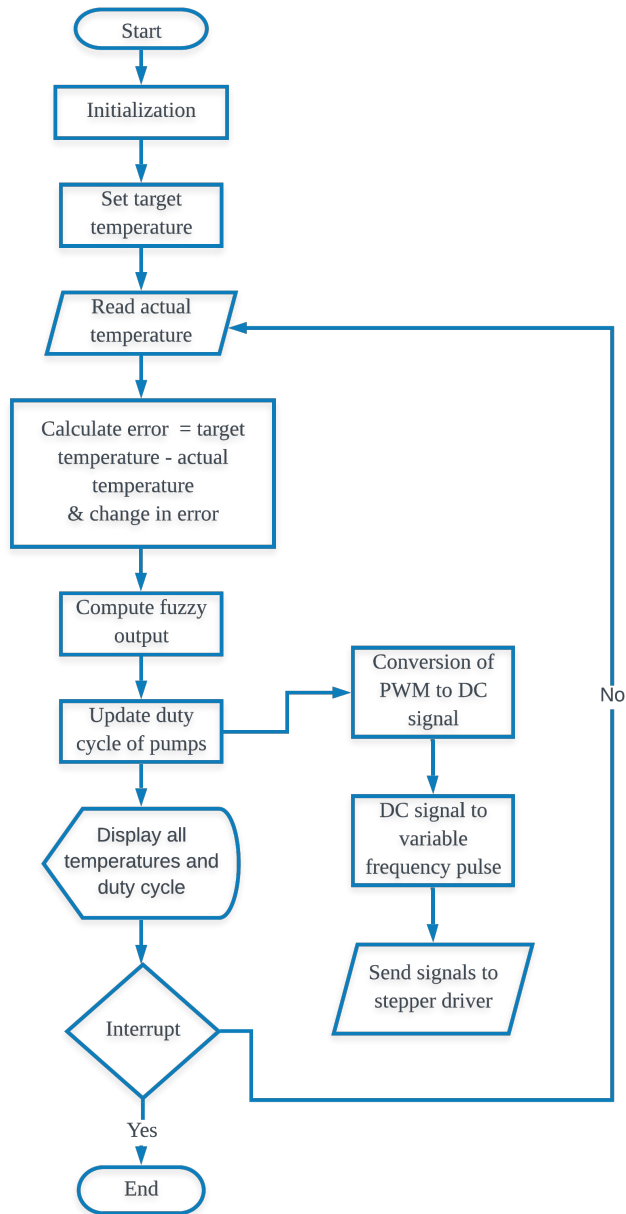


Figure 3.19 – Software flow chart for Phase 2 development.

The overall DTCM software was designed using MATLAB/Simulink environment. While the proposed FLC was designed using Fuzzy Logic Toolbox, which is a collection of functions in the MATLAB. It provides a tool to design fuzzy inference systems with the help of in-built graphical user interface (GUI) and also to integrate the fuzzy systems into simulations with Simulink seamlessly. This includes the definition of fuzzy inputs, outputs, membership functions, rule base and fuzzy inference engine properties for the FLC design process. The overall model was formed using several block diagrams, corresponding

MATLAB functions and parameters. Similarly, the MATLAB functions were used to read the temperature from the sensors using 1-wire communication bus. Moreover, additional Simulink blocks for Raspberry Pi provide the access to its I/O ports, which also enables to send PWM signals to the controller. Simulink provides the environment to deploy it to hardware directly by defining its unique IP address. It also enables to run it in external mode, which allows to communicate with host computer and target hardware during run-time. This makes the FLC implementation effective using its Simulink block.

3.7 Subsystem performance and interfacing

The performance and interfacing of input/output subsystem plays a vital role in defining the overall system performance. The ability of performance evaluation method is to identify good design potentials in terms of accuracy, usefulness and workload tolerance. In this study, interfacing the proposed components such as sensors and actuators with the microcontroller and individual performances were assessed. In addition, the input/output subsystems were calibrated without compromising on accuracy. This would eventually reduce the troubleshooting process before assembling the complete prototype.

This method enables to analyse and verify the subsystem performance individually according to the system requirements. The performance evaluation and interfacing method of subsystems in Phase 1 and Phase 2 are explained in the following sections.

3.7.1 Phase 1

Initially, the components such as heaters, float switches, pumps and temperature sensors were tested individually by interfacing the microcontroller. This method is to test

the functionality according to the prototype requirements. In addition, it would help to calibrate the temperature sensors with the known digital thermometer at different temperatures ranging from 20°C to 40°C. Similarly, the speed of pumps was calibrated with the known water rotameters. The range was chosen according to nominal dialysis parameter values.

The overall functionality of the Phase 1 subsystem was then verified by interfacing the components with Arduino UNO. One of the most vital performance evaluations of this phase is to evaluate the PID temperature control of two storage tanks. The PID parameters were varied by trial and error method to achieve the optimum result. Even though, there are many PID tuning methods, trial and error method is easy and effective way for applications without a mathematical model [115]. This method allows to tune the parameters while the system is working. When a PID controller is tuned optimally, the system responds to disturbances and reaches setpoint with minimal overshoot. However, the performance of PID temperature control was monitored using the GUI created in Megunolink Pro software. Additionally, float-switches mechanisms were tested in order to prevent the fluid teeming from the storage tanks. Therefore, various tests in different scenarios such as varying tank level, ambient temperature, initial temperature etc., have been performed to analyse its efficiency and repeatability. The detailed performance evaluation is discussed in section 6.4.1.

3.7.2 Phase 2

At the initial stage, the peristaltic pumps were tested separately by interfacing with stepper motor driver and microcontroller. Additionally, the temperature sensors were interfaced with Raspberry Pi. This would enable to evaluate the individual

performance according to the prototype specification. However, the temperature sensors and flow rate of peristaltic pumps were calibrated using similar method mentioned in section 3.7.1. The stepper motor driver was tuned for certain parameters such as driving current, micro steps etc., to drive the peristaltic pump efficiently.

The most important performance evaluation of this phase is to optimize the fuzzy parameters and analyse the controlling actions of peristaltic pumps. This method demonstrates the efficiency of a controller alone in real-time implementation. However, the FLC performance mainly depends on certain fuzzy parameters such as fuzzy inference engine, fuzzy rule base and membership functions. Therefore, a simplified design of temperature controller based on DTCM design concept was created in order to optimize the fuzzy logic design. Furthermore, numerous fuzzy logic designs were created by varying the fuzzy parameters for input and output of the prototype. As a result, the temperature responses were examined in terms of accuracy and the time response incorporating with its computational performance. The computational performance was analysed during the execution time in Simulink and it was found to be identical throughout the experiments without any noticeable delay. The detailed optimization of fuzzy logic design for DTCM is explained in Chapter 5. Hence, the optimized fuzzy logic design can be used for testing and validation of DTCM prototype.

3.8 Prototype construction and assembly

In this section, the circuits of phase 1 and 2 were assembled in order to evaluate the overall performance of the prototype. Figure 3.20 shows the design of cart that resembles the initial version of DTCM prototype. The PID and FLC circuits were enclosed in a user-designed cart which can be easily interfaced to existing HD machines. The cart

consists of two sections; upper section consists of electrical circuits, while the lower section consists of transport of fluids, heater and storage tanks. The initial tank imitates the final dialysate after preparation flows at a temperature of approx. 30°C. Whereas the final tank represents the dialysate, which eventually goes through the dialyzer after the individualized temperature control. Therefore, the initial tank and final tank were placed to analyse the temperature data for the in-vitro experiments and these tanks can be disconnected when HD connects to DTCM. In addition, the cart was designed to give importance to certain elements such as accessibility, portability, cost-effectiveness and, safety. Since, the module could interface by connecting the fresh dialysate from HD and temperature-controlled dialysate to dialyzer, the DTCM module would be accessible and portable. This in turn avoids additional expense of another HD machine with active temperature control. In terms of safety, DTCM does not become contact with blood and able to maintain within permissible limits (35°C - 38°C) [65].

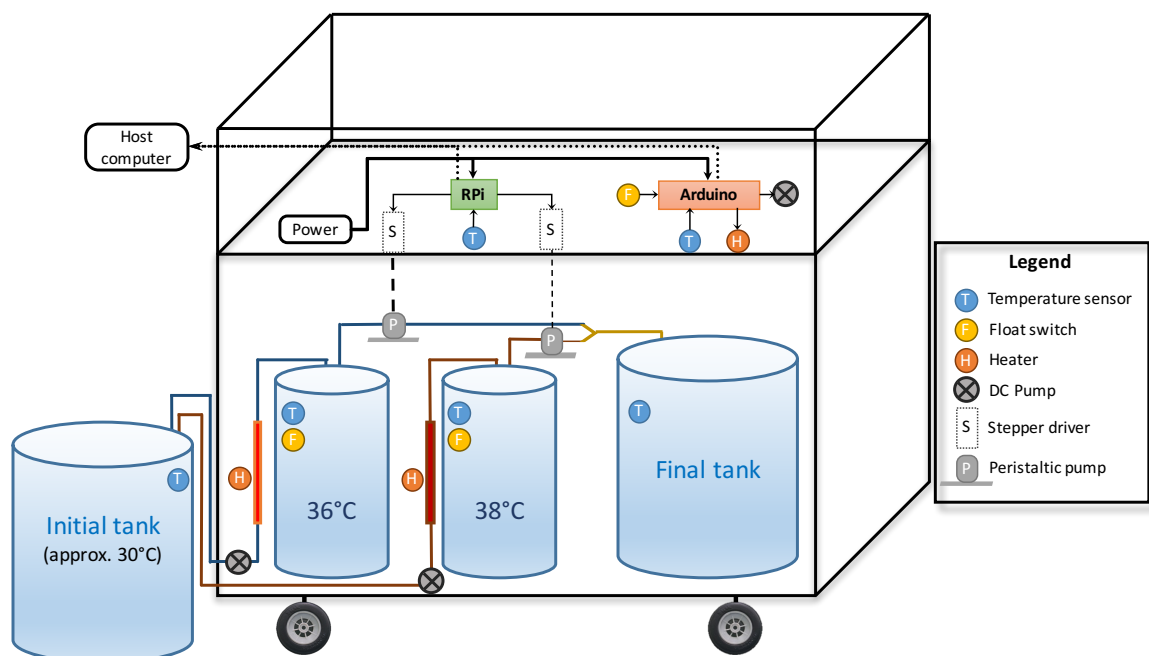


Figure 3.20 – Illustration of DTCM prototype design comprising of PID and fuzzy control.

3.9 Testing & validation

This section emphasizes on the evaluation of system capability and functionality of DTCM prototype. The prototype testing was performed to examine the body temperature trend under various physiological and machine conditions. These various conditions were based on patient's core temperature, variation in arterial temperature, recirculation, blood flow rate, dialysate flow rate, and ambient temperature. This method enables the prototype to validate the controller performance in terms of accuracy, repeatability, easy to interface, and individualized control adapting to patient's condition.

A model based approach was adopted to verify the DTCM prototype. In certain conditions such as target body temperature, variation of arterial temperature and recirculation were initialized in Simulink environment. While other conditions depending on thermal energy balance model, the model parameters were then updated and initialized in Simulink for DTCM analysis. This would allow to monitor the effect of body temperature with an active regulation of dialysate temperature.

3.10 Evaluation

This method involves in assessing the prototype performance, validation results and then verifies with the proposed objectives. Subsequently, this would affirm the development of DTCM prototype according to the hypothesis.

INVESTIGATION ON HEAT TRANSFER IN A DIALYZER MEMBRANE MODEL FOR THE DEVELOPMENT OF DIALYSATE TEMPERATURE CONTROLLER MODULE

4.1 Introduction

The patient's thermal instability plays an important role in the onset of hypotension, which shows that a slight fluctuation in body temperature is sufficient to cause life threatening complications [33]. The heat transfer taking place in extracorporeal circuit is considered as one of the factors that are responsible for change in body temperature. According to medical trials, a long term study showed that the highest mortality was observed in patients whose post-dialysis body temperature increased or decreased, irrespective of baseline body temperature [15]. The most common practices to control body temperature is to alter the dialysate temperature in extracorporeal circuit, which was first described by Maggiore et al. in the 1980's [30]. Several studies have revealed a remarkable improvement on the hemodynamic stability compared to traditional settings by altering the dialysate temperature [28], [35], [40]. Yet, more research is required to define the precise temperature at which maximum benefit is achieved without any complications. Thereby, the feedback control of dialysate temperature is vital for preserving patient's hemodynamic stability.

In addition to the transport of toxins and fluids, there is also heat exchange taking place between blood and dialysate in the dialyzer. Anticipating heat loss from the blood lines to the environment, the analysis of heat transfer in dialyzer need to be considered for the development of an effective temperature controller. Mathematical and computational models of dialyzer models may help to investigate the heat transfer and how other conditions affect the blood temperature differences, while at the same time reducing time consuming and expensive experiments. In the last few years, numerous computational models of dialyzer have been proposed to describe the transport phenomena of solutes in dialyzer. Until now, majority of the models emphasizes on the solute removal performance by analysing flow behaviour of blood and dialysate across the porous membrane [101], [102] and other design concepts of hollow fiber bundle [103], [116], [117]. Only a few of these numerical models have been used to validate and compare the flow behaviour with the experimental study [118], [119]. Over these years, these models have improved from one dimensional to three-dimensional study with minimal assumptions in blood and dialysate flow behaviour, which assisted to optimize the dialyzer design. However, to the best of the authors' knowledge, a detailed analysis on the influence of the heat transfer in dialyzer has yet to be reported. This hinders to identify the cause of heat loss/gain during HD and makes it difficult to optimize dialysate temperature controller design, which is the focus of our current research.

Apart from the heat exchange in dialyzer, there is also thermal energy balance, which is affected in extracorporeal circuit consisting of arterial and venous blood lines due to certain factors such as environmental temperature, tubing material, blood flow rate etc. A study has proposed a thermal energy model of extracorporeal circuit with the intention to estimate the overall thermal exchange to guarantee the stable patient core

temperature during the treatment [79]. However, the heat transfer in dialyzer is vital for determining overall thermal energy model due to the diffusion of blood and dialysate at different temperatures.

In this simulation, a single fiber of a dialyzer membrane namely Polyflux 210H was investigated using COMSOL Multiphysics® software. The primary aim is to investigate the effect of heat transfer taking place in dialyzer under various circumstances. In addition, the heat transfer relation in a dialyzer can be considered for modelling an overall heat transfer model of extracorporeal circuit, which enables to estimate the venous temperature for in-vitro analysis of DTCM prototype development.

4.2 Simulation methodology

An overview of a multi-layered dialyzer membrane namely Polyflux 210H (Gambro, Hechingen, Germany) is shown in Figure 4.1. The external housing contains a bundle of approx. 12000 hollow fibers and it is assumed that the fibers are uniformly spaced and arranged for this study. In this work, the heat transfer taking place in a dialyzer was investigated numerically with the commercially available COMSOL Multiphysics software. The membrane was modelled by following the dimensions of actual Polyflux 210H membrane [104], [105]. The basic assumptions of this model are axial symmetry, fully developed laminar flow in the blood and dialysate compartment, transport of momentum and mass occurs in 2D, incompressible fluid, Newtonian fluids, isotropic porous membrane consisting of three different layers, strongly diluted solutes and null ultrafiltration. The blood was considered as Newtonian fluid with the assumption of high shear rate through the membrane.

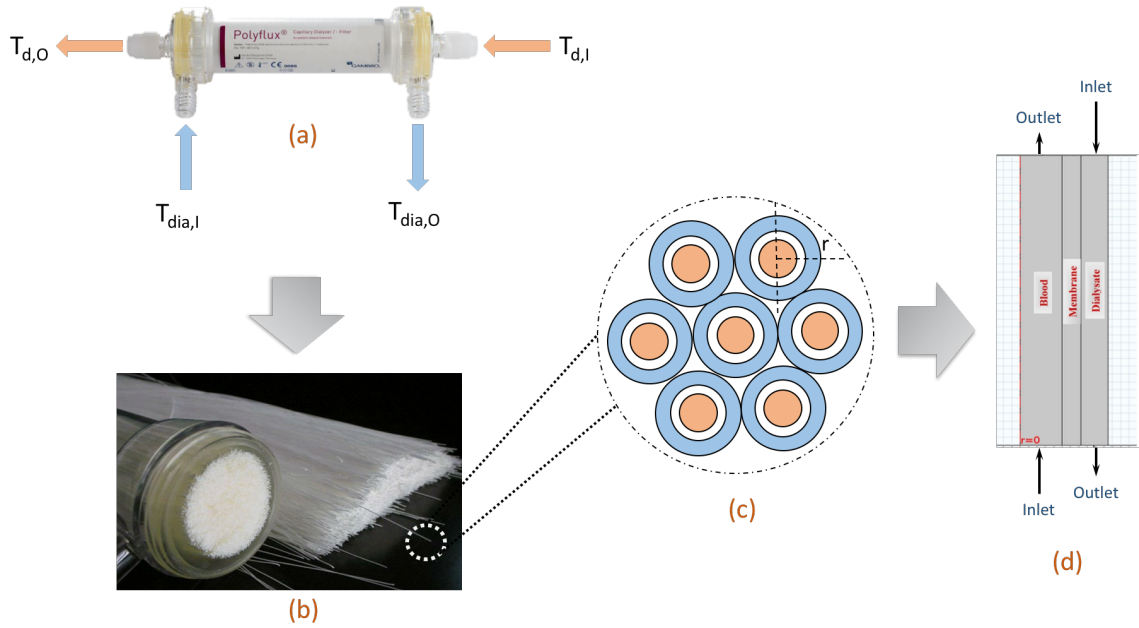


Figure 4.1 - Evolution of Polyflux 210H dialyzer membrane from actual dialyzer to a simulation model comprising of (a) overview of actual dialyzer, (b) bundle of hollow fibers packed inside the housing, (c) cross sectional view of hollow fiber in a dialyzer and (d) 2D geometrical model of single fiber membrane.

In this model, only one layer of membrane has been considered to ease the computation and the heat transfer across the layers is assumed to be negligible. Nonetheless, all other dimensions of geometry were created according to Polyflux 210H membrane. The width of path for dialysate flow was calculated using the following equation 4.1 [120],

$$W = R_{ext} \left(\sqrt{\frac{\pi}{2\sqrt{3}\phi}} - 1 \right) \quad (4.1)$$

where, W is the width of path for dialysate flow, ϕ is the fiber packing density of Polyflux 210H dialyzer i.e., 45% and R_{ext} is the outer radius of the fiber (m). The blood flows through the fibers while the dialysate flows over the membranes in a counter-current manner. The geometry of a dialyzer membrane was then created as shown in Figure 4.2.

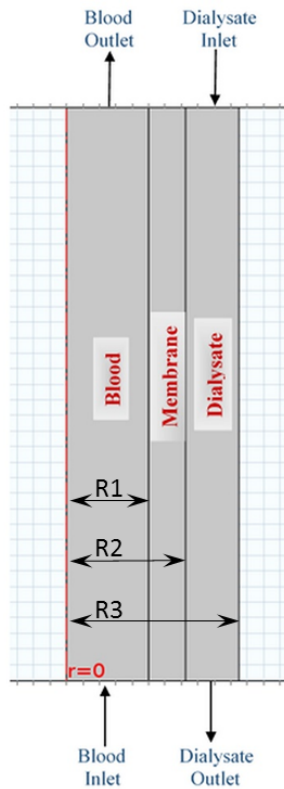


Figure 4.2 – Dialyzer membrane model showing blood, membrane and dialysate domain and other boundaries.

The types of physics applied for this study were *The Heat Transfer in Fluids* and *Porous Media*. *The Heat Transfer in Fluids* interface was used for both blood and dialysate flow. Likewise, *The Heat Transfer in Porous Media* was used for the dialyzer membrane. The material properties required for the physics were then added. The properties of blood such as density, thermal conductivity and heat capacity at constant pressure are shown in Table 4.1, while the dialysate uses the pre-defined properties of water. It was a challenging task to acquire the properties of Polyflux 210H membrane due to its unique blend of polymer exclusively used for this application. However, the bulk density, ρ_{bulk} of Polyflux membrane was estimated to be 857.60 kg m^{-3} .

This was calculated with the assumption that that entire polymers were equally distributed, as shown in equation 4.2.

$$\rho_{particle} = 0.33(\rho_a) + 0.33(\rho_b) + 0.33(\rho_c) \quad (4.2)$$

$$Porosity = 1 - \frac{\rho_{bulk}}{\rho_{particle}} \quad (4.3)$$

Where, $\rho_{particle}$ denotes the particle density, consisting of ρ_a , ρ_b , ρ_c denoting the polymers used in the Polyflux 210H membrane. The porosity of three layers from blood side to dialysate side were found to be 0.1, 0.27 and 0.4 respectively, whereas the porosity of the middle layer of membrane was estimated. The approximated values of heat capacity and thermal conductivity was based on the Polyamide, which is one of the materials used in Polyflux 210H membrane.

Table 4.1 – Material parameters of blood, dialysate and membrane used in this model

Parameters	Blood	Dialysate	Polyflux 210H membrane
Density, ρ (kg m ⁻³)	1060 [121]	Used same properties of water from material library.	857
Thermal Conductivity, k (W m ⁻¹ K ⁻¹)	0.543 [122]		0.25 [123]
Heat capacity at constant pressure, C_p (J kg ⁻¹ K ⁻¹)	4180 [122]		1590 [123]
Ratio of specific heats	1 [122]		-

With *Heat transfer in fluids*, the governing equation is the heat equation, which is based on the energy conservation equation. The same equation was used in dialysate flow model to estimate the temperature. The heat equation is shown in equation 4.4.

$$\rho C_p u \cdot \nabla T = \nabla \cdot (k \nabla T) + Q \quad (4.4)$$

Where C_p denotes the heat capacity at constant pressure ($\text{J kg}^{-1}\text{K}^{-1}$), k is the thermal conductivity ($\text{W m}^{-1}\text{K}^{-1}$), T is the temperature (K), and Q is the heat source (J) term and u is the velocity of fluids (m s^{-1}).

The inlet velocity of blood, v_b and dialysate, v_d along the axial direction were calculated using the equations 4.5 and 4.6 [124].

$$v_b = \left(\frac{2Q_b}{\pi R_1^2 n} \right) \left[1 - \left(\frac{r}{R_1} \right)^2 \right] \quad (4.5)$$

$$v_d = \frac{2Q_d}{\pi \left(\frac{3R_3^4}{4} + \frac{R_2^4}{4} - R_2^2 R_3^2 - R_3^4 \ln \left(\frac{R_3}{R_2} \right) \right) n} \left[r^2 - R_2^2 - 2R_3^2 \ln \left(\frac{r}{R_2} \right) \right] \quad (4.6)$$

where Q_b and Q_d denotes the flow rate of blood and dialysate respectively (ml min^{-1}), r denotes the radial coordinate, n denotes the number of fibers in a dialyzer (for Polyflux 210H dialyzer, $n = 12000$) and R_1, R_2, R_3 denotes the radius of the fiber (m), which is illustrated in Figure 4.2.

In *Heat Transfer in Porous Media*, the equation used was the same as that for fluids. The effective thermal conductivity of porous media was estimated based on volume averaging theory [125]. The modified equations are shown as equation 4.7 and 4.8.

$$\rho C_p u \cdot \nabla T = \nabla \cdot (k_{eff} \nabla T) + Q \quad (4.7)$$

$$k_{eff} = \theta_p k_p + (1 - \theta_p) k \quad (4.8)$$

Where k_{eff} denotes the effective thermal conductivity, θ_p denotes the packing density of membrane, k_p denotes the thermal conductivity of membrane and k denotes the thermal conductivity of fluid.

The transfer of heat through the membrane was defined as convective heat flux and the governing equation is shown in equation 4.9,

$$q = h.(T_{ext} - T) \quad (4.9)$$

Where h denotes the convective heat transfer coefficient and T_{ext} denotes the external temperature of the membrane. In many studies, it was mentioned that the calculation of heat transfer coefficient is a challenging task. However, COMSOL Multiphysics® provides many conditions to approximate the value of convective heat transfer coefficient, h ($\text{W m}^{-2} \text{K}^{-1}$). Since this model has two membrane boundaries, the blood side boundary was considered as the internal forced convection, while the dialysate side boundary was considered as the external forced convection. The internal forced convection was selected as the blood is forced to flow inside the membrane, whereas the dialysate fluid is forced to flow over the membrane surface in the dialyzer. Hence, this heat transfer system involves both internal and external convection simultaneously. The polymers are considered as thermal insulators, which means it reduces the heat transfer during the process [126], [127]. Thus, the heat transfer coefficient in the polymers are very low (range between $0.4 - 40 \text{ W m}^{-2} \text{K}^{-1}$) [128]. Therefore, the required inlets, outlets and boundaries were initialized for this model. Then the temperature of blood, dialysate and membrane are then solved using COMSOL Multiphysics® until a converged solution is obtained.

4.3 Results and discussion

4.3.1 Heat transfer in a dialyzer

In this model, a stationary study was carried out in order to investigate the effect of dialyzer in reaction to the difference in temperature from blood and dialysate fluids. Based on recent literatures, the use of cool dialysate (35°C) had significant effect on hemodynamic stability of dialysis patients when compared to standard dialysate temperatures (37°C) [36], [129]. Whereas, the prescription of standard dialysate temperature of 37°C would lead to heat accumulation and thereby to an excessive drop in blood pressure. So, the temperature at the inlet of blood and dialysate were initialized as 37°C and 35°C respectively and the flow rate of blood and dialysate were kept constant at 300ml min⁻¹ and 450ml min⁻¹ respectively. The dialysate flow rate were acquired by taking into consideration of the ratio $Q_b:Q_d = 1:1.5$ as prescribed in modern dialysis machines [130]. The simulated results showing the effect of temperature taking place in dialyzer is shown in Figure 4.3. The arrows in Figure 4.3(b) indicate the velocity magnitude and direction of blood and dialysate compartments.

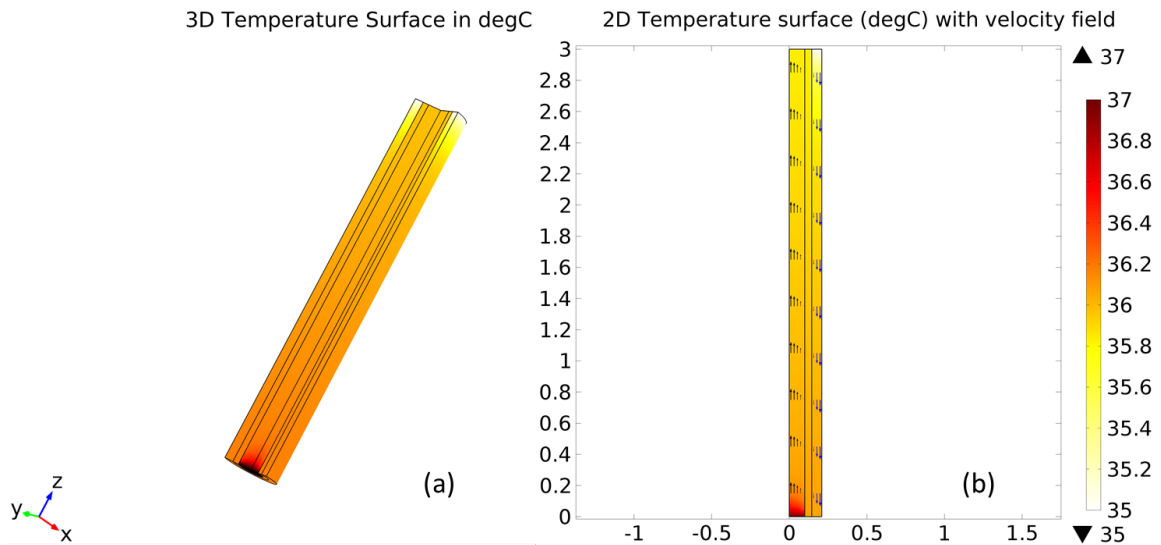


Figure 4.3 - (a) 3D representation and (b) 2D representation of Temperature surface when inlet temperature of blood and dialysate at 37°C and 35°C respectively flows through dialyzer at $Q_b = 300 \text{ ml min}^{-1}$ and $Q_d = 450 \text{ ml min}^{-1}$.

The temperature at the inlet and outlet of blood and dialysate were analysed and shown in Figure 4.4. It can be observed that the actual blood temperature has decreased by about 1.16°C and the dialysate temperature has increased about 1.08°C along the membrane. The difference in temperature change is very small (approx. 0.08°C), which may be due to the difference in the blood and dialysate flow rates.

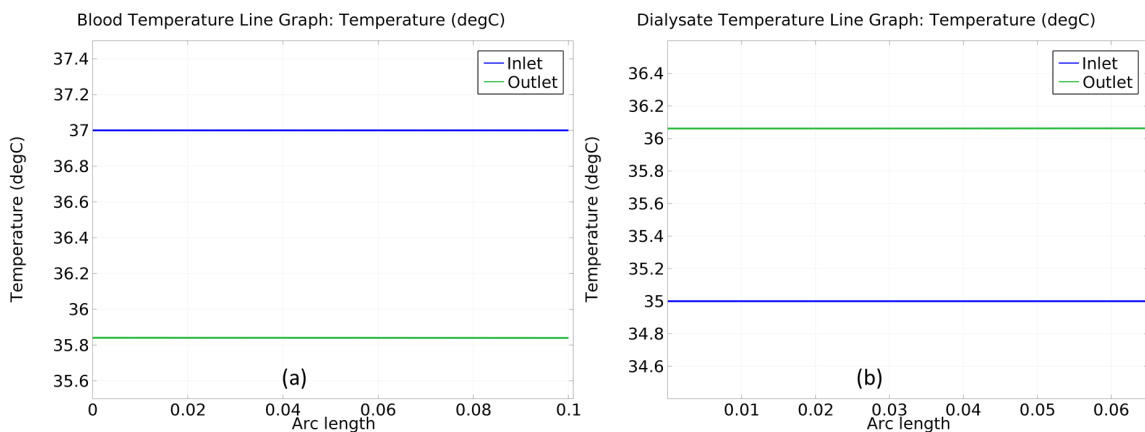


Figure 4.4 - The graph of (a) blood and (b) dialysate temperature at the inlet and outlet of this model.

4.3.2 Effect of heat transfer by varying dialysate temperature

Figure 4.5 shows the effect of blood and dialysate temperature by various inlet dialysate temperatures for normal body temperature at 37°C. The dialysate temperature was varied from 34°C to 38°C to investigate the heat loss and the flow rate of blood and dialysate were kept constant at 300ml min⁻¹ and 450ml min⁻¹ respectively. It is assumed that only negligible (≈ 0) heat loss occurs from blood line to environment. At 37°C of dialysate temperature, it can be seen that the blood and dialysate is in thermal equilibrium. However, dialysate temperature higher than the body temperature shows an increase in blood temperature, which can lead to many complications. Respectively, dialysate temperature lower than the body temperature shows a decrease in blood temperature. Similarly, the outlet dialysate temperature shows increase and decrease with the decrease and increase in inlet dialysate temperature respectively. This is most likely due to the fact that heat loss/gain is taking place across membrane from blood to dialysate and vice versa.

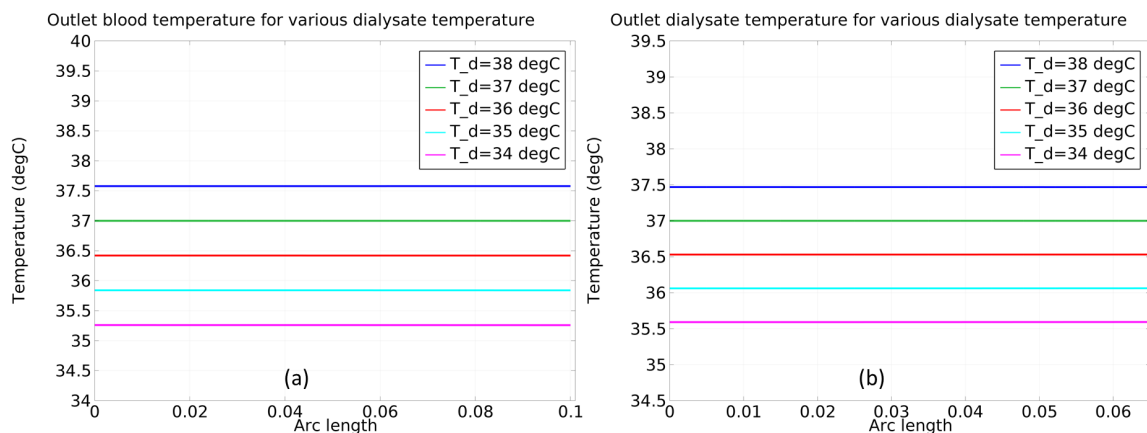


Figure 4.5 - The outlet (a) blood temperature and (b) dialysate temperature for various dialysate temperatures under normal body temperature.

It was found that the heat transfer taking place in dialyzer is mainly due to the difference in temperature between blood and dialysate. From a medical perspective, the

thermal aspects of HD mainly depends on the physiologic effects of patients, which responds to changes in body temperature [20]. This implies that the body temperature could not be stabilized if blood and dialysate temperature were the same. However, continuous research is progressing in merging physiological and extracorporeal thermal transfers [79]. Hence, it is probably best to analyse the thermal exchange in extracorporeal circuit, especially the dialyzer.

4.3.3 Effect of heat transfer by varying blood and dialysate flow rate

The different types of dialyzers such as low-flux and high flux membranes have different optimal blood and dialysate flow rates to undergo an efficient HD treatment. Thereby, the analysis on heat transfer for various blood and dialysate flow rate was investigated. Thus, the three commonly used dialysate flow rate such as 400 ml min⁻¹, 450ml min⁻¹, and 500 ml min⁻¹ of the Polyflux 210H dialyzer were considered for the study. While, the blood flow rates were varied from 200 ml min⁻¹ to the maximum of dialysate flow rate were considered. The flow rates were selected according to the Polyflux dialyzer datasheet [104]. The inlet temperatures of the blood and dialysate were kept constant at 37°C and 35°C respectively for this study. The simulations were carried out and plotted in the graph as shown in Figure 4.6. From the graph, it can be observed that the dialysate temperature increases with the increase in blood flow rate, while the blood temperature decreases. Moreover, there was only a slight change in temperature at around 0.01°C. However, there was no noticeable change in temperature when the blood flow rate increases by 50 ml min⁻¹. Furthermore, the blood temperature loss in dialyzer was found to be lesser in high dialyzer flow rate, while the loss is higher in low dialyzer flow rate. Similar relations were found with the increase in dialysate

temperature. Specifically, the change in temperature for the nominal blood flow rate at 300 ml min⁻¹ with increasing dialysate flow rate were 1.164°C, 1.159°C and 1.155°C respectively, which shows a negligible difference in temperature loss with a magnitude of less than 0.005°C. Most importantly, the gradient of the temperature change in different dialyzer flow rates were fairly similar. This shows a generalized trend of heat transfer in dialyzer for different prescriptions of HD.

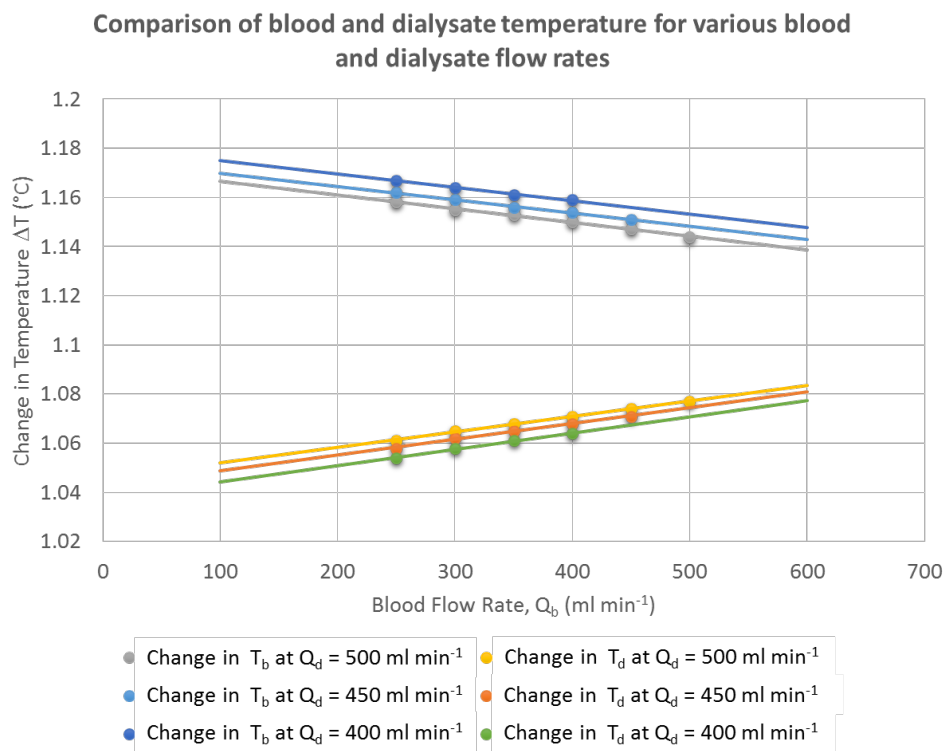


Figure 4.6 - Comparison of change in blood and dialysate temperature along the membrane for various blood flow rate, Q_b , and dialysate flow rate, Q_d

4.3.4 Relationship between inlet and outlet blood temperature

The inlet blood temperature, $T_{d,I}$ and outlet blood temperature, $T_{d,O}$ were analysed for various blood and dialysate flow rates in order to deduce a heat transfer relation of a dialyzer. This will benefit in achieving an overall thermal energy relation of extracorporeal circuit including arterial and venous line. Therefore, the outlet blood temperatures were computed within various inlet blood and dialysate temperature, T_d .

These temperatures were kept beyond normal range from 34°C to 38°C to deduce a generalized expression. The relationship between inlet blood and outlet blood temperatures were plotted in terms of dialysate temperature for $Q_b = 300\text{ml min}^{-1}$ and $Q_d = 450\text{ml min}^{-1}$ as shown in Figure 4.7. From the graph, it can be seen that the relationship between the inlet and outlet blood temperature is linear and the relationship can be expressed as a linear equation. The gradient was then calculated to deduce an expression in terms of $T_{d,O}$, $T_{d,I}$ and T_d as shown in equation 4.10.

$$T_{d,O} = k_a T_{d,I} + k_b T_d + k_c \quad (4.10)$$

Where, k_a , k_b and k_c denotes the coefficients of linear heat transfer equation of dialyzer.

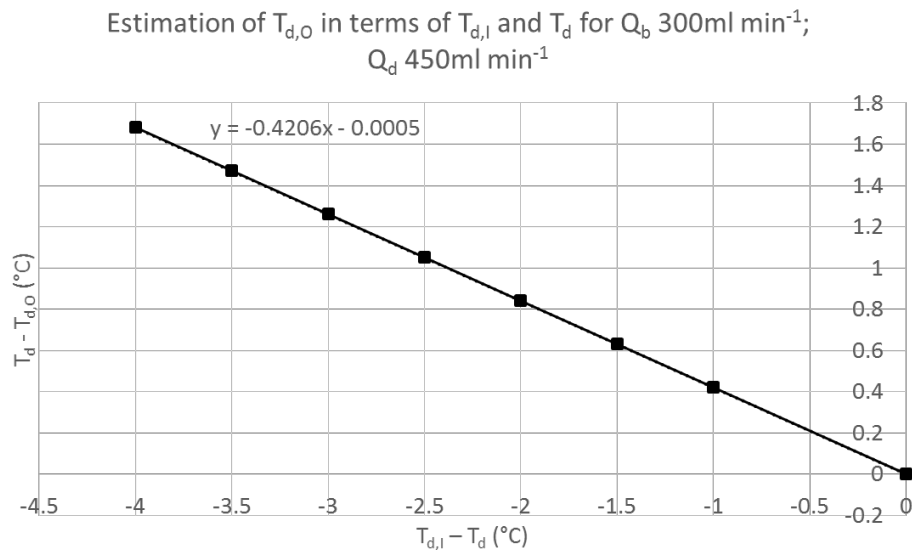


Figure 4.7 – Graph of relation between outlet blood temperature in terms of inlet blood and dialysate temperature for $Q_b 300\text{ml min}^{-1}$; $Q_d 450\text{ml min}^{-1}$

Similarly, the outlet blood temperature was computed for different dialysate flow rates of 350 ml min^{-1} and 400 ml min^{-1} , while keeping the blood flow rate constant at 300 ml min^{-1} . In the same way, the outlet blood temperature was also computed for different blood flow rates of 200 ml min^{-1} and 400 ml min^{-1} by keeping constant dialysate flow rate

at 450 ml min^{-1} . From this analysis, the coefficients of the linear equation were tabulated as shown in Table 4.2. In this current work, the defined range of blood flow rate were selected as it is used commonly for normal patients, while the usual dialysate flow rates needs to be less than 1.5 times the blood flow rate [131].

Table 4.2 – Coefficients of inlet blood and dialysate temperature for various Q_b and Q_d

Q_b ml min^{-1}	Q_d ml min^{-1}	k_a	k_b	k_c
200	450	0.4178	0.5822	0.0005
300	450	0.4206	0.5794	0.0005
400	450	0.4234	0.5766	0.0005
300	350	0.4148	0.5852	0.0006
300	400	0.4181	0.5819	0.0008

As this is an initial study on heat transfer in dialyzer, there are many limitations and assumptions adopted such as isotropic medium, negligible work done by pressure changes, approximations of membrane material properties etc., were considered. Moreover, the results were mainly biased to high flux dialyzers such as Polyflux 210H, which hinders to approximate the characteristics of other dialyzers with different properties. However, the model can be easily modified to the specific dialyzer properties using the COMSOL software. To the best of authors' knowledge, there has been no simulation study based on the heat transfer in the dialyzer. Therefore, the outlet blood temperature in dialyzer were validated with clinical studies while assuming negligible heat loss between dialyzer and venous line.

From the initial 3D representation of the dialyzer as shown in Figure 4.3 (a), it can be seen that there is notable transfer of heat taking place between blood and dialysate

across the membrane. This means the temperature of blood drops along the fiber, while the temperature of dialysate rises using the cool dialysate at 35°C. Also, it shows that the blood leaves the dialyzer in thermal equilibrium with the dialysate. It can also be seen that the temperature of the blood returning to the body is also influenced by that of the dialysate, which confirms that the dialyzer acts as an almost perfect heat exchanger [19], [33], [132], [133]. Studies have shown that the drop in blood temperature in venous line is within the range of 0.5°C – 1°C [19], [65]. An earlier study showed that the venous temperature has dropped to 0.9±0.4°C in an isothermic HD [66]. From this simulation work, it can be concluded that the temperature change along the dialyzer membrane is one of the factors which leads to a drop in blood temperature as shown in the literatures. The direction of velocity shows strong agreement with the fully developed laminar flow theory, which shows the velocity is higher away from the membrane. Moreover, the model shows that the blood flow rate has insignificant dependency on the effect of heat transfer in dialyzer.

To further strengthen the development of an efficient temperature controller, more useful information on various dialysis operating conditions need to be investigated. Thus, the important temperature gradient was analyzed by various dialysate temperature, dialysate flow rates and blood flow rates. As a result, the inlet and outlet blood temperature trend in a dialyzer need to be utilized to account for overall thermal energy transfer in extracorporeal circuit. Thereby, the venous temperature can also be estimated from the overall extracorporeal model, which serves as an important parameter for monitoring the efficiency of a temperature controller. Hence, the numerical results can serve as a guide for further design and development.

In future, this model can be used to design an optimal dialyzer membrane not only limiting to membrane design parameters such as pore radius, dimensions of fiber, material properties, flow rates of blood and dialysate etc., but also heat transfer properties. The study further strengthens our research that heat transfer in the dialyzer due to its inherent mass transfer necessitates a system to control and regulate the dialysate temperature. This could serve as a simple and efficient way to compensate the heat loss/gain in extracorporeal circuit.

4.4 Conclusion

In conclusion, the model had shown that there is also a heat transfer taking place in dialyzer other than heat loss from blood lines to environment. The model exhibited a trend in temperature profile across the dialyzer membrane and the blood temperature has decreased up to 1.16°C using cool dialysate settings. The blood temperature slightly decreased for increasing blood flow rates with a constant dialysate temperature. Whereas, the decrease in blood temperature in dialyzer showed a similar trend for different dialysate flow rates. It can be verified that the dialyzer acts as a heat exchanger during HD. Most importantly, the linear equation expressing the heat transfer in a dialyzer can be favourably used for the in-vitro evaluation of DTCM prototype. In future, it is hoped that inclusion of temperature controller in HD machine by incorporating the heat loss will reduce the hypotension episodes as well as other complications during dialysis.

IMPLEMENTATION AND PERFORMANCE EVALUATION OF FUZZY LOGIC CONTROL WITH RASPBERRY PI

5.1 Introduction

In the last few years, artificial intelligence (AI) based techniques in the control system has seen an emerging trend in various applications. In fact, AI technique offers the science of producing intelligent systems, which are effective and better solution to tackle different problems and tasks. AI consists of several techniques such as Neural Networks, Fuzzy Logic, Expert Systems, Evolutionary computing techniques and many more. One of the AI techniques widely used in the field of control system is fuzzy logic techniques. Fuzzy logic control (FLC) is mainly based on the logic and decision mechanism, which is realization of human control strategy. However, FLC delivers superior performance over a classical controller due to its decision-making capability and ability to operate in presence of uncertainties and external disturbances [134]. Unlike other control techniques, it does not require complete system knowledge which requires analytical model. In contrary, other AI techniques would require complete system knowledge for its development. However, this study emphasizes on the best possible solution to the problem rather than giving importance to the different control techniques. Therefore, FLC is considered as a convenient technique which can be applied to real systems with multiple inputs and outputs.

Today, engineers and researchers are considering fuzzy logic algorithms to implement intelligent controls in embedded systems. This would lead to a natural choice

of using embedded systems for solving complex real-world problems. However, the performance of an FLC strongly depends on its fuzzy parameters such as membership functions, rule base, and fuzzy inference system (FIS) of the process to be controlled [135]. Although a FLC does not have a systematic procedure in the design process, it requires proper tuning of fuzzy parameters to improve the performance. Many studies have shown the optimization can be based on trial and error [136], artificial neural network (ANN) [137], genetic algorithms (GA) [138], and particle swarm optimization (PSO) [139]. The trial and error method use initial system knowledge and estimates the fuzzy parameters until an optimal performance is obtained. Other learning algorithms like GA, ANN, and PSO have proven that these methods work very well. But, they are hybrid systems that combines other intelligent methods with fuzzy logic. Studies have shown that the implementation of hybrid systems [140] and combination of classical control techniques such as Fuzzy PID, Fuzzy PI etc., are on rising trend [141]–[143]. Moreover, the hybrid systems are also powerful and adaptive, although they require high level algorithms with time consuming processes that may not be desirable in certain control applications.

In recent years, numerous studies have reported on the FLC implementation in embedded systems such as field-programmable gate array (FGPA) [144], [145], digital signal processor (DSP) [146], and microcontrollers [147], [148] in various applications. In addition, a low-cost microcontroller Arduino has successfully implemented FLC in certain control applications such as liquid level control [149], temperature control [109], robotics [150], speed control for DC motors [151] and many more. These studies show an encouragement in FLC implementation for applications that require better performance compared to conventional control techniques. Likewise, some studies have reported on

the FLC implementation in powerful low-cost microcontroller Raspberry Pi. But, most of the studies were on applications that are based on facial recognition [152], Internet of Things (IoT) [110], [153], [154], navigation applications [155] etc. However, the implementation of speed control [156], robot control [111], [157], and temperature control system [158] using FLC looks promising. In a comparative study, the control behavior of FLC in Raspberry Pi was found to be better compared to Arduino in fluid flow control application [159]. The implementation of FLC in the literatures are mostly modeled for specific applications, not for general cases.

This chapter focusses on the implementation of FLC in a low-cost microcontroller Raspberry Pi and its algorithms for fuzzification, rule evaluation and defuzzification of a closed loop control system as stated in section 3.7.2. The effect of fuzzy parameters was compared and analyzed in real environment to achieve an optimal control. Thus, a fuzzy-logic based temperature control system consisting of a sensor, actuator and microcontroller was designed. The main goal of this work is to find a fuzzy logic model with an optimal combination of fuzzy parameters for the implementation in Raspberry Pi. Therefore, the optimal fuzzy logic model can be then applied to implement in DTCM.

5.2 Design and methodology

5.2.1 Experimental design

In this work, a simplified temperature controller model consisting of two tanks at a stable temperature of 34.5°C and 28.5°C has been proposed as shown in Figure 5.1. The proposed design concept was similar to the DTCM prototype except for the pre-heated tank. As this study emphasizes on optimization of fuzzy parameters, heated water and water at normal temperature were considered. The temperature was then controlled

according to the target temperature by varying the flow rates from the two different temperature tanks. At the same time, actual temperature was monitored using a sensor at the final tank and the final flow rate was maintained at 450 ml/min. Hence, the control of peristaltic pumps by varying the flow rates would be vital for the efficiency of the temperature control system. The experimental setup of the simplified temperature controller is shown in Figure 5.2.

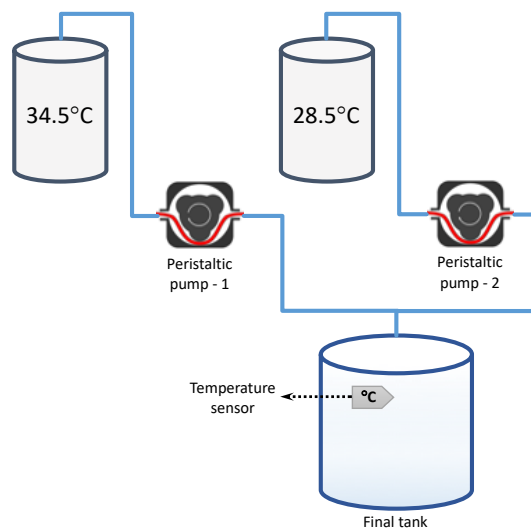


Figure 5.1 - Simplified temperature controller schematic for fuzzy logic optimization



Figure 5.2 – Experimental setup for a simplified temperature controller.

5.2.2 Fuzzy logic control design

In this study, a MISO (multiple input and single output) FLC was designed for the temperature control application as shown in Figure 5.3. As this study emphasizes on the implementation and optimization on FLC in Raspberry Pi, several fuzzy logic designs were considered using fuzzy logic toolbox in MATLAB. However, the approach of the design optimization was based on ‘trial and error’ method by considering certain factors such as model simplicity and computational efficiency for hardware implementation. Likewise, a normalized fuzzy system was chosen in order to eliminate the intervention on fuzzy logic design if any changes to be made on the controller.

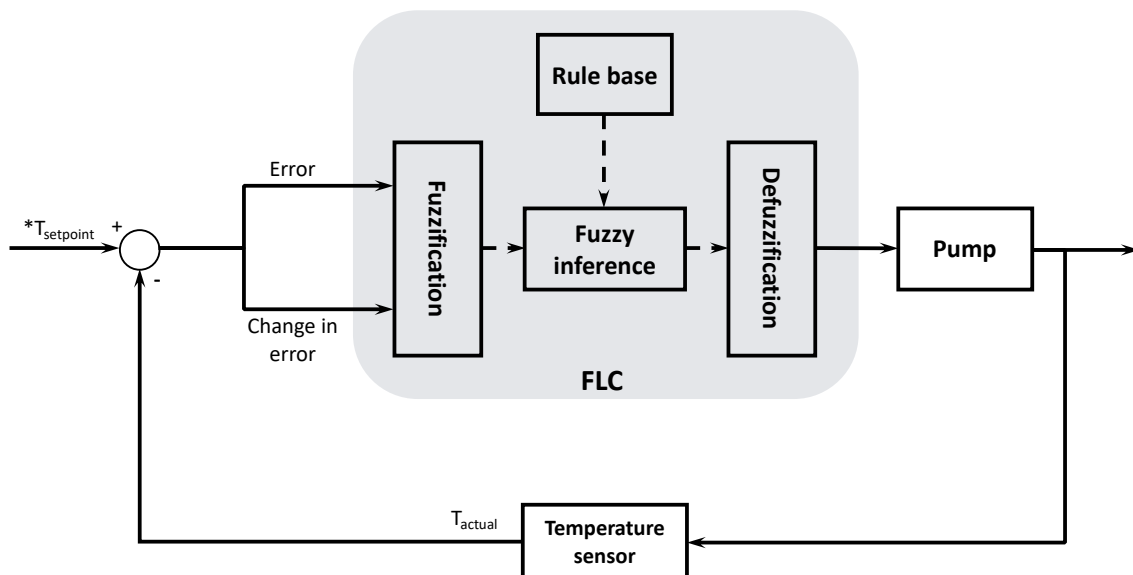


Figure 5.3 - Schematic diagram of FLC used for the proposed model.

The inputs error (e) denotes the error between setpoint and actual temperature and change in error (ce) denotes the difference between the present error (e_k) and the previous error (e_{k-1}) given by equations 5.1 and 5.2 respectively, where k is the sampling instance. Whereas the output ‘Pump’ (Δu) denotes the change of duty cycle signal to vary the speed is expressed in equation 5.3. The universe of discourse is set to fit into interval $[-1;1]$ for all the variables. A total of four designs were created and compared in

terms of fuzzification, rule base and defuzzification in the following sections. In order to select the most efficient model for the FLC temperature control interface, a comparison between two fuzzy models widely utilized have been tested in each design: Mamdani FIS and Sugeno FIS.

$$e(k) = T_{setpoint} - T_{actual} \quad (5.1)$$

$$ce(k) = e_k - e_{k-1} \quad (5.2)$$

$$u_k = u_{k-1} + \Delta u_k \quad (5.3)$$

5.2.2.1 Design-1

In this initial design, triangular membership functions were used to fuzzify the inputs as shown in Figure 5.4(a) and 5.4(b), whereas, triangular membership function was used for Mamdani output and singleton membership function was used for Sugeno output as shown in Figure 5.4(c) and 5.4(d). The membership functions were partitioned equally into three subsets for each input which are negative (N), zero (Z) and positive (P), whereas the three subsets for output are low (L), normal (N) and high (H).

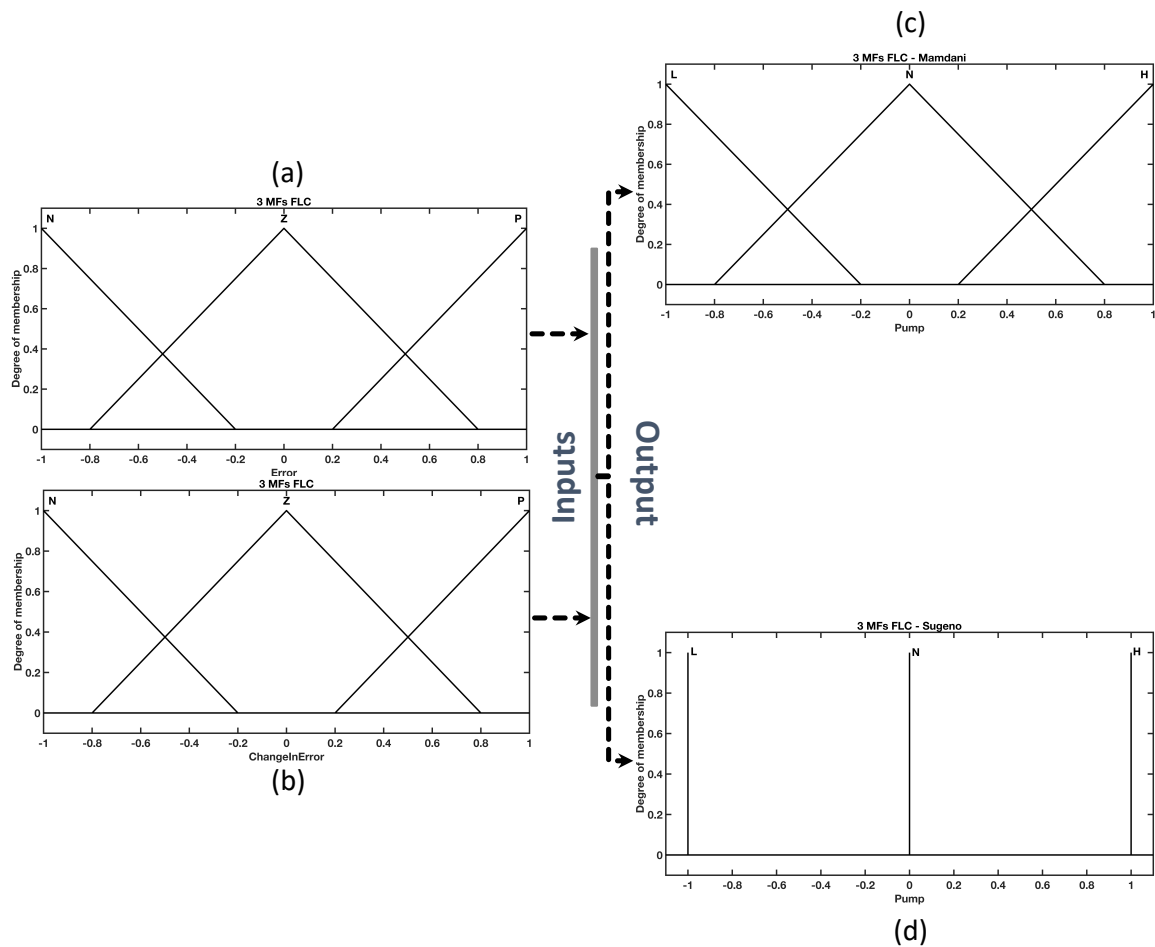


Figure 5.4 – Design-1 membership function of inputs (a) error and (b) change in error, while (c) and (d) shows the output membership function in Mamdani and Sugeno FIS respectively.

The fuzzy rules serve as the knowledge and skills of human operator who can make necessary modifications to run the system with faster response and minimal error. Therefore, the input signal signs e and ce are used to determine the signs of control signal Δu , which determines the FLC to increase or decrease the overall control action to the controlled system. According to the generalized approach in rule base construction, the sign of Δu should be positive if the final output u is required to be increased and vice versa [160]. In this model, the same approach has been considered for creating the rule-base table. By considering the three-membership function for inputs and outputs, a rule base table with nine rules were formed and shown in Table 5.1. Based on this design

approach, the normal (N) membership function was placed on the main diagonal separating the positive and negative parts; shown in Table 5.1. From the Table, a sample rule format is as follows,

Rule 1: IF error (e) is N AND change in error (ce) is N THEN pump (Δu) is L.

Table 5.1 – Rule base for Design-1

$\Delta e \backslash e$	N	Z	P
N	L	L	N
Z	L	N	H
P	N	H	H

The final control output signal is the crisp value that is defuzzified from the inference processes of the fuzzy rule base. In Mamdani FIS output, the most commonly used technique for defuzzification; centroid has been applied as shown in equation 5.4. While, the commonly used defuzzification method for Sugeno FIS is Weighted average, which is expressed in equation 5.5.

$$\Delta u = \frac{\sum_i^n u_i \cdot \mu(u_i)}{\sum_i^n \mu(u_i)} \quad (5.4)$$

$$\Delta u = \frac{\sum_j^n u_j \cdot w_j}{\sum_j^n w_j} \quad (5.5)$$

Here, Δu denotes output value, u_i denotes the value of membership function centroid, $\mu(u_i)$ denotes the degree of membership, w_j denotes the output weights and n denotes the number of elements in a sample. The control surface that illustrates the complete operation of the FLC is shown in Figure 5.5. It can be seen that the output surface of Mamdani FIS has an effect of a larger area around zero compared to Sugeno

FIS, which means the stability point will be focused on zero. Moreover, the control surface of Sugeno can be approximated by linear surface than Mamdani FIS.

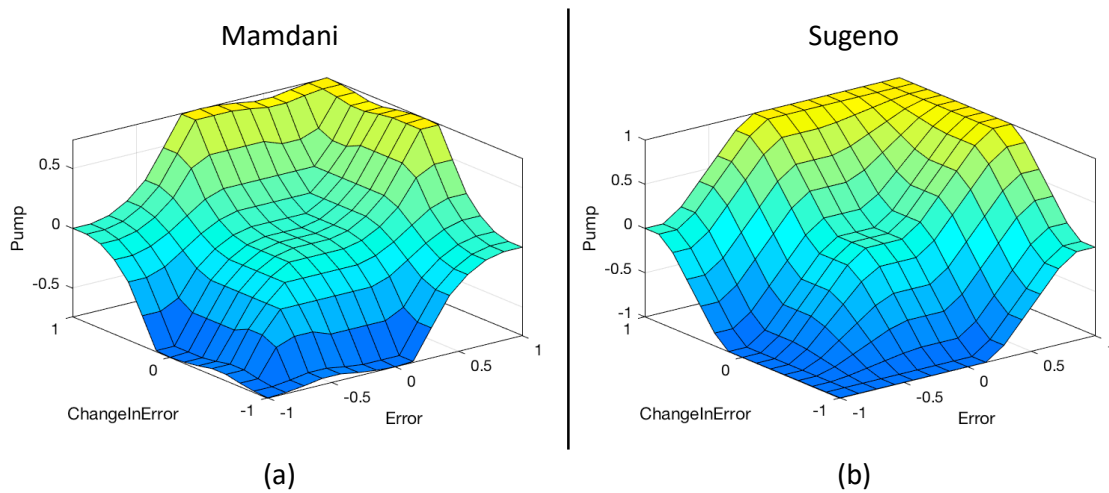


Figure 5.5 - Control surface of (a) Mamdani FIS and (b) Sugeno FIS for Design-1

5.2.2.2 Design-2

In this design, triangular membership functions were used to fuzzify the inputs and Mamdani output, while Sugeno output uses singleton function as shown in Figure 5.6. A five membership function was used for the input 'error' and the input 'change in error' employs a three membership function, the same as in Design-1. Also, a five membership function was utilized for the output 'pump' with the intention to improve the resolution. The five membership function for input 'error' was represented by linguistic variables such as negative large (NL), negative small (NS), zero (Z), positive small (PS) and positive large (PL). Similarly, five membership function was assigned to output 'Pump' and represented as very low (VL), low (L), normal (N), high (H) and very high (VH).

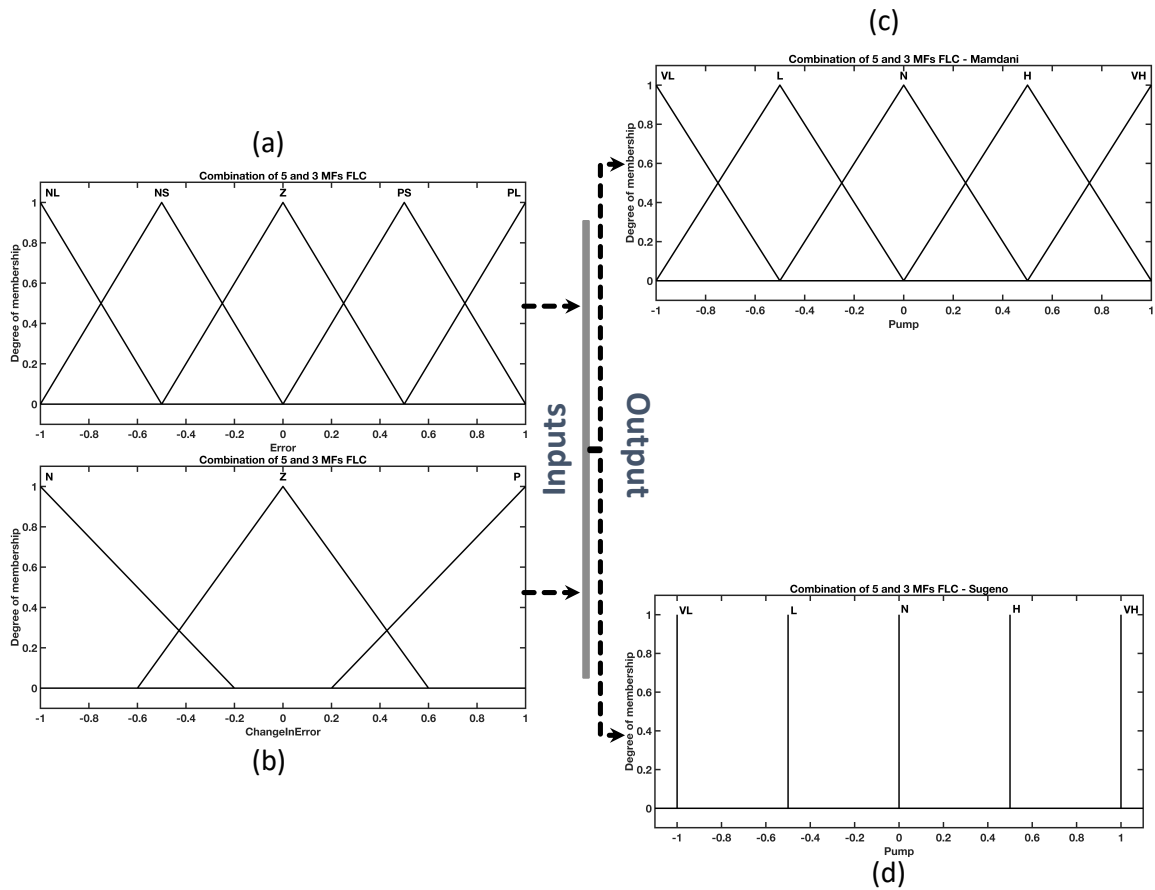


Figure 5.6 - Design-2 membership function of inputs (a) error and (b) change in error, while (c) and (d) shows the output membership function in Mamdani and Sugeno FIS respectively.

Since this design employs two different number of membership functions in inputs and output, a rule base table with a total of 15 fuzzy rules was formed and shown in Table 5.2. Since this is a non-symmetrical matrix, the assigned rules were mainly based on the dynamic of the error signal behaviour. The output control signal was defuzzified using the same technique as mentioned in Design-1. The control surface that illustrates the complete operation of the FLC is shown in Figure 5.7.

Table 5.2 - Rule base for Design-2.

Δe \ e	NL	NS	Z	PS	PL
N	VL	VL	L	N	N
Z	L	L	N	H	H
P	N	N	H	VH	VH

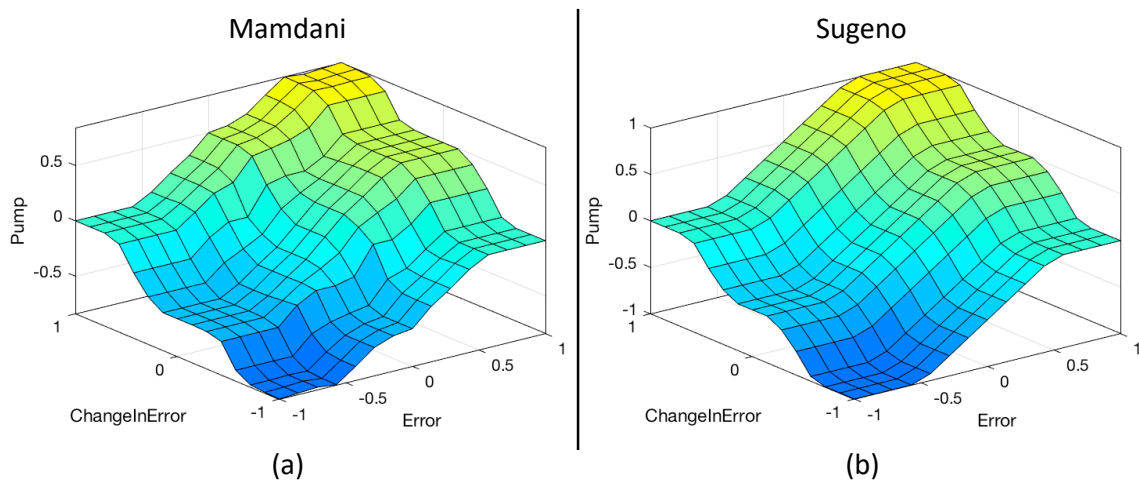


Figure 5.7 - Control surface of (a) Mamdani FIS and (b) Sugeno FIS for Design-2

5.2.2.3 Design-3

In this design, a trapezoidal membership was assigned on the extreme boundaries of both the inputs, while the triangular membership functions were used in the middle range as shown in Figure 5.8. Meanwhile, the output membership function remained the same as Design-2. This approach was intended to alter the type of membership function rather than increasing the number of membership functions. As this design utilizes the same number of membership functions, the rule base table from Design-2 was utilized for this design as shown in Table 5.2. The output control signal was defuzzified using the same technique as mentioned in Design-1. The control surface that illustrates the complete operation of the FLC is shown in Figure 5.9.

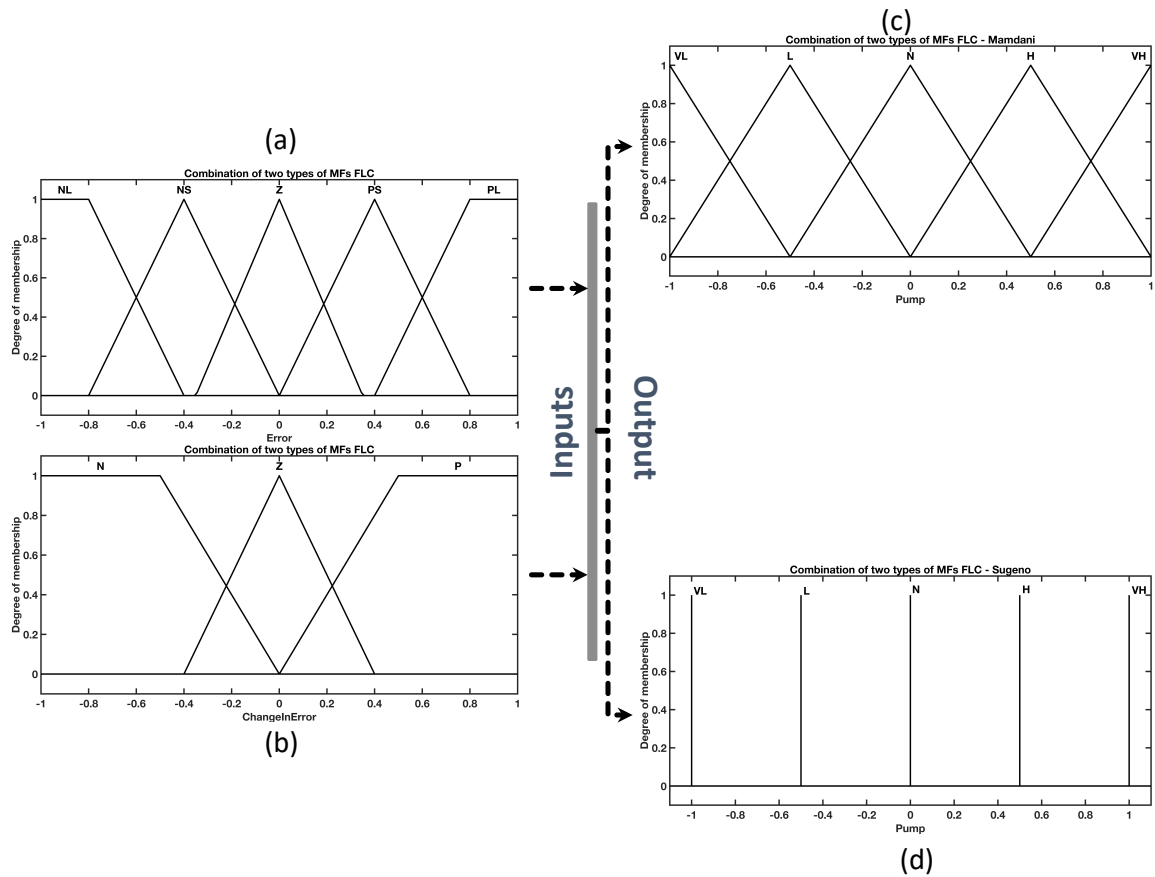


Figure 5.8 - Design-3 membership function of inputs (a) error and (b) change in error, while (c) and (d) shows the output membership function in Mamdani and Sugeno FIS respectively.

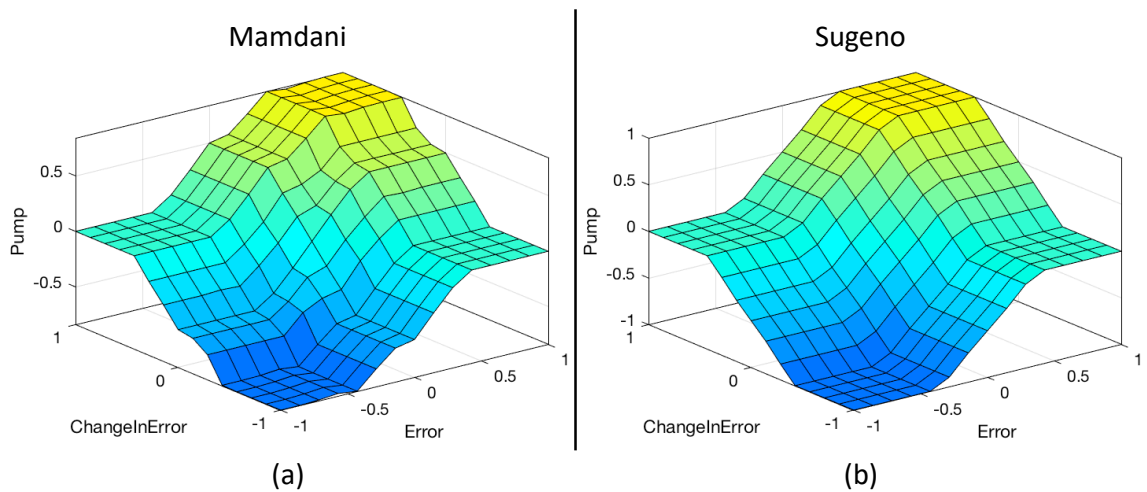


Figure 5.9- Control surface of (a) Mamdani FIS and (b) Sugeno FIS for Design-3

5.2.2.4 Design-4

This design utilizes same strategy as Design-1 with the triangular membership functions for inputs and Mamdani output, while Sugeno uses the usual singleton

membership function. The only difference comparing to Design-1 is the number of membership functions. In this design, the membership functions were equally portioned into five subsets for each inputs and output as shown in Figure 5.10.

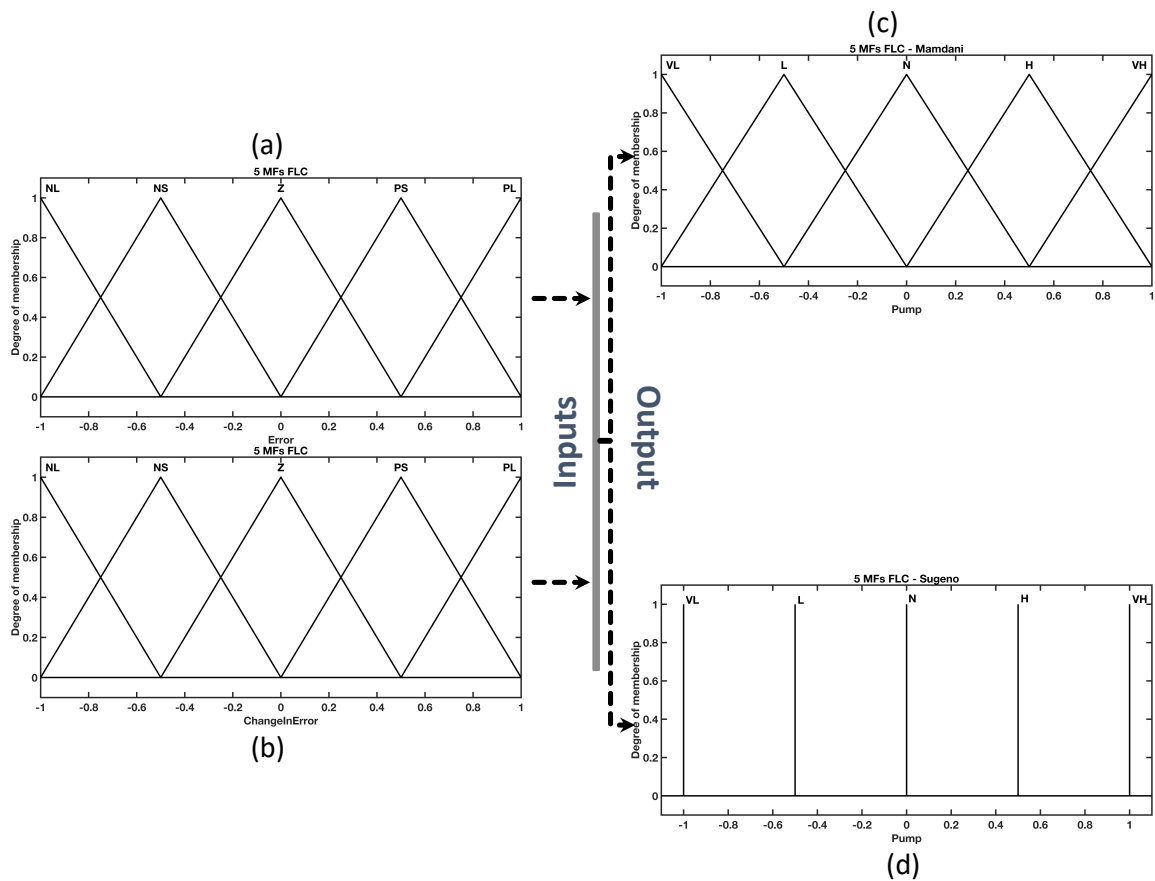


Figure 5.10 - Design-4 membership function of inputs (a) error and (b) change in error, while (c) and (d) shows the output membership function in Mamdani and Sugeno FIS respectively.

Based on the generalized approach of rule base construction, the normal (N) membership function were placed on the main diagonal; while separating the positive and negative parts were divided into sub-regions such as VL, L, H and VH as shown in Table 5.3. As a result, a symmetrical matrix with a total of 25 fuzzy rules were obtained. However, the output control signal was defuzzified using the same technique as mentioned in Design-1. The control surface that illustrates the complete operation of the FLC is shown in Figure 5.11.

Table 5.3 - Rule base for Design-4

Δe \ e	NL	NS	Z	PS	PL
NL	VL	VL	VL	L	N
NS	VL	VL	L	N	H
Z	VL	L	N	H	VH
PS	L	N	H	VH	VH
PL	N	H	VH	VH	VH

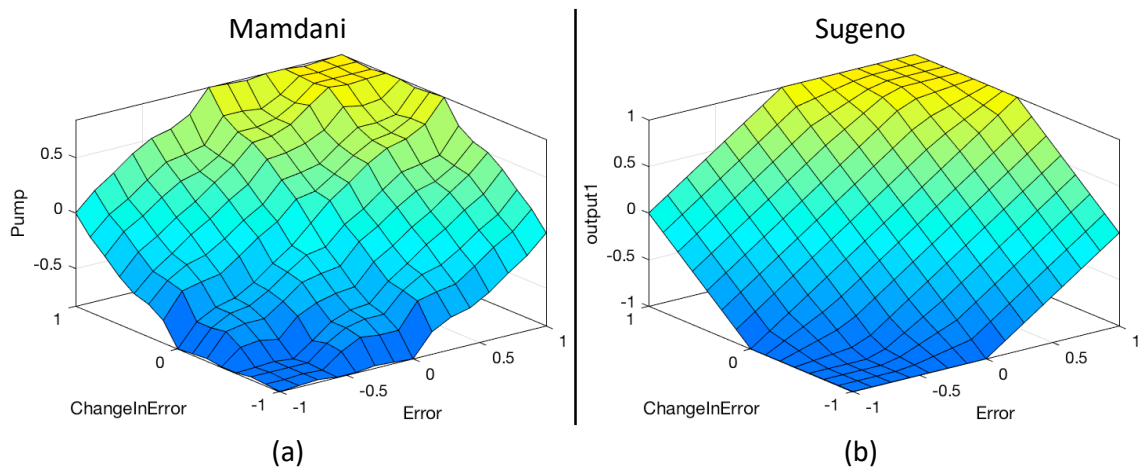


Figure 5.11 - Control surface of (a) Mamdani FIS and (b) Sugeno FIS for Design-4

5.2.3 Implementation design

The hardware components of DTCM prototype that were used for the proposed model is mentioned in section 3.6.1.2. It was then interfaced to Raspberry Pi and executed the proposed model externally using MATLAB/Simulink as stated in section 3.6.2.2. In addition, scaling factors were introduced for the flexibility of the system. By changing the scaling factor, the user can easily modify the control circuit. In other means, the scaling factor in the inputs were utilized to keep the values between $[-1,1]$ for the fuzzy inputs. Similarly, FLC generates the output signal in the range $[-1,1]$, that is further multiplied by a scaling factor; obtaining the final modification of the control at each

sample time. The final modification of duty cycle is updated according to equation 5.3. The range of variation is limited between 0 and 255 by saturation block. The fuzzy signal was fed to one of the peristaltic pumps with an appropriate duty cycle, while the other was fed with the remaining duty cycle in order to achieve a stable flow rate at the final tank. The overall Simulink model is shown in Figure 5.12.

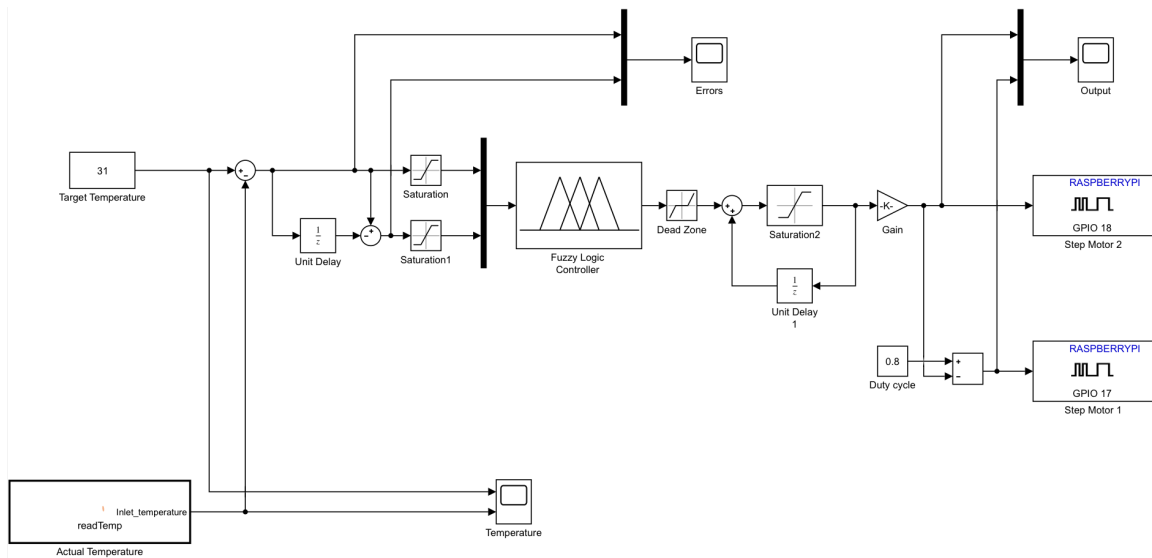


Figure 5.12 – Simulink model for the proposed temperature control system.

5.2.4 Evaluation factors

To compare the different types of fuzzy logic designs, several practical aspects have been considered in this study as they are critical to the success of the DTCM prototype application. The control system performance is initially measured by applying a step function as the setpoint and then measuring the response of the process variable. The basic factors in transient response such as overshoot, rise time, and peak values were analysed from the controller output. Moreover, the commonly used performance indices namely Integral absolute error (IAE), integral squared error (ISE) and integral time absolute error (ITAE) were used to quantitatively measure the performance of the system. These performance indices were analysed during steady state output to fall

within a 2% threshold of setpoint (t_s) until infinity (∞). Therefore, the control objective is to minimize the errors of each performance index. Mathematical equations for such quantitative measure are given in equations 5.6, 5.7 and 5.8. Among the proposed four designs, an optimal fuzzy logic design was then considered for the multiple setpoint response in order to evaluate the implementation in DTCM prototype.

$$IAE = \int_{t_s}^{\infty} |e(t)| dt \quad (5.6)$$

$$ISE = \int_{t_s}^{\infty} e^2(t) dt \quad (5.7)$$

$$ITAE = \int_{t_s}^{\infty} |e(t)|t dt \quad (5.8)$$

5.3 Results and discussion

The working of temperature controller based on FLC was implemented and verified on low-cost microcontroller Raspberry Pi for different scenarios by the step response for a user-specified set point temperature. The system presents the response of setpoint temperature at 31°C, which lies in between temperature of the two tanks. The actual temperature from the sensor was monitored at a sample time of 0.50 seconds in real-time using Simulink environment. Besides, an error tolerance band was introduced within 1% error from the setpoint to analyse the effectiveness of temperature controller. The tolerance band was set to be narrower band than the existing HD system tolerance band of $\pm 0.5^\circ\text{C}$. The controller response for each design were compared against both FIS – Mamdani and Sugeno as shown in the following sections.

5.3.1 Design-1

Figure 5.13 depicts experimental behavior of the temperature controller responses at the pre-defined setpoint. From the response, it can be observed that the

temperature has reached the setpoint from the room temperature after 45 seconds for Mamdani FIS, while Sugeno FIS has taken 48.5 seconds after the overshoot. However, the steady state condition was then achieved with a minute deviation of $\pm 0.25^{\circ}\text{C}$, which lies within the specified tolerance band. In addition, it was noticed that output temperature settles after an overshoot of 2.02% and 1.21% for Mamdani and Sugeno FIS respectively; which goes beyond the tolerance band. This is attributed to the design utilizing minimum number of rules and membership functions. As a result, the controller couldn't adapt to small margin of error or sudden minor changes in the output.

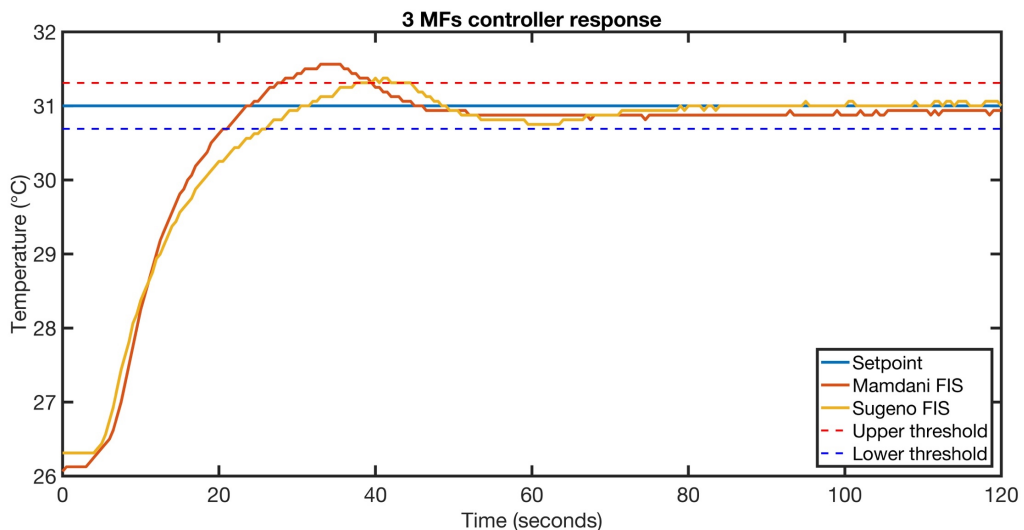


Figure 5.13 – Controller response for Design-1

The peristaltic pumps output, which plays a key role in actuating the heating system in the controller were plotted as shown in Figure 5.14. The actuator consists of two pumps namely HT pump that transfers high temperature fluid, while LT pump transfers low temperature (also known as room temperature) fluid. From the graph, it can be seen that both FIS results a steady output after reaching the steady state. However, Sugeno FIS have made a slight adjustment in order to minimize the steady state error, since the output temperature has reached an error of -0.25°C . Furthermore, the

combined duty cycle of the two pumps was found to be 80%, which substantiates the required flow rate.

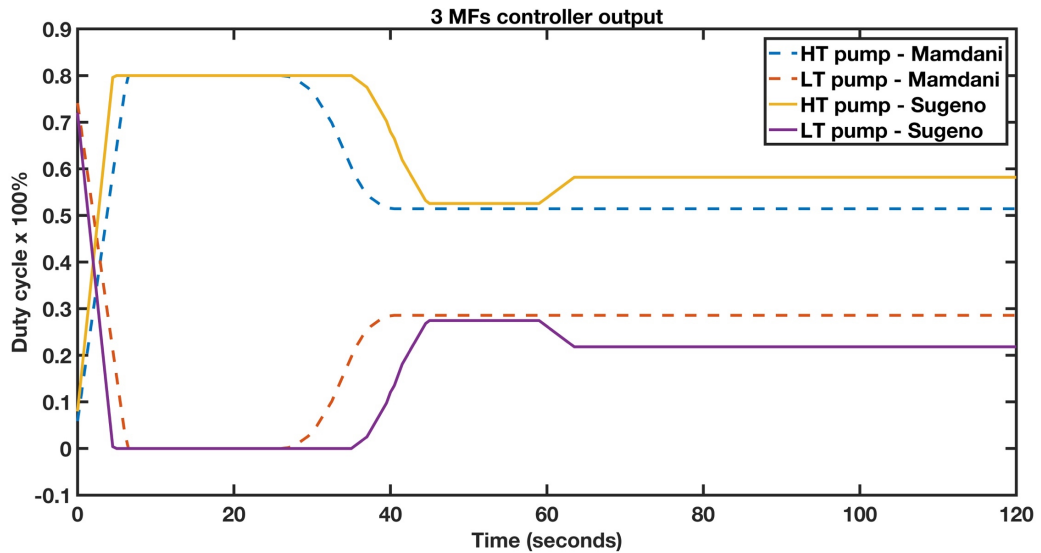


Figure 5.14 – Pump output response for Design-1

Recent study revealed an implementation of fuzzy logic based temperature control system which utilized heating resistor as an actuator [109]. The study employs Sugeno FIS with a similar rule base and fuzzy logic design implemented in an Arduino board for the purpose. As a result, an overshoot of 0.5°C was observed for the setpoint of 37°C in the published literature, while the proposed method shows an overshoot of 0.375°C in Sugeno FIS. The difference of the overshoot can be due to the difference in setpoint and actuator properties as both the response started from the room temperature. This validates the behaviour of FLC temperature controller in real-time environment.

5.3.2 Design-2

With the introduction of five triangular membership functions for an input and output, the overshoot has reduced in the temperature control response as shown in Figure 5.15. However, the temperature reaches the setpoint after 31.5 seconds and 28

seconds for Mamdani and Sugeno FIS respectively. The faster time is due to the higher room temperature at the beginning. Again, the temperature response for both FIS results in a persistent oscillation, yet still lies under the tolerance band throughout the experiment. To be precise, the Sugeno FIS shows lesser deviation of $\pm 0.19^{\circ}\text{C}$ compared to Mamdani FIS with a deviation of $\pm 0.31^{\circ}\text{C}$. Most importantly, the overshoot for both FIS were eliminated significantly compared to Design-1.

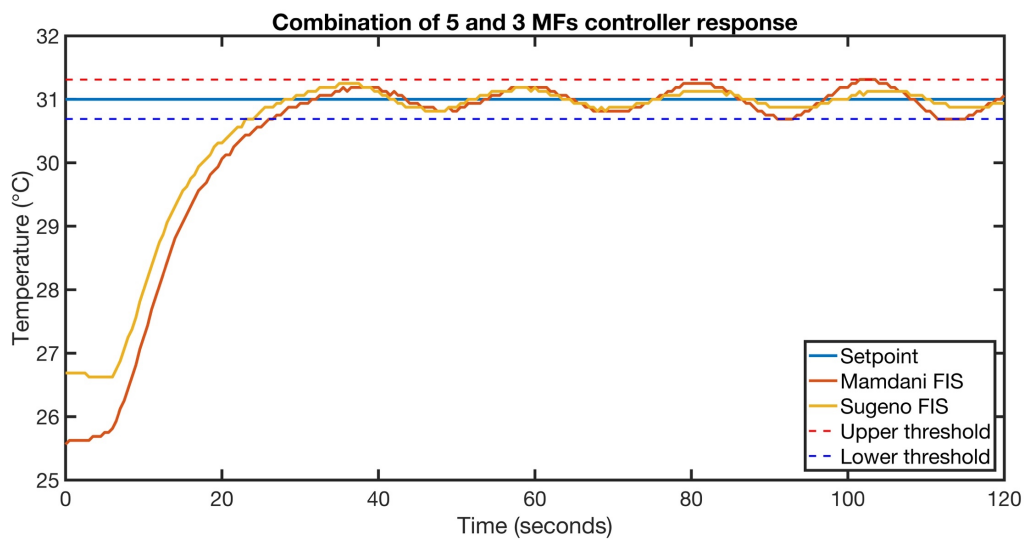


Figure 5.15 - Controller response for Design-2

Figure 5.16 shows the output control signal for the peristaltic pumps and it can be seen that the duty cycle is oscillating during steady state condition. An experimental study for the direct torque control in an Induction machine utilizing the similar Mamdani FIS based fuzzy logic design was reported [144]. Furthermore, a wall-following robot with different number of membership functions for input and output was implemented in a Raspberry Pi microcontroller [111]. The controller response with a similar oscillations trend were observed in both studies. This can be due to the design utilizing different number of membership functions for the input, which results in a non-symmetrical rule base table.

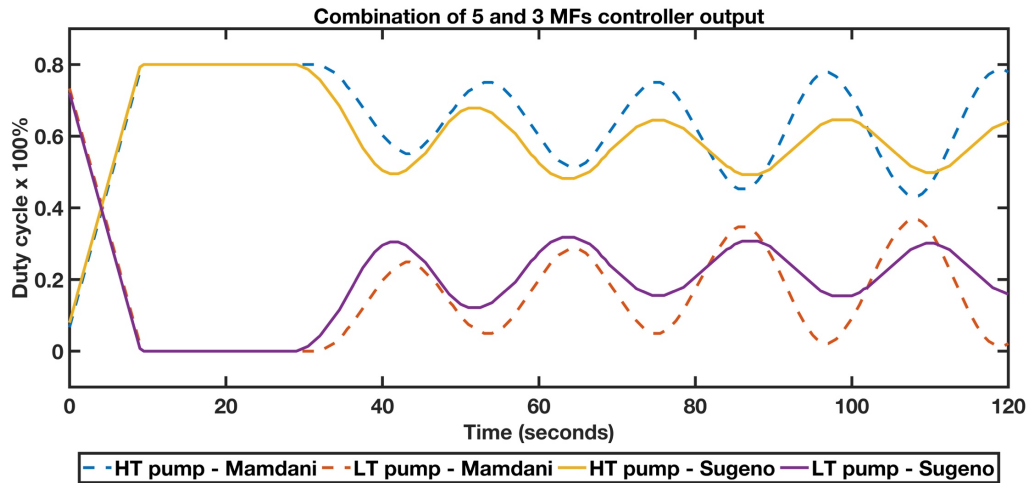


Figure 5.16 - Pump output response for Design-2

5.3.3 Design-3

Figure 5.17 depicts the temperature response for the design consisting of triangular and trapezoidal membership functions for inputs. According to the graph, it can be observed that the temperature has reached the setpoint after 31 seconds for Mamdani FIS, while Sugeno has taken 40.5 seconds. However, the overshoot for both FIS were eliminated, similar to Design-2. Subsequently, the steady state condition for the Sugeno FIS was found to be encouraging with a small deviation of $\pm 0.06^{\circ}\text{C}$. In contrary, Mamdani FIS response was unstable within 1% tolerance band. Some studies have reported the performance comparison of Mamdani and Sugeno FIS, which shows insignificant differences between their responses [137], [161]. As expected, the output control signal for both FIS was found to be oscillating as shown in Figure 5.18. Studies have reported similar fuzzy logic designs utilizing Mamdani FIS for temperature control and speed control [147], [148]. Those results show that there is a slight fluctuation in the steady state response, similar to Design-3 controller response. Moreover, a preliminary result on fuzzy logic based dialysate temperature control system was reported in a recent study [78]. It was implemented using STM32F4 microcontroller utilizing the combination

of trapezoidal and triangular membership functions. In that work, the temperature response with a deviation of $\pm 0.5^{\circ}\text{C}$ during steady state was reported in a real time experiment. This could be due to the difference in number and type of membership functions used for inputs, resulting in a sinusoidal output signal response.

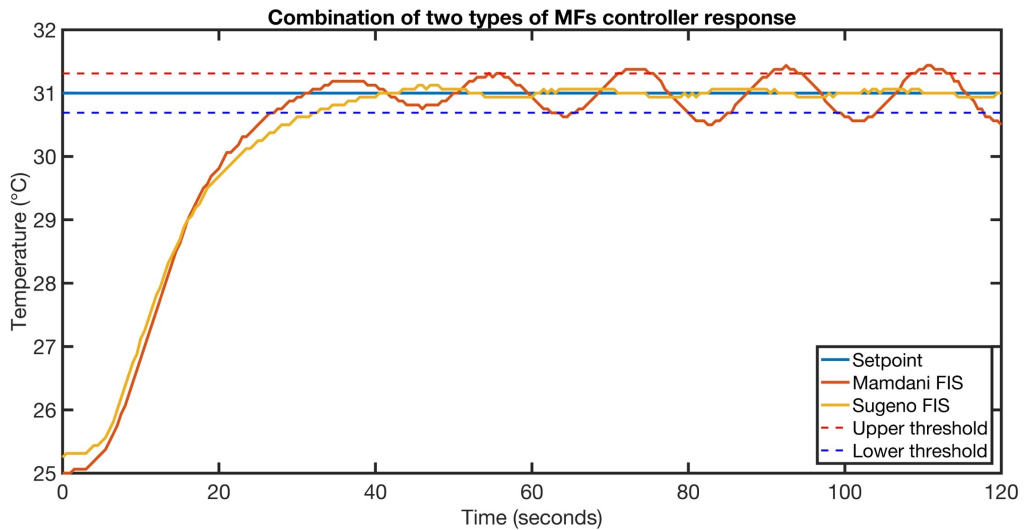


Figure 5.17 - Controller response for Design-3

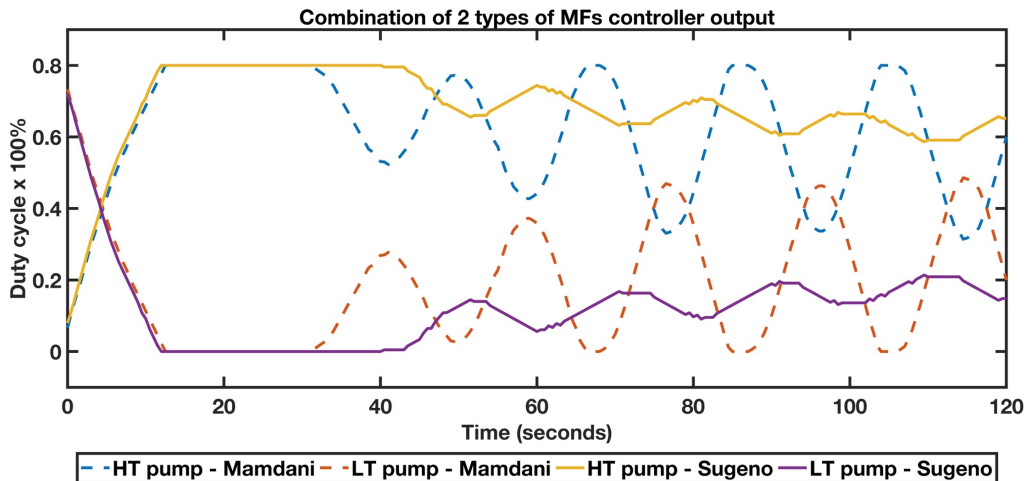


Figure 5.18 - Pump output response for Design-3

5.3.4 Design-4

The temperature response consisting of five triangular membership functions for inputs and output is shown in Figure 5.19. According to the graph, it can be seen that the responses of both FIS were encouraging without any overshoot. However, the

temperature reached the setpoint after 39 seconds for Mamdani FIS, while Sugeno FIS has taken 34.5 seconds. Moreover, the steady state region was reliable with a negligible deviation of $\pm 0.125^\circ\text{C}$ for both FIS, which absolutely lies inside the tolerance band. A similar experimental fuzzy logic design was reported for a DC-DC power boost converter application [81]. The experimental response revealed a negligible overshoot and steady state error compared to PI control. Figure 5.20 shows the control output signal for the Design-4. It can be observed that the output signal oscillates during the initial steady state region and slowly settles without a significant change in temperature. This shows a potential approach towards the symmetrical membership functions and rule base design strategy for certain applications.

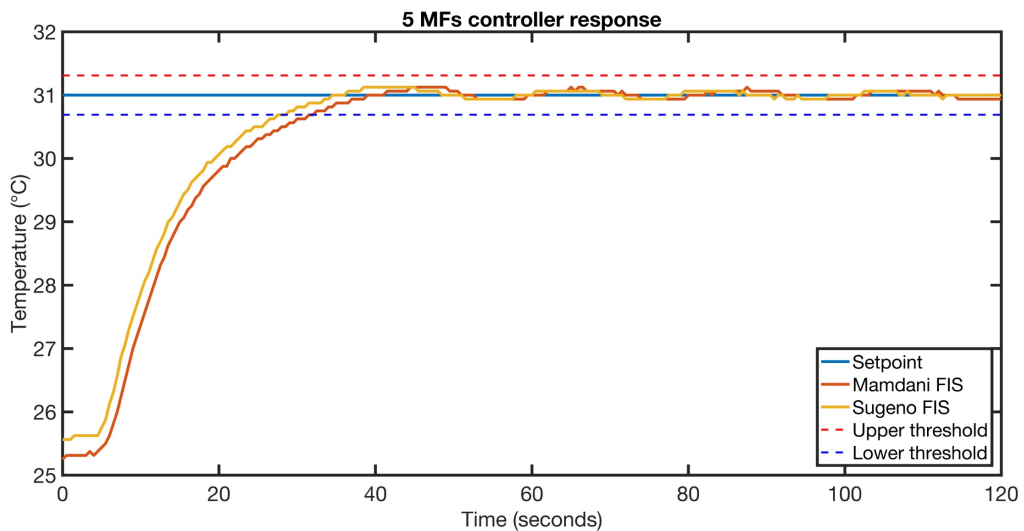


Figure 5.19 - Controller response for Design-4

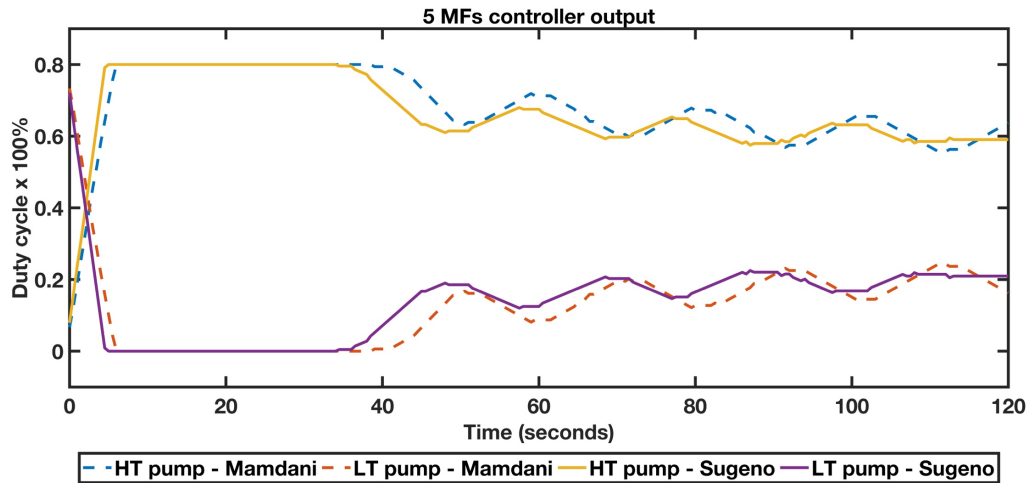


Figure 5.20 - Pump output response for Design-4

5.3.5 Summary of results

The performance indices such as IAE, ISE and ITAE were evaluated in order to demonstrate the performance of the proposed designs. Figure 5.21 summarizes the performance analysis. From the graph, it can be inferred that the performance of Design-4 is excellent compared to other designs. In Design-4, Sugeno FIS has exhibited slightly lesser error during steady state with IAE = 6.99, ISE = 1.61 and ITAE = 330.14 compared to Mamdani FIS with IAE = 8.09, ISE = 1.85 and ITAE = 447.03. The large value of error demonstrates the higher value in ISE than IAE. But, IAE expresses the cumulative error magnitude and ISE expresses the square of error. These values indicate better performance in the steady state for Design-4 FLC compared to other proposed designs. However, the error difference between Sugeno and Mamdani FIS were found to be small in Design-4.

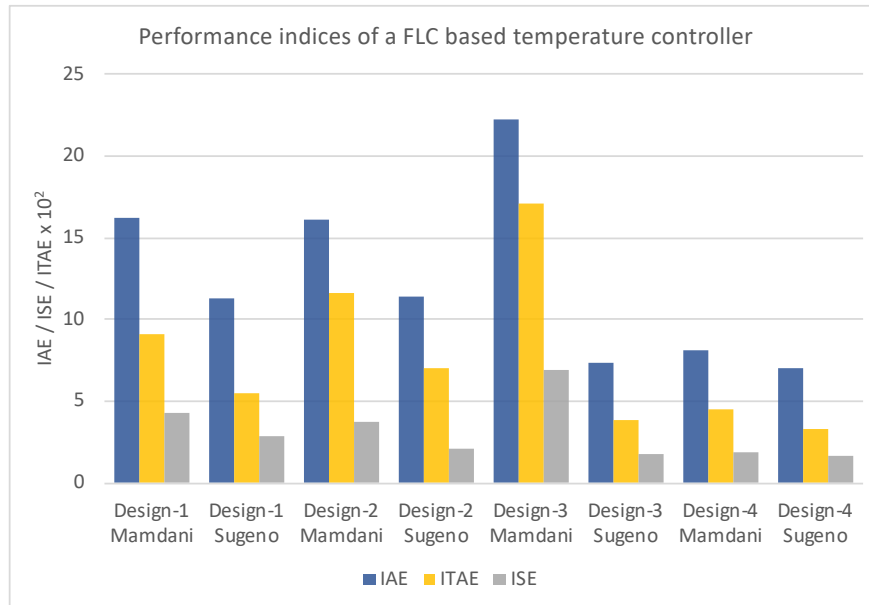


Figure 5.21 – Bar graph showing the comparison of performance indices among the proposed designs

Conversely, Mamdani FIS in Design-3 has shown larger error values due to their high deviation in temperature during steady state as shown in Figure 5.17. Also, it shows larger error difference between its Sugeno FIS performance. Therefore, it can be seen that the Sugeno FIS outperforms Mamdani FIS proportionally in all designs except in Design-3. This could be due to their linear surface of output, which allows the change of output linearly. In the other case, the IAE and ISE (7.31 and 1.73 respectively) of Design-3 Sugeno FIS was found to be minimum, while the ITAE (384.41) was larger compared to Design-4. As ITAE depends on the time factor, it will penalize the error heavily on the later stage of steady state. Therefore, Sugeno FIS in Design-3 illustrates slightly higher error deviation compared to Design-4.

Table 5.4 – Comparison of transient response among the proposed designs

Designs	FIS	Rise time (seconds)	Overshoot (%)	Peak (°C)
Design-1	Mamdani	12.6	2.02	31.562
	Sugeno	17.17	1.21	31.375
Design-2	Mamdani	17.13	0.81	31.312
	Sugeno	12.96	1.01	31.25
Design-3	Mamdani	14.35	3.07	31.437
	Sugeno	20.87	0.4	31.125
Design-4	Mamdani	19.43	0.61	31.125
	Sugeno	18.19	0.4	31.125

The basic control characteristics namely the rise time, overshoot and peak temperature were tabulated in Table 5.4. As expected, both FIS in Design 1 were subjected to an overshoot with a peak temperature of 31.562°C for Mamdani FIS and 31.375°C for Sugeno FIS. Minimal overshoot was noticed for both FIS in Design-4 and Sugeno FIS in Design-3. It can be seen that the peak has decreased with the increase in membership functions. Lesser importance was given to rise time analysis as the initial temperature varies in every experiment. Also, it can be observed that there is a dead time at the initial time of temperature response graphs. The dead time indicates the time taken by the fluid to reach the temperature sensor to return the data for computation. Considering these factors, Design-1 have shown faster rise time with overshoot, while Design-4 shows slower response with maximum accuracy. Therefore, the fuzzy logic design in Design-4 was considered as the optimal design to be implemented for further analysis.

5.3.6 Multiple setpoint of optimized design

The optimal fuzzy logic is then evaluated for the user-defined multiple setpoints of temperature 31.5°C, 29.5°C and 31°C at a regular interval of 50 seconds. The setpoints were selected within the range of inlet temperatures. This study enables us to analyse the optimal control behaviour in the case of changing setpoints over time, which is crucial in certain applications especially in dialysate temperature controller. As mentioned earlier, it was introduced with a 1% tolerance band to analyse the effectiveness of the controller. The temperature response of the multiple setpoint temperature is shown in Figure 5.22.

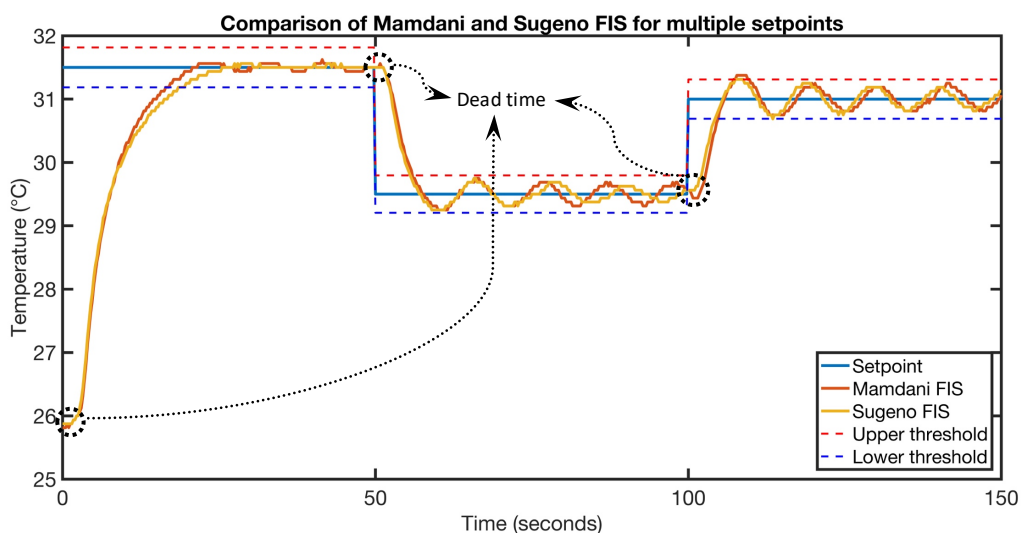


Figure 5.22 – Controller response for multiple setpoint of optimized design

From the response, it can be observed that both FIS performs exceptionally well in different setpoints as expected. More importantly, the controller was able to maintain the temperature within the tolerance band, which shows the effectiveness and controllability in the design optimization. The performance of Mamdani and Sugeno FIS works almost in identical fashion without any large effect in the response as mentioned in literatures [137], [161]. As expected, the similar response of both FIS was mainly due

to the utilization of similar defuzzification techniques. In terms of performance indices, both FIS shows a negligible effect as shown in Table 5.5. The temperature has reached the 1st setpoint after 21 seconds, and then temperature cooled down to 2nd setpoint after 7 seconds and then increased the temperature to 3rd setpoint after 5.5 seconds. The response time for changing setpoints were encouraging. Especially, the sudden fall in temperature response for 2nd setpoint was superior compared to conventional heater control design. In addition, the dead time was observed on all setpoints and labelled in Figure 5.22. The dead time can be reduced by reducing the length of tubing resulting in a faster fluid transfer to the final tank since the flow rate needs to be controlled. Generally, the fuzzy logic design comprises of symmetrical rule base and membership functions revealed a better response compared to other fuzzy logic design through real-time experiments.

Table 5.5 – Performance indices for the multiple setpoints

Setpoints	FIS	IAE	ISE	ITAE
31.5->29.5->31	Mamdani	68.74	184.92	2489.5
	Sugeno	66.93	179.56	2246.8

Numerous studies have implemented and experimentally validated the fuzzy logic-based temperature controller for various applications [113], [148], [162]. The performance of the proposed optimal fuzzy logic design was found to be superior when compared to the published studies. In comparison with a recent experimental study of fuzzy based temperature controller has reported the response with 0.5°C of overshoot, 0.25°C of undershoot and 216.5 seconds of rise time to heat up about 7°C of fluid; is shown in Figure 5.23 [109]. This shows a remarkable improvement in the response time and accuracy of the proposed model. However, the better performance indicates the

efficiency in the process design considering the pump as actuator, while other studies have used heaters as actuators [109], [148]. This would benefit in achieving the setpoint temperature with a quick response time. On the negative side, the proposed design could be able to regulate the temperature only within the range of temperature in storage tanks. In the proposed system design, the temperature in storage tanks were kept constant, yet it would be subjected to a temperature tolerance of $\pm 0.5^{\circ}\text{C}$ as the tanks were not insulated appropriately. Hence, the temperature in storage tank should be insulated to keep it constant especially for application that requires a longer duration of usage.

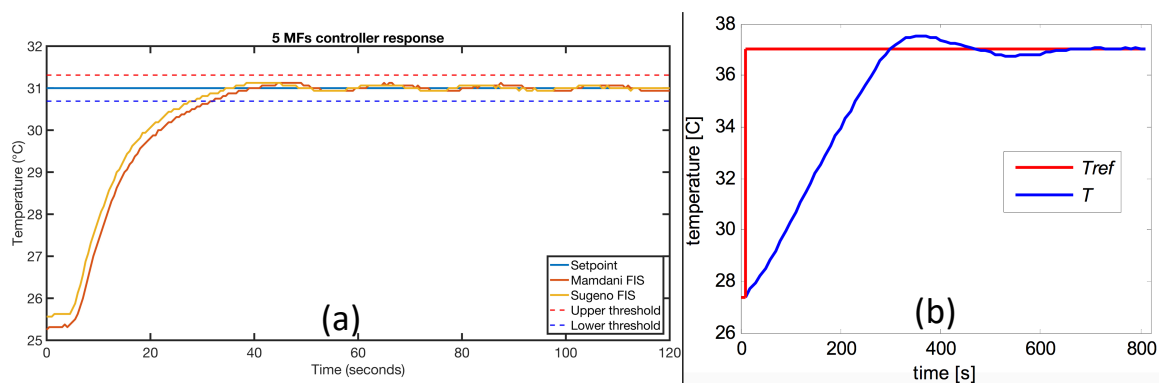


Figure 5.23 – Comparison of (a) optimized fuzzy logic design temperature setpoint response with (b) published fuzzy logic temperature control response [109].

Considering the proposed fuzzy logic designs, only triangular and trapezoidal membership functions were utilized, even though there are many membership functions such as Gaussian, sigmoidal, and polynomial based membership functions that are accessible. This is mainly because of its simplicity and computationally efficient, while other utilizes non-linear functions, which results in increase in computational time. This is why the triangular and trapezoidal membership functions are widely implemented in real applications.

It can be realized that the performance of Mamdani FIS and Sugeno FIS were fairly identical in the optimized fuzzy logic design. Successively, the FIS selection for the DTCM prototype becomes quite challenging as both FIS have pros and cons. Based on literatures, it can be inferred that Mamdani FIS allows the system to be more intuitive, which performs like human knowledge even in the case of any unforeseen disturbances, yet it consumes more computational power [163]. On the other hand, Sugeno FIS is more compact and computationally efficient. However, no noticeable delay in executional performance was observed in both FIS throughout the experiments. It might be due to the seamless interface between Raspberry Pi and the MATLAB environment. In addition, the Sugeno FIS is mainly widely used for adaptive techniques along with other control techniques such as ANFIS, PID etc., as it allows customization [150], [164]. Although, the Sugeno FIS demonstrates higher accuracy than Mamdani FIS, Mamdani FIS demonstrates high consistency in results [165]. Therefore, Mamdani FIS was selected for the DTCM prototype by considering the factors such as consistency and wide acceptance.

In comparing the experimental results of various fuzzy logic designs, an optimized fuzzy logic design was achieved for a temperature controller application. An optimal fuzzy logic design of its parameter values is very important to achieve the performance of the fuzzy controller, which is beneficial to the development of the DTCM prototype. Furthermore, this chapter illustrates the generalized optimization approach which shows the effect of fuzzy logic parameters on their real outputs in implementation with faster effective response to solve real-world problems.

5.4 Conclusion

In conclusion, a fuzzy logic based temperature controller was evaluated in terms of performance indices such as IAE, ISE and ITAE for the proposed fuzzy logic designs. The results showed that Design-4 with a symmetrical rule base and highest number of overlapping triangular membership functions was superior in its system performance. The minimum peak temperature of 31.125°C with less deviation in steady state was achieved for the optimized fuzzy logic design, which implies a better response than those presented in literatures of fuzzy logic based temperature controllers. However, the Mamdani and Sugeno FIS showed fairly identical performance in both single setpoint and multiple setpoint experiments that is in line with the published literatures. In future, the optimized fuzzy control design can be utilized for certain applications that requires narrow range of output with high accuracy. The results from this chapter provide a better understanding of implementation and optimization of fuzzy logic control in cost-effective microcontroller Raspberry Pi and a motivation factor to implement the optimal fuzzy logic design in the DTCM prototype.

IMPLEMENTATION OF DIALYSATE TEMPERATURE CONTROL MODULE PROTOTYPE AND ITS IN-VITRO EVALUATION

6.1 Introduction

Temperature is considered as one of the vital parameters for dialysis performance in terms of patient's quality of life. During HD treatment, it would cause a significant quantity of heat loss in extracorporeal circuit, which can be usually compensated by dialysate and cyclic blood in dialyzer. Generally, the dialysate for the entire treatment was set to a constant temperature using a heater in the dialysate circuit. Several studies have reported on various dialysate temperature settings for the benefits of patient's hemodynamic stability during the treatment as mentioned in section 2.2. From the literatures, it was clear that the individualized and seamless temperature control in hemodialysis is much required to minimize the complications.

Until now, there has been only one commercially available device built into a HD machine that was able to measure and control the body temperature and thermal balance of the extracorporeal circuit - Blood Temperature Monitor (BTM) by Fresenius® [57], [65]. The controller is equipped with sensors to measure the venous and arterial temperature and the required dialysate temperature is calculated on the basis of results from temperature measurement, actual blood flow and several other constraints in order to get the precise outcome. However, with the usage of BTM, the hypotensive episode

was reduced from 50% to 25% during dialysis session with better hemodynamic stability [19]. Also, dialysis adequacy was not influenced by temperature control [66]. On the other side, studies based on BTM and other temperature biofeedback systems were quite sparse, and it was less renowned in the current society especially third world countries [23]. In fact, the BTM module allows its implementation only in Fresenius HD machine, which makes it a proprietary module.

Since there is no other economically feasible dialysate temperature control module to avoid such hemodynamic complications, there is a major requirement to look into its implementation. Preliminary studies have reported the on-going research on dialysate temperature control with a modification of dialysate proportioning method through simulation and experiments [77], [78]. This serves as a motivation factor for in-vitro evaluation of proposed DTCM prototype. In this research, a novel dialysate proportioning model has been proposed for the development of DTCM prototype. The DTCM prototype was designed to control the temperature of a dialysate fluid after the proportioning of bicarbonates flowing at an approximate 30°C of temperature, as mentioned in section 3.6, whereas, the optimized fuzzy logic design has been utilized for the temperature control technique.

Earlier, a preliminary study has reported a simple model of extracorporeal circuit with the intention to study the removal of thermal energy during HD [20]. However, the estimation of venous temperature depends only on dialysate temperature by neglecting the blood temperature in arterial line. As the DTCM prototype has to be evaluated through in-vitro studies, an extracorporeal thermal energy balance was introduced in order to estimate the venous and arterial temperature. The utilization of extracorporeal

model is mainly due to the limitation in facilitating medical experiments involving patients. The effect of the DTCM prototype was then analysed for various physiological and ambient parameters such as patient temperature, gradient of patient's temperature, ambient temperature, blood flow rate, dialysate flow rate, and recirculation.

6.2 Extracorporeal thermal energy balance model

An extracorporeal thermal energy balance model of HD was considered for the prediction of arterial and venous temperature with respect to active regulation of dialysate temperature. In this model, the thermal energy transfer in extracorporeal circuit divided into three sections namely arterial side, dialyzer and venous side were considered as shown in Figure 6.1. The arterial and venous side energy transfer models were developed from a recent study [79], while the thermal energy transfer takes place in dialyzer was developed from the proposed COMSOL Multiphysics simulation as mentioned in Chapter 4.

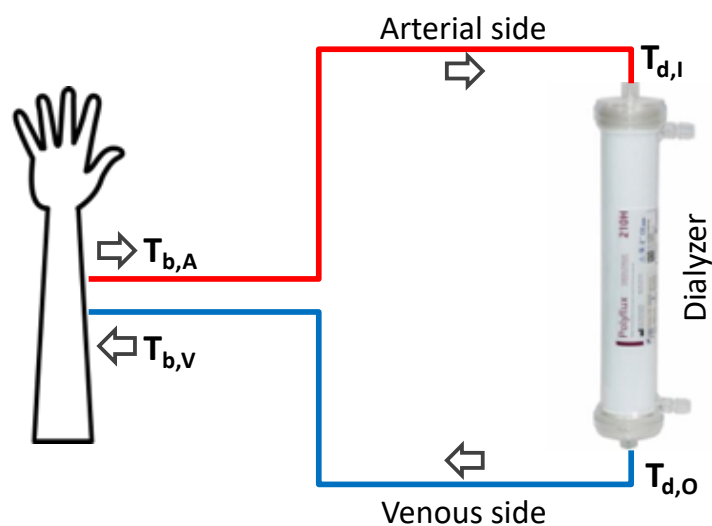


Figure 6.1 - Block representation of extracorporeal circuit.

Initially, an arterial branch of the extracorporeal circuit was considered, which leads the blood from the patient to the dialyzer through a tubing with a uniform

diameter, D (m) and total length of the tubing, L_a (m) such that one dimensional model was considered. It was assumed that the ambient temperature, T_{amb} (K) is lower than the blood temperature, T_b (K) and blood flow rate is uniform. Hence, the thermal energy transfer, $E_{l,l}$ (W) by the blood flowing in the arterial side based on energy conservation equation is given in equation 6.1.

$$E_{l,l} = \int_0^{L_a} U\pi D(T_b - T_{amb})dl = (\dot{m}c)_b \cdot (T_{b,A} - T_{d,l}) \quad (6.1)$$

Where, U denotes the overall heat transfer coefficient ($W m^{-2} K^{-1}$), \dot{m} denotes the blood flow rate ($kg s^{-1}$), c denotes the specific heat capacity of the blood ($J kg^{-1} K^{-1}$), $T_{b,A}$ denotes the arterial blood temperature and $T_{d,l}$ denotes the blood temperature at the inlet of dialyzer. The overall heat transfer coefficient, U is estimated by using equation 6.2.

$$\frac{1}{U} = \frac{1}{\lambda_b} + \frac{\delta_w}{\alpha_p} + \frac{1}{\lambda_{env}} \quad (6.2)$$

Where, λ_b denotes the convective heat transfer coefficient of blood ($W m^{-2} K^{-1}$), δ_w denotes the wall thickness of tubing (m), α_p denotes the thermal conductivity of tubing ($W m^{-1} K^{-1}$) and λ_{env} denotes the convective heat transfer coefficient of the environment ($W m^{-2} K^{-1}$).

However, the blood temperature, T_b along the path of the tubing was assumed to be H.H. Pennes' revisited equation – Bio Heat Transfer Equation (BHTE), as expressed in equation 6.3.

$$e^{-l/l^*} = \frac{T_b(l) - T_{amb}}{T_{d,l} - T_{amb}} \quad (6.3)$$

Where, l^* denotes the characteristic length to be evaluated from equation 6.3 for $l = L_a$ as shown in equation 6.4. In addition, solving equation 6.1 combined with equation 6.3, the characteristic length, l^* can also be expressed as shown in equation 6.5.

$$l^* = -\frac{L_a}{\ln\left(\frac{T_b - T_{amb}}{T_{d,I} - T_{amb}}\right)} \quad (6.4)$$

$$l^* = \dot{m}c_b U \quad (6.5)$$

The relation of T_b can be estimated in terms of $T_{d,I}$ by solving equation 6.4 and 6.5. According to equation 6.1, U and T_b can be determined and the other parameters are known, and such expression allows $T_{b,A}$ to be evaluated by non-invasive measurement in order to estimate the temperature at the entry of dialyzer, $T_{d,I}$.

Similarly, the thermal energy transfer in venous side can also be estimated by the same technique as thermal energy transfer in arterial side. Thereby, the venous temperature, $T_{b,V}$ can be determined by the expression of the thermal energy transfer, $E_{l,O}$ by the blood flowing in the venous side as shown in equation 6.6.

$$E_{l,O} = \int_0^{L_v} U\pi D(T_b - T_{amb})dl = (\dot{m}c)_b \cdot (T_{d,O} - T_{b,V}) \quad (6.6)$$

Where L_v denotes the length of tubing in venous side and $T_{d,O}$ denotes the temperature at the outlet of dialyzer. Since, the tubing in venous side is identical to arterial side, the overall heat transfer coefficient was utilized from equation 6.2. Thus, T_b was estimated through the same method as shown in equation 6.7 and 6.8.

$$e^{-l/l^*} = \frac{T_b(l) - T_{amb}}{T_{d,O} - T_{amb}} \quad (6.7)$$

$$l^* = -\frac{L_v}{\ln\left(\frac{T_b - T_{amb}}{T_{d,O} - T_{amb}}\right)} \quad (6.8)$$

The trend of the thermal energy transfer in dialyzer was analyzed for various inlet temperatures and dialysate temperatures in order to determine the dialyzer outlet temperature, $T_{d,O}$ as shown in equation 6.9.

$$T_{d,O} = k_a T_{d,I} + k_b T_d + k_c \quad (6.9)$$

Where, k_a , k_b and k_c denotes the coefficients of the linear equation of heat transfer in dialyzer. However, these gradients can vary for blood and dialysate flow rates as mentioned in section 4.3.4. Therefore, the venous temperature, $T_{b,V}$ can be estimated using equation 6.6 by substituting all the other known parameters. Finally, the venous temperature can be rearranged in a generalized expression for implementation in Simulink as shown in equation 6.10.

$$T_{b,V} = k_f \cdot \left(\left[\frac{k_a}{k_e} \cdot (T_{b,A} + k_d) \right] + k_b T_d + k_c \right) + k_g \quad (6.10)$$

Where, k_d , k_e , k_f , and k_g are the coefficients in the simplified expression of venous temperature expression. The mixed venous temperature, which demonstrates the blood back to patient from the extracorporeal circuit and combines with arterial temperature resulting in an alternate marker of body temperature, T_b . Therefore, the body temperature was determined by considering the heat transfer between venous and arterial temperature in the body as shown in equation 6.11. The equation is based on the conservation of energy with the assumption that both the bloods have identical mass and specific heat capacity.

$$T_b = \frac{T_{b,A} + T_{b,V}}{2} \quad (6.11)$$

In addition, the blood temperature from the patient's access does not necessarily reflect the mixed venous temperature because of possible access and cardiopulmonary recirculation [20]. So, the body temperature, T_b requires amending the arterial and venous temperature with a recirculation factor, R as shown in equation 6.12.

$$T_b = T_{b,A} \left(\frac{1}{1-R} \right) - T_{b,V} \left(\frac{R}{1-R} \right) \quad (6.12)$$

In order to utilize this model in DTCM prototype, the body temperature needs to be updated on every cycle as shown in equation 6.13.

$$T_{b,k} = T_{b,k-1} + \Delta T_b \quad (6.13)$$

The arteriovenous temperature gradient has been evaluated to determine the temperature difference between arterial and venous blood as shown in equation 6.14.

$$\Delta T_{A,V} = T_{b,V} - T_{b,A} \quad (6.14)$$

In this way, the estimation of venous temperature and arterial temperature can be ensured to compensate the thermal energy transfer in extracorporeal circuit. This can be realised by iterating the control algorithms and active regulation of dialysate temperature in order to reach the pre-dialysis body temperature.

6.3 Design and methodology

6.3.1 Experimental design

In this chapter, the overall model of the DTCM prototype consisting of initial tank, phase 1 and phase 2 as mentioned in section 3.8 has been assembled as shown in Figure 6.2. The overall hardware design and components of the DTCM prototype were mentioned in section 3.6.1. As the initial tank mimics the flow of dialysate at 30°C after the preparation, a standalone PID temperature control along with a stirrer was utilized

to maintain the uniform temperature in the tank. The standalone controller sends the control signal through a solid state relay, which drives the submersible heater in the initial tank. However, the accuracy of the controller is limited to $\pm 0.5^{\circ}\text{C}$, which is adequate for this purpose. As this study emphasizes on the in-vitro evaluation, water was considered to mimic the dialysate fluid. Finally, the final temperature was measured using a temperature sensor at final tank after going through active control of temperature processes of DTCM prototype.

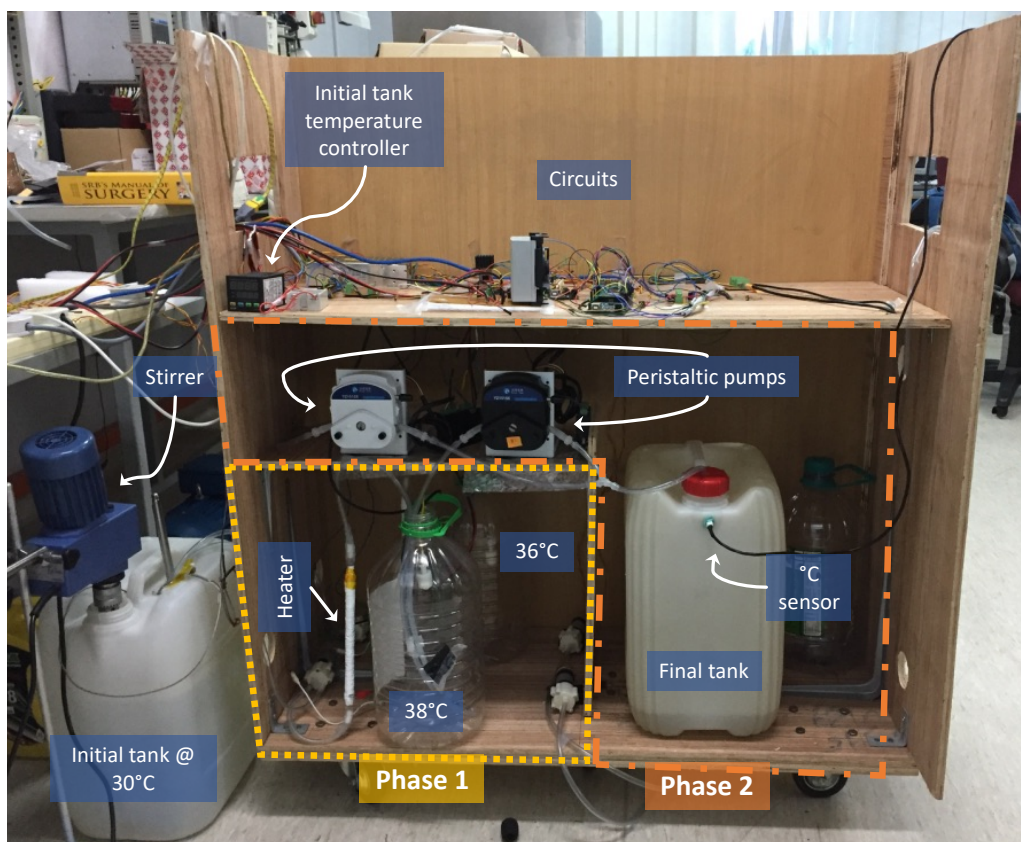


Figure 6.2 – Experimental setup for in-vitro evaluation of DTCM prototype.

6.3.2 Phase 1 design

In this design, the pre-heated tanks contain the fluid at constant temperatures of 36°C and 38°C respectively. The temperature controller of the pre-heated tanks has been accomplished by using the PID control technique as mentioned in section 3.6.2.1. Commonly, the PID control signal drives the inflow heaters by means of PWM signal fed

into power MOSFETS for each tank. In fact, the pump transfers the fluid from initial tank to pre-heated tanks at 250 ml min^{-1} to extract a decent performance from heaters. However, the speed of the pump is determined by the microcontroller through a NPN transistor. The circuit of the phase 1 of DTCM prototype consisting of PID temperature controller is shown in Figure 6.3. To achieve an optimal performance, the PID parameters such as $K_p = 180$, $K_i = 5$ and $K_d = 90$ were chosen for both pre-heated temperature controllers as both heaters shows similar specifications.

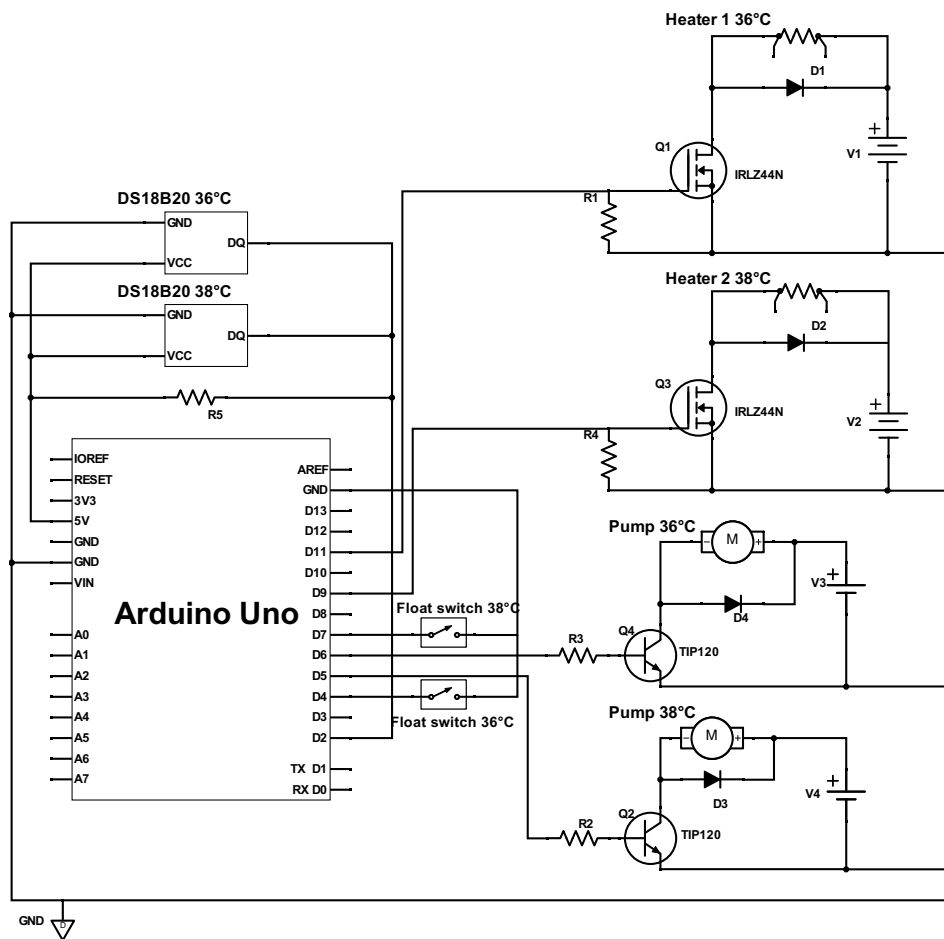


Figure 6.3 – Circuit diagram for phase 1 of DTCM prototype.

6.3.3 Phase 2 design

In this study, the optimal fuzzy logic design was utilized for the phase 2 of the DTCM prototype as shown in Figure 6.4. The same design approach has been followed

for the fuzzy logic parameters including MFs, rule base and defuzzification as discussed in Chapter 5. In HD, the input parameters should be capable of reflecting the hemodynamic status of patient and should be measurable by using non-invasive sensors, while the output parameters should be adjustable. So, one of the inputs determines the error between the target temperature and arterial temperature; other input of FLC determines its change in error. Whereas, the output determines the actuator of DTCM prototype, which is the control signal of the peristaltic pump.

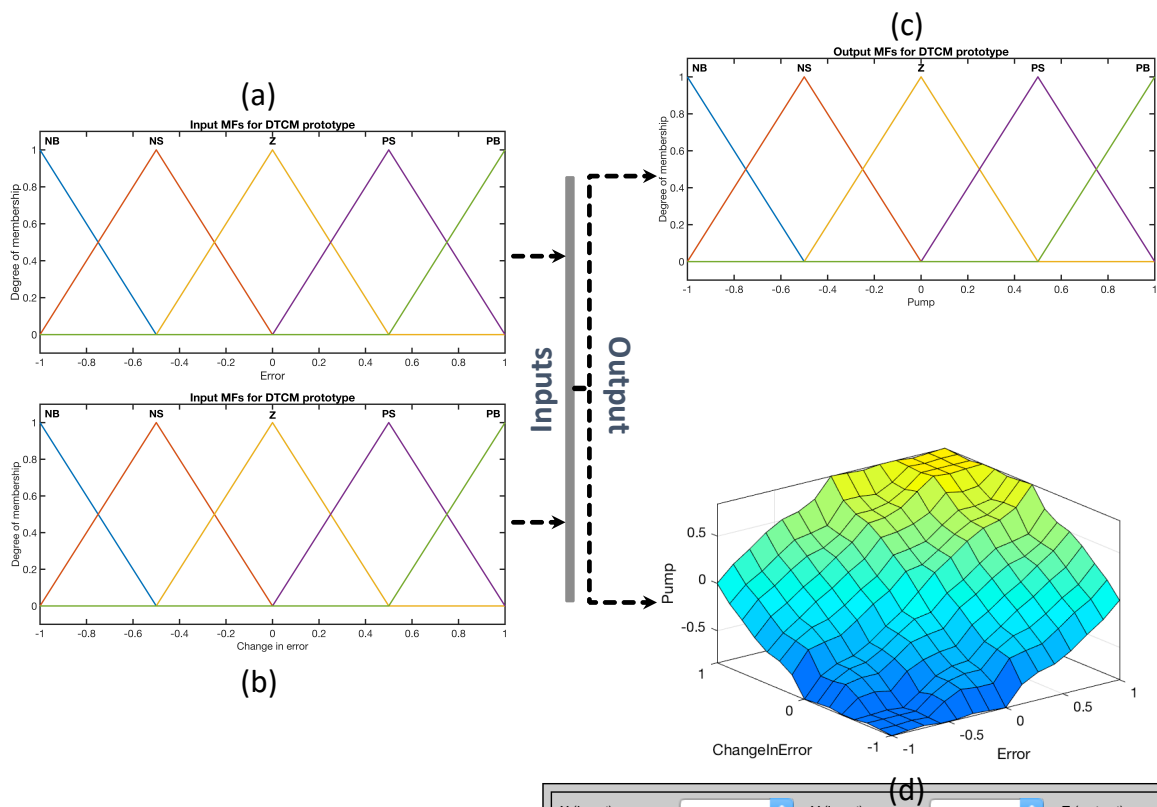


Figure 6.4 – Optimized fuzzy logic design for DTCM prototype consisting of (a) error input MFs, (b) change in error input MFs, (c) pump output MFs and (d) output surface for the Mamdani FIS output.

The overall circuit for the phase 2 of DTCM prototype was constructed as shown in Figure 6.5. As the stepper driver requires 5V logic level, a logic level converter has been used to convert the 3.3V logic level of Raspberry Pi. The speed of peristaltic pump can be controlled by the PWM signal of Raspberry Pi, which converts PWM signal to analogue

signal and then high frequency pulses for the stepper driver. The stepper driver supplies the current of 1.9A to the stepper motor with a micro-step of 1600 to transfer the fluid evenly with a peristaltic pump head load.

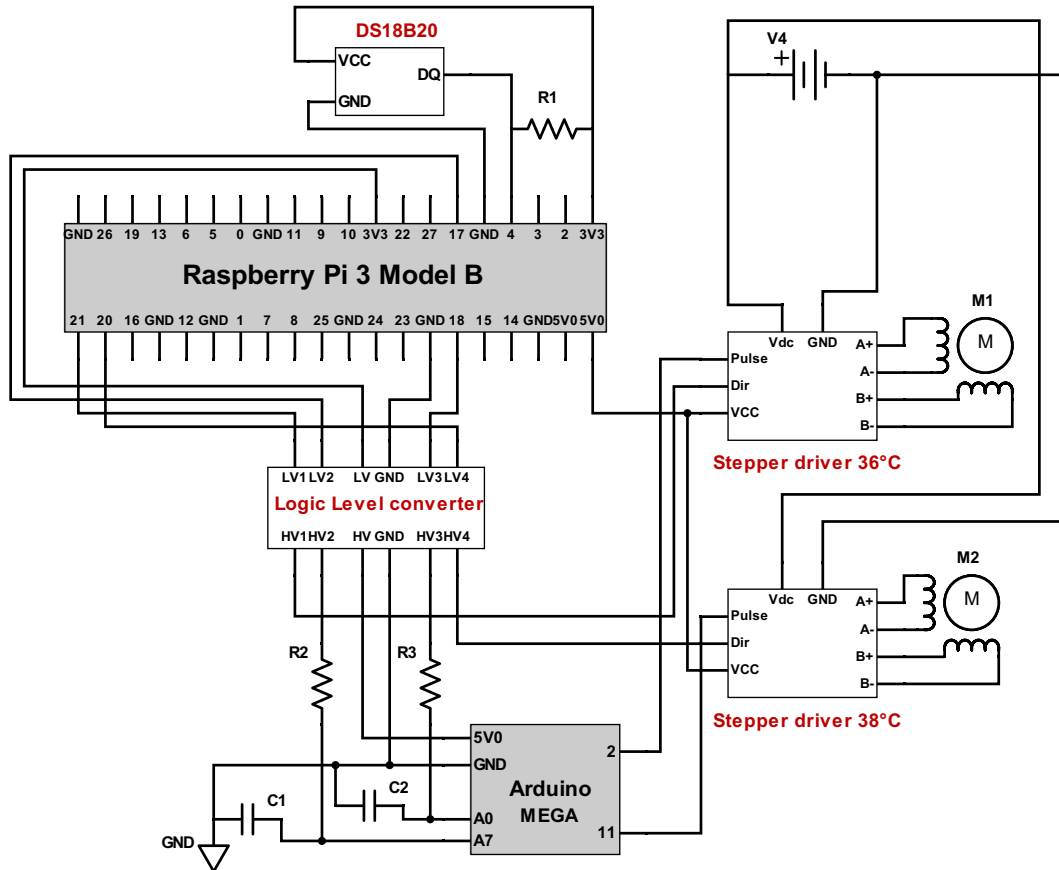


Figure 6.5 – Circuit diagram for phase-2 of DTCM prototype.

6.3.4 Implementation design

The DTCM prototype was then implemented by assembling the initial tank, phase 1 and phase 2 systems along with the thermal energy balance model for extracorporeal circuit for its in-vitro evaluation. A similar Simulink model to the simplified temperature controller stated in section 5.2.3 has been utilized for the DTCM prototype, which is also presented in Appendix A. In fact, the phase 1 systems were implemented in Arduino microcontroller and monitored the performance in Megunolink Pro software as mentioned in section 3.6.2.1. While, the phase 2 systems were implemented in Raspberry

Pi and analyzed the evaluation performance in Simulink environment as mentioned in 3.6.2.2. Moreover, the thermal energy balance model was defined in Simulink environment to estimate the venous and arterial temperatures. The overall flow chart of DTCM controller implementation design is shown in Figure 6.6.

The initial body core temperature was considered as target temperature, because the body temperature would change during the treatment. This is due to the thermoregulatory mechanism of a body. The same strategy has been applied to set the target temperature in Simulink environment. The measurement and calculations were continuously repeated at a defined sample time during the experiment and the dialysate temperature increases or decreases if any changes in arterial temperature to ensure the target temperature is maintained. The effect of body temperature under several cases by varying physiological and machine parameters were analyzed. Such cases were implemented in Simulink environment for the in-vitro evaluation of the DTCM prototype.

Normally, the treatment time for a session of hemodialysis would last up to 4 hours [166]. In this study, the duration for DTCM prototype evaluation was considered as 250 seconds. This would be sufficient to emphasize the temperature control under various situations except for toxin clearance. The DTCM prototype will commence the operation when the PID temperature control reaches a stable temperature.

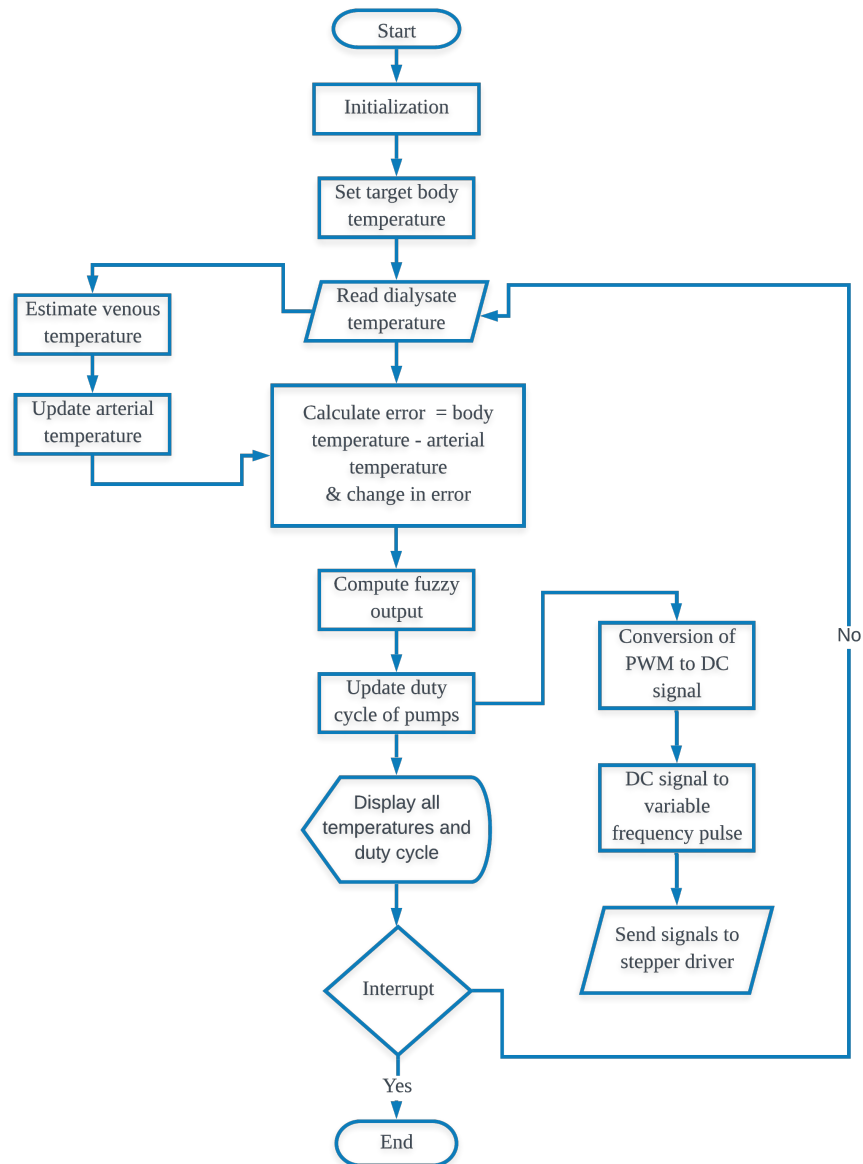


Figure 6.6 – Flow chart of implementation design of DTCM prototype.

6.4 Results and discussion

6.4.1 PID temperature control system

The performance of the DTCM prototype strongly depends on the temperature of fluid in storage tanks. Figure 6.7 (a) shows the PID controller response of temperature at 36°C throughout the experimental duration. It can be seen that the PID controller manages to reach the setpoint and maintain a stable temperature in steady state. The oscillatory response was observed at the later stage of steady state, which shows the

disturbance caused due to the change in quantity of fluid in 36°C storage tank. Whereas, the change in fluid quantity is due to controller behaviour of DTCM. In fact, the steady state temperature was found to be fairly stable with a positive deviation of 0.38°C and negative deviation of 0.31°C. It should also be noted that the PID controller manages to overcome the oscillatory response within a short span of time. The corresponding output response of PID temperature controller is shown in Figure 6.7 (b). This indicates an adequate performance and controllability for this purpose.

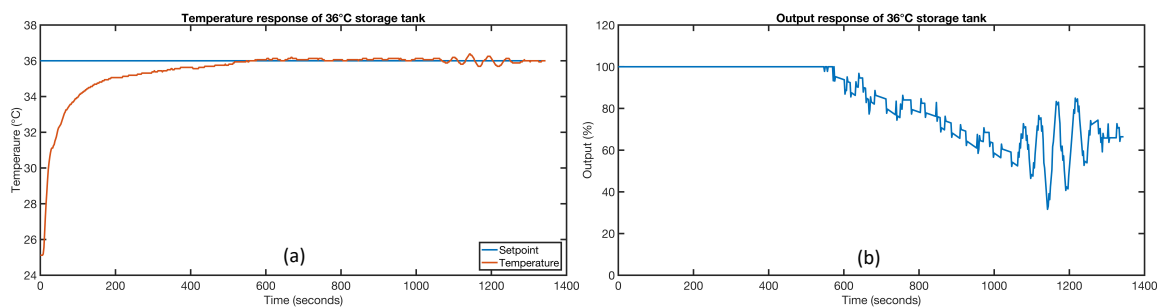


Figure 6.7 – The (a) temperature response and (b) output response for 36°C storage tank.

Similarly, PID controller response for 38°C storage tank is shown in Figure 6.8. It can be seen that the controller has shown a similar performance compared to 36°C storage tank with positive deviation of 0.19°C and negative deviation of 0.12°C. Even though, the quantity of fluid changes in this tank during the operation of the DTCM, the controller manages to eliminate such disturbances. The controller output response for the 38°C storage tank is shown in Figure 6.8 (b).

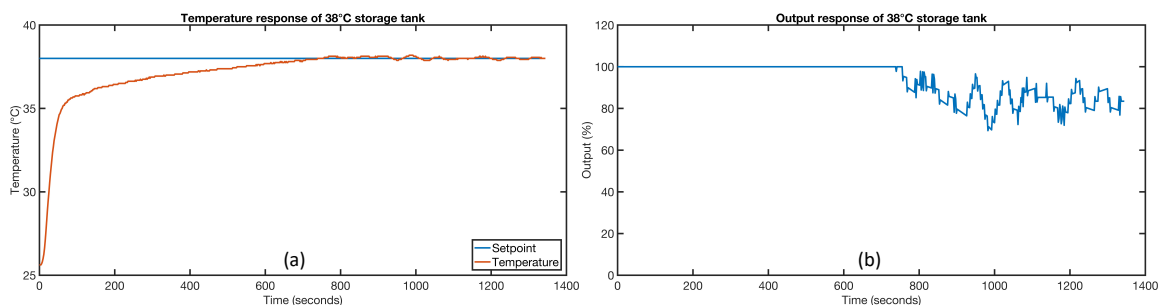


Figure 6.8 - The (a) temperature response and (b) output response for 38°C storage tank.

In comparison with 36°C storage tank, it can be observed that the time taken to reach the setpoint is higher in 38°C storage tank as shown in Figure 6.7 and 6.8. This means that the controller of the 36°C storage tank has taken 548.6 seconds, while the 38°C storage tank has taken 739.3 seconds to reach their respective setpoints. Moreover, a similar response from the PID controller was observed for all in-vitro evaluation tests carried out for the DTCM prototype. Therefore, these results depict a well-suited controller for this purpose due to certain factors such as steady-state performance, controllability and repeatability.

6.4.2 Effect of body temperature with DTCM

The operation of the DTCM prototype was verified on a real-time environment for a pre-defined trend of body temperature. Figure 6.9 represents the system response of the body temperature setpoint at 36.5°C and their corresponding venous, arterial and dialysate temperatures. In fact, the venous and arterial temperature were estimated using the extracorporeal thermal energy model, while the dialysate temperature was measured using the temperature sensor. The parameters considered for this case are: $Q_b = 300 \text{ ml min}^{-1}$, $Q_d = 450 \text{ ml min}^{-1}$, $T_{amb} = 24^\circ\text{C}$ and recirculation = 10%. It has been observed that the body core temperature increases due to heat accumulation caused by blood volume reduction during HD [18], [33]. Thus, a ramp function was used to define the increasing behaviour of uncontrolled arterial temperature. From Figure 6.9, it can be observed that the arterial temperature was controlled according to the target temperature even though the uncontrolled arterial temperature is on the rise. Most importantly, the DTCM prototype has managed to control the arterial temperature with a maximum positive deviation of 0.08°C and negative deviation of 0.03°C. This is achieved

by an effective active regulation of dialysate temperature throughout the experiment, which results in a decrease in venous temperature. Moreover, a series of dead time of 6.5 seconds was observed for the temperatures, similar to section 5.3.6, which shows the time taken to transfer the fluid from storage tank to the temperature sensor in final tank.

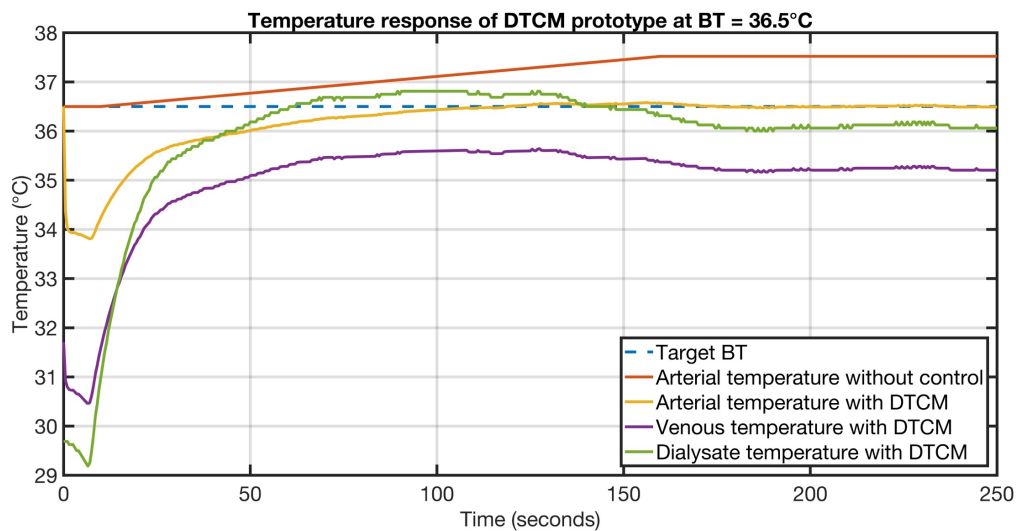


Figure 6.9 – Temperature response of DTCM prototype at BT = 36.5°C.

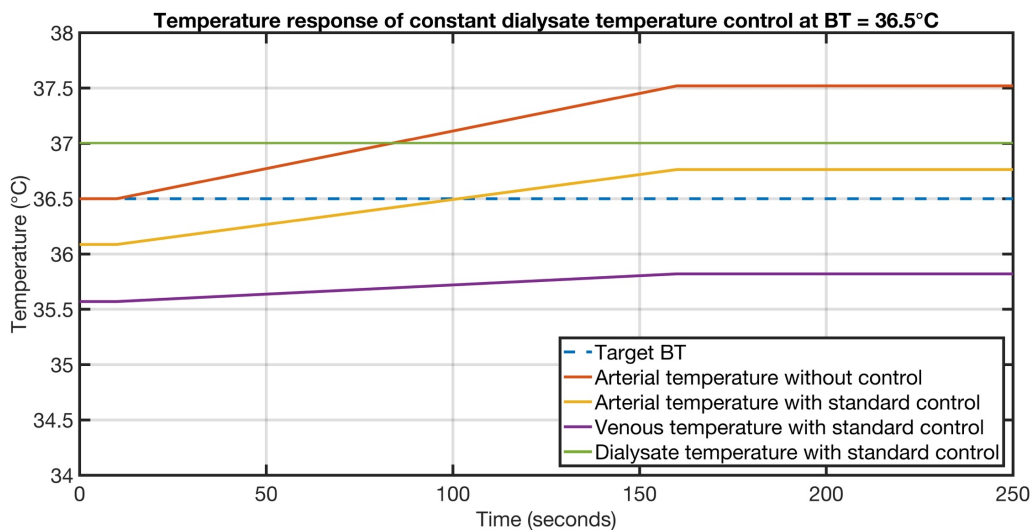


Figure 6.10 – Temperature response of standard dialysate temperature control at BT = 36.5°C.

In comparison with DTCM, a constant dialysate temperature was considered for the same body temperature at 36.5°C. The temperature responses of standard dialysate treatments were simulated using extracorporeal thermal energy balance model as shown

in Figure 6.10. It can be seen that the arterial temperature has increased up to 36.77°C during the experiment. Studies have reported a similar trend of increase in arterial temperature during the treatment. In an experiment consisting of nine HD patients utilizing standard dialysate temperature, the body core temperature has increased up to 0.5°C with a $Q_b = 300 \text{ ml min}^{-1}$ [44]. Similar experiments have reported the rise in body temperature in the range between 0.18°C to 0.4°C with the use of standard dialysate temperature [65], [74], [167]–[169]. However, the difference in the change in arterial temperature also depends on certain parameters such as blood flow rate, dialysate flow rate, ambient temperature etc. In the standard dialysate simulation, the arteriovenous temperature gradient was found to be -0.94°C, which shows a strong agreement with the published experimental data [44], [167]. In fact, the published data have reported the temperature gradient between -1°C and -0.5°C under standard dialysate temperature. In contrary, these temperature trends were based on the HD treatment duration of about 4 hours. This is why the uncontrolled arterial temperature was initialized to sharp increase unlike HD treatment. Withstanding, the entire treatment of temperature profile is been able to demonstrate in lesser duration through the proposed model. Therefore, it can be realized that the model for estimation of venous and arterial temperatures are in line with the published clinical data.

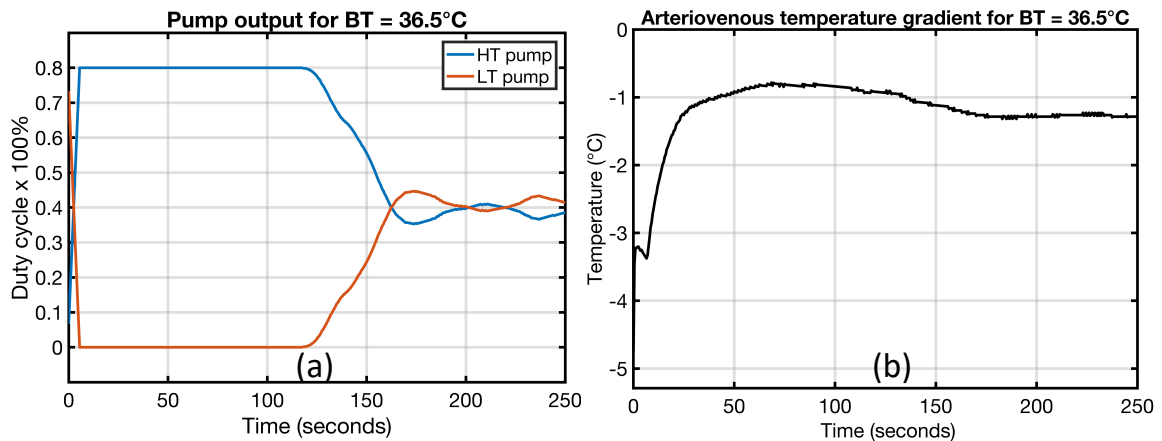


Figure 6.11 –Graphs shows (a) Output response and (b) Arteriovenous temperature gradient of DTCM prototype at body temperature = 36.5°C.

Figure 6.11 (a) shows the output response of peristaltic pumps in DTCM prototype, which results in change in dialysate temperature. It can be seen that the pump transferring the high temperature fluid reduces the flow once it reaches the setpoint at 117 seconds. Thereafter, the arterial temperature maintains at the defined setpoint by an efficient control of the pumps. It can be inferred that the novel dialysate proportioning method benefits the faster response in short duration of experiment as mentioned in Chapter 5. This results in an efficient active regulation of dialysate temperature during the treatment. Figure 6.11 (b) shows the arteriovenous temperature gradient during the experiment. It can be seen that the gradient is in negative value, which indicates the thermal energy is removed from extracorporeal circuit resulting in cooling of venous temperature. However, the active control of dialysate temperature leads to higher thermal energy removal compared to the standard dialysate, which strongly agrees to the published literature [44], [68]. In addition, the arteriovenous gradient for the DTCM prototype was found to be -1.3°C during the steady state as the venous temperature cooled down to 35.2°C . Similar arteriovenous temperature gradient was reported on multiple clinical studies based on a temperature-controlled HD using BTM module.

Specifically, Maggoire et al., has reported a vast experimental study consists of 116 HD patents resulting in a mean arteriovenous gradient of $-0.90 \pm 0.4^{\circ}\text{C}$ and the venous temperature at the end of treatment was 35.36°C [66]. In another study, the gradient was found to be -1.1°C and the final venous temperature was 35.6°C under an experimental study consisting of 13 HD patients with $Q_b = 300 \text{ ml min}^{-1}$ and $Q_d = 500 \text{ ml min}^{-1}$ [68]. In comparison, it can be seen that the DTCM arteriovenous temperature gradient was similar to the clinical data. The negligible difference could be due to the difference in blood flow rate and dialysate flow rate.

Multiple HD studies have been performed on the BTM with the intention to analyse the hypotensive episodes during the treatment. In T-control mode of BTM, the arterial temperature was kept constant throughout the treatment with an accuracy of $\pm 0.1^{\circ}\text{C}$ [18], [19], [28], [68], [71], [170]. In a study consisting of twenty patients, the control of arterial temperature were kept stable with the error between -0.07°C and 0.14°C [69]. In specific, a vast experimental study of BTM has revealed a mean accuracy of arterial temperature of $0.01 \pm 0.16^{\circ}\text{C}$. The trend in temperature responses of the treatment is shown in Figure 6.12 and 6.13 [66]. Significantly, the DTCM control of arterial temperature with a very small error by following the real trend of venous and dialysate temperature shows a strong potential of the DTCM over BTM.

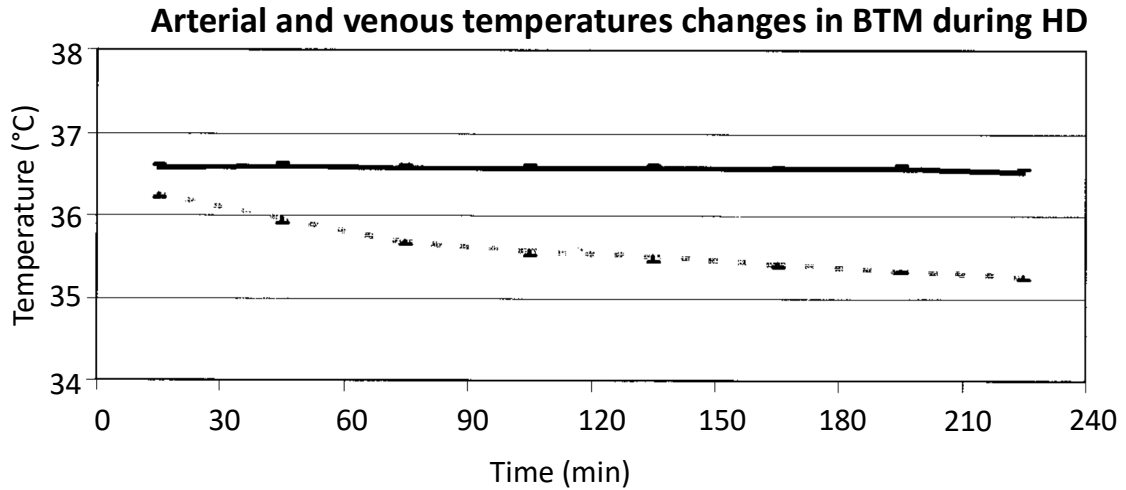


Figure 6.12 – Mean arterial (solid line) and venous (dotted line) temperature changes in BTM during HD [66].

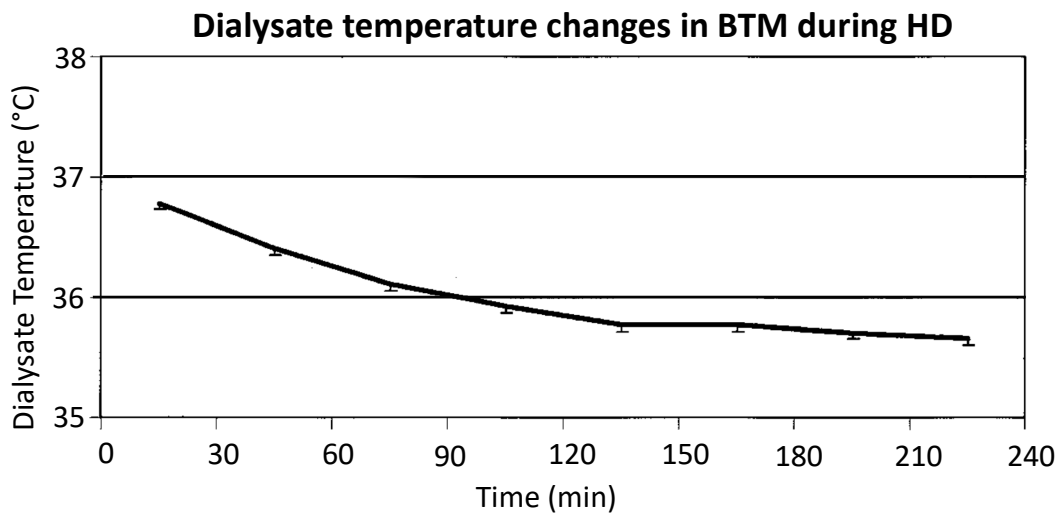


Figure 6.13 – Dialysate temperature changes in BTM during HD [66].

6.4.3 Effect of body temperature for various trends of arterial temperature

According to the literatures, the majority of HD patient's temperature lies between 36.2°C and 36.7°C [20], [33]. Overall, the mean HD patient's body temperature was found to be 36.5°C, which is lower than that of healthy individuals. In addition, the body temperature is expected to rise during HD due to certain factors such as reduction in blood volume, net energy loss to extracorporeal circuit, production of cytokines etc [27]. Hence, the DTCM were subjected to experiment under various physiological body

temperature, and different rising trend of body temperature. In this study, the target body temperature with a normal rise for 36°C (N36), 36.5°C (N36.5) and 37°C (N37) were analysed. In addition, the body temperature of 36.5°C with three different rise slopes; slow rise (S36.5), N36.5 and rapid rise (R36.5) were studied. While the experiments were performed under constant parameters such as $Q_b = 300 \text{ ml min}^{-1}$, $Q_d = 450 \text{ ml min}^{-1}$, $T_{amb} = 24^\circ\text{C}$ and recirculation = 10%.

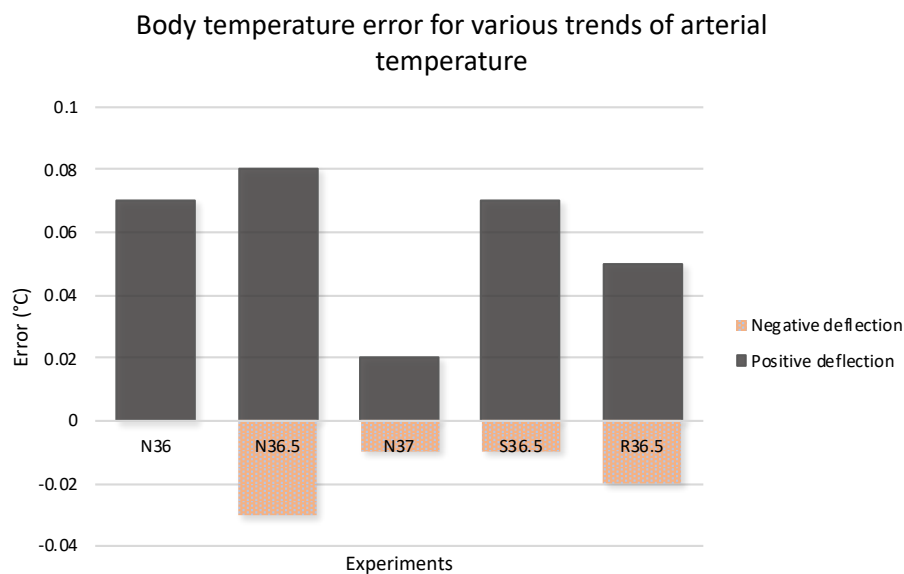


Figure 6.14 – Graph of body temperature error fluctuations for various trends of arterial temperature.

Figure 6.14 shows the steady state error fluctuation of DTCM response under these conditions. It can be seen that the maximum error was observed at N36.5 experiment with a positive deflection of 0.08°C and negative fluctuation of -0.03°C. On the other hand, the N37 shows the least error (+0.02°C and -0.01°C) during the experiment. Moreover, the DTCM were able to control within a tight tolerance in the event of dramatic sudden increase of temperature. This demonstrates the performance of DTCM is superior to the current BTM even though with a vigorous response in shorter

duration than real HD treatment. The temperature and output response under these conditions are shown in Appendix B.

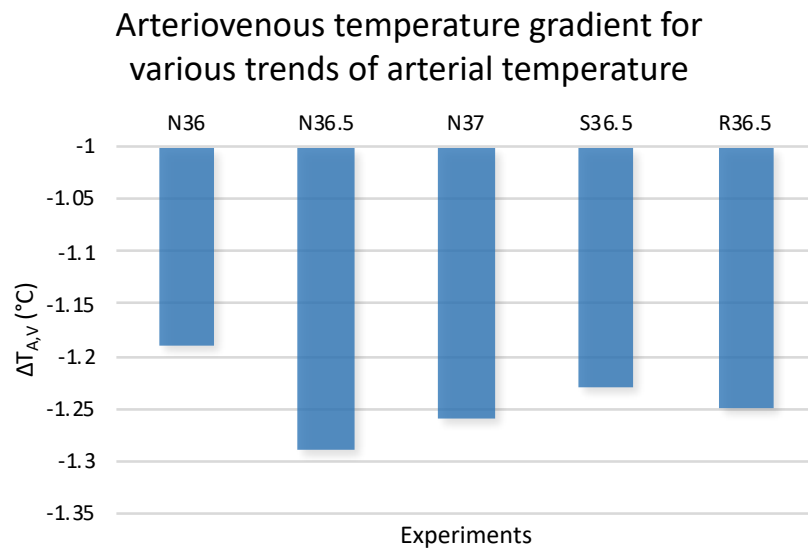


Figure 6.15 – Graph of arteriovenous temperature gradient for various trends of arterial temperature.

The steady-state arteriovenous temperature gradient was observed under these conditions as shown in Figure 6.15. This indicates the control of dialysate temperature affecting the arterial temperature through venous blood line under different arterial temperatures. In the case of different target temperature, the arteriovenous temperature gradient was found to be lower in N36 compared to other target body temperatures. In fact, the steady state dialysate temperature under these targets were $T_{d,N36} = 35.75^{\circ}\text{C}$, $T_{d,N36.5} = 36.06^{\circ}\text{C}$ and $T_{d,N37} = 36.69^{\circ}\text{C}$. As the dialysate temperature plays an important role in the thermal energy removal in extracorporeal circuit, the larger difference between the dialysate temperature and target temperature determines the arteriovenous temperature gradient. Similar dialysate temperature was found in a recent study of individualized dialysate of 0.5°C less than core temperature ($36.4 \pm 0.2^{\circ}\text{C}$), which reduces the cardiac complications at dialysate temperature of $35.9 \pm 0.2^{\circ}\text{C}$ [46]. On the

other side, studies have reported on shivering and cold sensation due to the individualized dialysate control [28], [47]. This reveals that certain patients with constant individualized dialysate temperature would result in lesser core temperature leading to shivering and other complications. Most importantly, there is no noticeable differences in the temperature gradient for different slope of the body temperature as it depends primarily on the controller's response time. Overall, the negative value of temperature gradient signifies that the DTCM are capable to prevent heat accumulation for avoiding intradialytic complications.

6.4.4 Effect of body temperature for various blood and dialysate flow rates

The blood and dialysate flow rates are one of the most vital parameters for the hemodialysis efficiency, which differs in patients according to their hemodialysis prescription [171], [172]. The common range of blood and dialysate flow rates that suits the dialyzer specification were considered for this study. The selected blood flow rates were 200 ml min^{-1} (Qb200), 300 ml min^{-1} (Qb300), and 400 ml min^{-1} (Qb 400) by keeping dialysate flow rate constant at 450 ml min^{-1} . On the other hand, the dialysate flow rates were 350 ml min^{-1} (Qd 350), 400 ml min^{-1} (Qd 400) and 450 ml min^{-1} (Qd 450) with a constant blood flow at 300 ml min^{-1} . Thereby, the dialysate flow rates were varied in DTCM using duty cycle of 50%, 65% and 80% for Qd350, Qd400 and Qd450 respectively. This is in accordance with the calibration data of peristaltic pump as shown in Appendix C. Similar to the last experiment, the steady state error fluctuation of body temperature control under these conditions is shown in Figure 6.16. It can be seen that the body temperature is kept in control with a maximum deflection of $(+0.08^\circ\text{C}$ and $-0.06^\circ\text{C})$ during the experiment. Among the flow rates, the Qd350 $(+0.05^\circ\text{C}$ and $-0.06^\circ\text{C})$ and Qb300

(+0.08°C and -0.03°C) shows the maximum error fluctuation compared to other blood and dialysate flow rates. The promising error tolerance infers the capability of DTCM in controlling the temperature under normal prescription of blood and dialysate temperature.

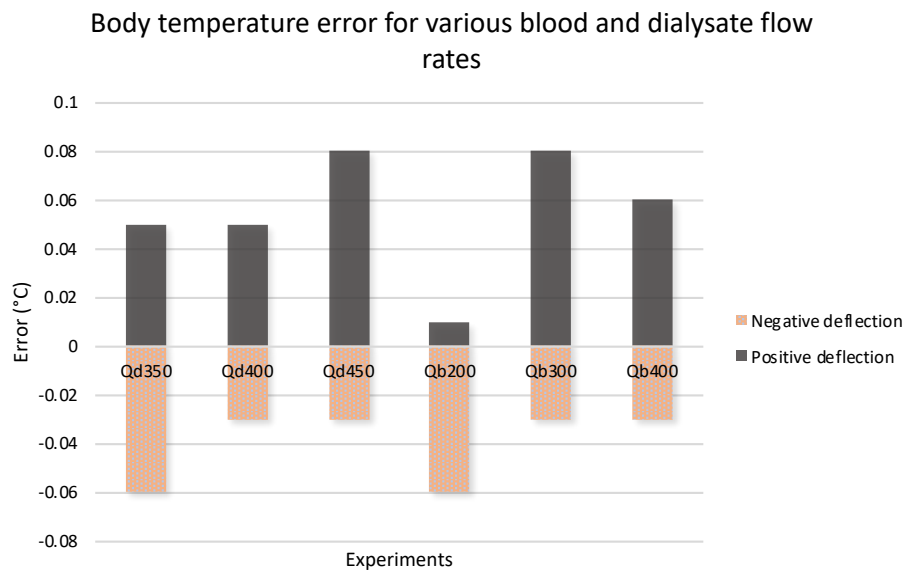


Figure 6.16 - Graph of body temperature error fluctuations for various blood and dialysate flow rates.

Figure 6.17 shows the steady state arteriovenous temperature gradient under these conditions. It can be seen that there is no significant difference in the temperature gradient by varying blood and dialysate flow rates. The negligible difference of temperature gradient in various dialysate flow rate are due to the heat transfer in dialyzer, whereas the dialysate flow rate is independent on arterial and venous side thermal exchange. On the other hand, the steady state dialysate temperatures for Qb200, Qb300 and Qb400 were found to be 36.88°C, 36.06°C and 35.62°C respectively. The difference in dialysate temperature demonstrates the temperature loss through blood lines at different blood flow rate. In other words, the thermal energy loss has been

compensated by active regulation of dialysate temperature in order to keep the body temperature constant.

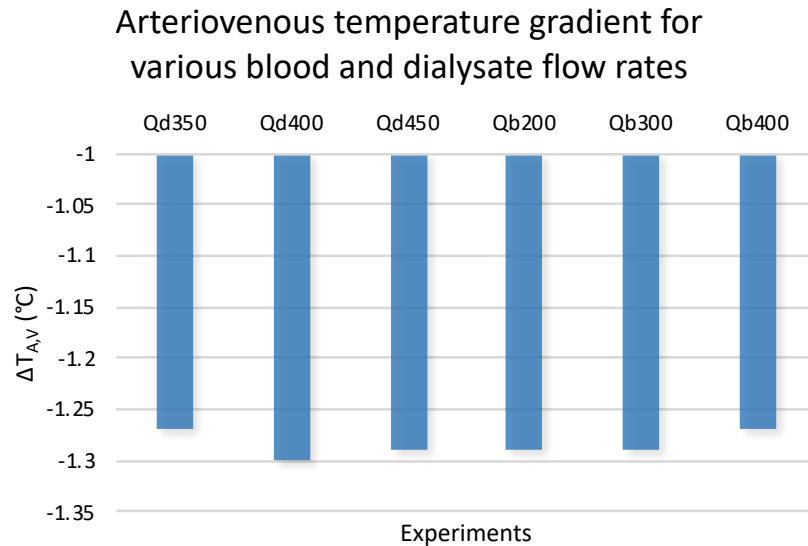


Figure 6.17 - Graph of arteriovenous temperature gradient for various blood and dialysate blood flow rates.

6.4.5 Effect of body temperature for various external factors

The major external factors such as recirculation and ambient temperature were discussed in this section since these factors intervenes the thermal energy balance during HD. In this study, the unavoidable recirculation factors such as 5% (Re5), 10% (Re10) and 15% (Re15) were considered, while above 15% requires an immediate further investigation on fistula leading to interruption of treatment [65], [173]. On the other hand, the possible ambient temperature of 24°C (T24), 23°C (T23) and 22°C (T22) were considered. Figure 6.18 shows the steady state error fluctuation of DTCM response under these conditions. The Re15 shows the highest positive deflection (+0.09) among all experiments, which illustrates the disturbances due to excess transfer of thermal energy between arterial and venous temperatures. Similarly, minimal error deflections were

found for various ambient temperature. This shows an impressive performance of DTCM under external disturbances.

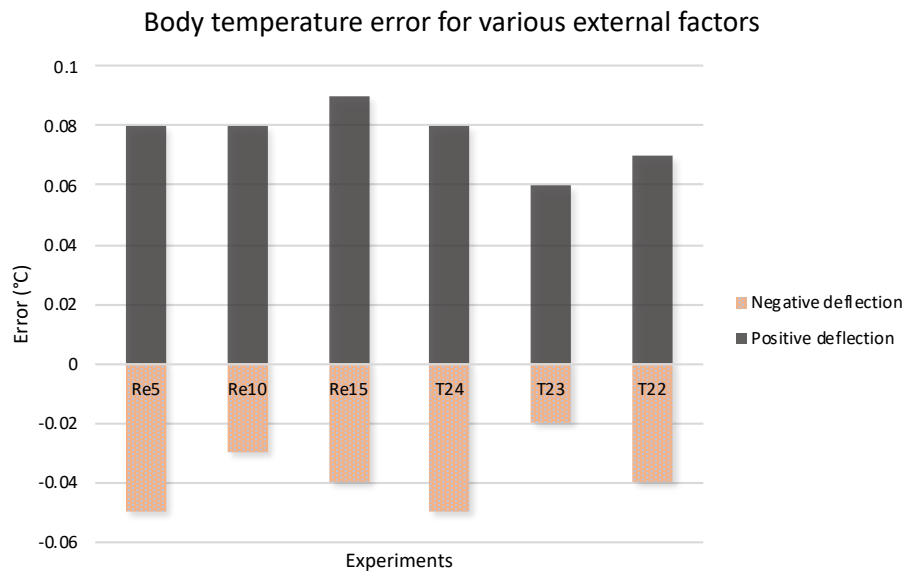


Figure 6.18 - Graph of body temperature error fluctuations for various external factors.

Figure 6.19 shows the arteriovenous temperature gradient under various recirculation and ambient temperatures. It can be seen that the temperature gradient decreases linearly with the increase in recirculation. In fact, the dialysate temperature also decreases with the increase in recirculation, which results in a decrease of venous temperature and then arteriovenous gradient. As expected, R15 shows high thermal energy loss compared to other recirculation. On the other hand, the arteriovenous temperature gradient decreases with the decrease in ambient temperature. As expected, the venous temperature reduces because of increased exposure to the cooler environment. This is in agreement to the results obtained in published literature [17].

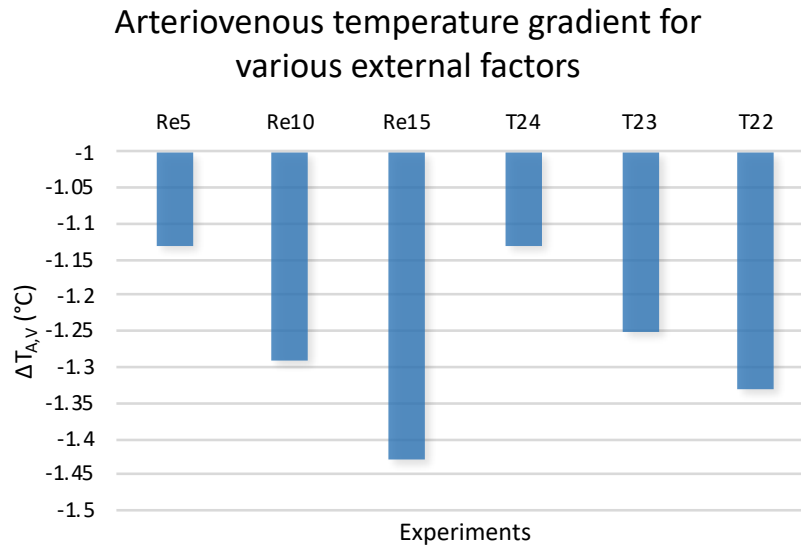


Figure 6.19 - Graph of arteriovenous temperature gradient for various external factors.

A long-term study has revealed a fascinating report on the relation between body temperature and mortality in HD patients [15]. In fact, the highest mortality was observed in patients with changing body temperature during the period, irrespective of baseline body temperature. Whereas, the lowest mortality was found in the group with the highest body temperature at baseline and with stable temperature during the treatment. Based on several experiments, it can be seen that DTCM has capability to control the body temperature during HD within a tolerance of $\pm 0.09^{\circ}\text{C}$. The stable body temperature during HD could prevent the chance of heat accumulation and thereby intradialytic hypotension and other complications to a great extent as discussed in published literature [73], [170].

There are some limitations and constraints for this study. Foremost, the DTCM performance was evaluated through in-vitro experiments comprising of a proposed thermal energy model, since the medical experiments including blood side are quite challenging at the initial stage development. Though adequately emphasized on the design implementation and evaluation of temperature control, the duration of DTCM

experiments was too short and done with less quantity of fluids. This is in consideration of constant input soon after the rise of arterial temperature due to the reduction of blood volume as mentioned in literatures [27]. Due to the lack in research regarding the rise in body temperature, the arterial temperature trend was approximated through simulated ramp input [18], [28], [66], [68]. In this study, unlike from typical controller evaluation, the rise time was not given importance for the experiments. This is because of the priming technique used in HD machine, which starts the treatment after the dialysate temperature setpoint has been reached. Generally, the treatment would start after reaching the required dialysate temperature at either 36°C or 37°C [33]. In addition, the extracorporeal thermal energy model was based on a single Polyflux 210H membrane. Furthermore, low-cost and best-in-class components such as sensors, actuators and microcontrollers were utilized as this is initial study on the development of the prototype.

Unlike other physiological variables, the body temperature has not received much attention to improve the hemodynamic stability during HD. To the best of authors' knowledge, an in-depth research on dialysate temperature control and its performance were quite sparse even though many studies have reported its importance in HD. The main focus on this research is the contribution to create awareness of the importance of temperature control in HD, which in turn filled a gap on this field of current research. Based on a series of experiments, the DTCM has shown a potential to improve the patients' quality of life and other complications. Furthermore, features such as modularity, cost-effective and competitive response time would facilitate with the existing HD machine, which would be beneficial for developing countries. Significantly, the performance of DTCM is in line with the hypothesis of this research. Yet, more research is needed in the field of dialysate temperature controllers especially DTCM

under long-term in-vivo experiments using arterial temperature sensors as controller input, which would enable the DTCM to operate independently.

6.5 Conclusion

In conclusion, the novel dialysate proportioning model comprising of phase 1 and phase 2 were formed for the benefit of temperature control in HD. Initially, the initial tank has controlled the fluid temperature at $30 \pm 0.5^{\circ}\text{C}$, which is then fed into the PID temperature control system. The temperatures were kept constant on both storage tanks at $36 \pm 0.38^{\circ}\text{C}$ and $38 \pm 0.19^{\circ}\text{C}$ throughout the experiment, which is one of the most vital part of DTCM performance. There has been no research that has focussed on the dialysate temperature control system and in-depths study on its performance. Therefore, an extracorporeal thermal energy balance model was validated in order to evaluate the performance of the DTCM prototype. In the current dialysate temperature, the consequences of rise in body temperature was found to be undesirable. In contrast, the DTCM prototype showed a significant response in maintaining the body temperature with a very small error tolerance of $\pm 0.09^{\circ}\text{C}$. These values were quite impressive even with the shorter duration and abrupt disturbances unlike in actual HD treatment. In the current study, the DTCM justifies the potential to control the body temperature within the specified tolerance under various physiological and other practical experiments. The active control of dialysate temperature has showed the decreasing trend in the arteriovenous gradient and thermal energy removal in extracorporeal circuit, which plays an important role in preventing the heat accumulation. The current study would benefit many researchers to contribute further to the development of a dialysate temperature

controller, which is an unexplored hemodynamic variable with proven hemodynamic stability during the treatment.

CONCLUSION AND FUTURE WORKS

7.1 General Conclusion

The present study illustrates the development of dialysate temperature control module (DTCM) with emphasis on control of body temperature during HD treatment. A comprehensive study of dialysate temperature controller design and in-vitro analysis of body temperature during HD have not been reported elsewhere to date. An innovative design of a dialysate proportioning model by varying flow rates was proposed to control the body temperature efficiently. In addition, the performance of fuzzy logic control was evaluated in real environment for effective implementation in DTCM. Then, in-vitro analysis of DTCM prototype under various conditions such as blood flow rate, dialysate flow rate, blood temperature, ambient temperature and recirculation were analysed. As a result, the effective body temperature control from DTCM could, not only reduce the hypotensive episodes but also improves the patient's quality of life. Hence, the HD treatment with DTCM can be introduced into market as it has the potential to minimize the intradialytic complications and thereby its associated mortality.

This study has reported the following significant findings:

- I. The novel design of dialysate proportioning method for DTCM was proposed in such a way that it can interface with existing HD machines. The prototype of DTCM was developed emphasizing on temperature parameter, which implies that only well-prepared dialysate will enter into DTCM prototype. Unlike conventional heaters, the DTCM employs two different temperature tanks flowing at different flow rate for effective

temperature control. The design of DTCM prototype has shown the potential for the current society.

- II. The heat transfer in a dialyzer showed a trend in temperature profile across the membrane and the blood temperature has decreased up to 1.16°C under cool dialysate. The loss of blood temperature could be one of the consequences of venous temperature cooling as reported in literature. However, the heat transfer in a dialyzer was then deduced in terms of linear equation under various conditions. This would help in estimating the overall heat transfer in extracorporeal circuit in HD as well as arterial and venous temperatures.
- III. The FLC based temperature controller was implemented in Raspberry Pi microcontroller and optimized through numerous real time experiments. The fuzzy logic design with symmetrical rule base and highest number of overlapping triangular membership functions was found to be optimal performance compared to other designs. However, the performance indices of optimized design were fairly similar for both Mamdani and Sugeno FIS without any large effect in the response time as cited in literature (IAE: 68.74 and 66.93; ISE: 184.92 and 179.56; ITAE: 2489.5 and 2246.8 for Mamdani and Sugeno FIS respectively). Moreover, the optimized design shows remarkable improvement in accuracy ($\pm 0.125^{\circ}\text{C}$) and response time compared to the accuracy ($\pm 0.5^{\circ}\text{C}$) in published experimental study.
- IV. At the initial processes of DTCM, the accuracy of PID temperature control storage tanks were reported within $\pm 0.38^{\circ}\text{C}$. Under standard dialysate

trial, the estimated arterial temperature showed an increase up to 36.77°C and arteriovenous gradient as 0.94°C, which are in line with published literature. This validated the overall extracorporeal thermal energy model incorporating the heat transfer in dialyzer.

- V. BTM reported a mean tolerance of $\pm 0.16^{\circ}\text{C}$ under various experiments and it showed a substantial reduction in intradialytic complications. In comparison, the active control of dialysate temperature in DTCM showed a slight improvement in error tolerance of $\pm 0.09^{\circ}\text{C}$ during the in-vitro experiments. However, even the slight improvement over BTM may result in significant impact on long-term mortality.

7.2 Future works

The studies carried out have revealed that the development of DTCM prototype could be beneficial for maintaining body temperature and thereby reducing intradialytic complications during HD treatment. The potential of DTCM thus developed could be further explored to provide a commercialized dialysate temperature controller for healthcare industry. Therefore, the following future works are recommended:

- I. Analyse the DTCM prototype performance for entire HD treatment duration (up to 240 minutes) including entire quantity of dialysate fluid. Similarly, in-vitro experiments with BTM will be beneficial in determining an in-depth comparison of performances.
- II. Implementation of FLC in high-performance industrial controllers for DTCM in order to interface with HD machine with maximum durability. In

addition, implementation of medical grade sensors and actuators will be advantageous for further evaluation.

- III. Analyse the performance of DTCM through in-vivo studies independent of extracorporeal thermal energy model. Therefore, the body temperature including arterial and venous temperatures can be acquired using the non-invasive temperature sensors. This would help to validate clinically the HD treatment with DTCM.
- IV. From section 4.3.4 of this thesis, it is shown that the heat transfer equation of dialyzer is limited to a single product. Even though, there are many commercially available dialyzers, it was selected according to the available adequate data for validation. Thus, the expressions for different dialyzers from different manufacturers would be valuable to generalize the heat transfer in a dialyzer.
- V. Pre-commercialization studies consists of cost analysis, statistical analysis, durability, compact design, easy-interface with other HD machines, etc., of DTCM would be beneficial to provide economical treatment and global awareness for HD patients especially in third world countries.

BIBLIOGRAPHY

- [1] J. G. Webster, *Bioinstrumentation*. John Wiley & Sons, Inc., 2004.
- [2] W. H. Fissell, A. J. Fleischman, H. D. Humes, and S. Roy, "Development of continuous implantable renal replacement: past and future," *Transl. Res.*, vol. 150, no. 6, pp. 327–336, 2007.
- [3] Wikipedia, "Schematic of Hemodialysis circuit." <https://upload.wikimedia.org/wikipedia/commons/9/9/>, 2008.
- [4] W. Bradshaw and P. N. Bennett, "Asymptomatic Intradialytic Hypotension: The Need for Pre-Emptive Intervention," *Nephrol. Nurs. J.*, vol. 42, no. 5, pp. 479–485, 2015.
- [5] S. M. Toth-Manikowski and S. M. Sozio, "Cooling dialysate during in-center hemodialysis: Beneficial and deleterious effects," *World J. Nephrol.*, vol. 5, no. 2, pp. 166–171, 2016.
- [6] S. Al Shamsi, A. Al Dhanhani, M. M. Sheek-Hussein, and O. Bakoush, "Provision of care for chronic kidney disease by non-nephrologists in a developing nation: a national survey," *BMJ Open*, vol. 6, no. 8, pp. 1–7, 2016.
- [7] V. Jha, G. Garcia-Garcia, K. Iseki, Z. Li, S. Naicker, B. Plattner, R. Saran, A. Y.-M. Wang, and C.-W. Yang, "Chronic kidney disease: global dimension and perspectives," *Lancet*, vol. 382, no. 9888, pp. 260–272, 2013.
- [8] K. J. Jager and S. D. S. Fraser, "The ascending rank of chronic kidney disease in the global burden of disease study," *Nephrol. Dial. Transplant.*, vol. 32, no. suppl_2, pp. 121-128, 2017.
- [9] S. L. White, S. J. Chadban, S. Jan, J. R. Chapman, and A. Cass, "How can we achieve global equity in provision of renal replacement therapy?," *Bull. World Health Organ.*, vol. 86, no. 3, pp. 229–237, 2008.
- [10] L. Y. Ngo, "11th Report of the Malaysian Dialysis and Transplant Registry 2003,"

Malaysian Soc. Nephrol., pp. 13–25, 2003.

- [11] G. Ahmad, G. B. Leong, L. Y. Ngo, O. L. Meng, and L. D. Guat, “24th Report of the Malaysian Dialysis and Transplant Registry 2016,” *Malaysian Soc. Nephrol.*, pp. 6–30, 2016.
- [12] G. T. Obrador, X. Rubilar, E. Agazzi, and J. Estefan, “The Challenge of Providing Renal Replacement Therapy in Developing Countries: The Latin American Perspective,” *Am. J. Kidney Dis.*, vol. 67, no. 3, pp. 499–506, 2016.
- [13] T. Liyanage, T. Ninomiya, V. Jha, B. Neal, H. M. Patrice, I. Okpechi, M. Zhao, J. Lv, A. X. Garg, J. Knight, A. Rodgers, M. Gallagher, S. Kotwal, A. Cass, and V. Perkovic, “Worldwide access to treatment for end-stage kidney disease: a systematic review,” *Lancet*, vol. 6736, no. 14, pp. 1–8, 2015.
- [14] B. F. Palmer and W. L. Henrich, “Recent advances in the prevention and management of intradialytic hypotension.,” *J. Am. Soc. Nephrol.*, vol. 19, no. 1, pp. 8–11, 2008.
- [15] L. A. Usvyat, J. G. Raimann, M. Carter, F. M. Van Der Sande, J. P. Kooman, P. Kotanko, and N. W. Levin, “Relation between trends in body temperature and outcome in incident hemodialysis patients,” *Nephrol. Dial. Transplant.*, vol. 27, no. 8, pp. 3255–3263, 2012.
- [16] M. Fu, W. Weng, W. Chen, and N. Luo, “Review on modeling heat transfer and thermoregulatory responses in human body,” *J. Therm. Biol.*, vol. 62, pp. 189–200, 2016.
- [17] F. Lopot, S. Sulkova, M. Fortova, and B. Nejedly, “Temperature and thermal balance monitoring and control in dialysis,” *Hemodial Int*, vol. 7, no. 2, pp. 177–183, 2003.
- [18] F. M. van der Sande, L. M. Rosales, Z. Brener, J. P. Kooman, M. Kuhlmann, G. Handelman, R. N. Greenwood, M. Carter, D. Schneditz, K. M. Leunissen, and N. W. Levin, “Effect of ultrafiltration on thermal variables, skin temperature, skin blood flow, and energy expenditure during ultrapure hemodialysis,” *J. Am. Soc. Nephrol.*, vol. 16, no. 6, pp. 1824–1831, 2005.

- [19] D. Schneditz, C. Ronco, and N. Levin, "Temperature control by the blood temperature monitor," *Semin. Dial.*, vol. 16, no. 6, pp. 477–482, 2003.
- [20] D. Schneditz, "Temperature and thermal balance in hemodialysis.," *Semin. Dial.*, vol. 14, no. 5, pp. 357–364, 2001.
- [21] A. Santoro, E. Ferramosca, and E. Mancini, "Biofeedback-driven dialysis: where are we?," in *Contributions to Nephrology*, vol. 161, pp. 199–209, 2008.
- [22] P. Presta, G. Mazzitello, L. Fuiano, M. Andreucci, V. Piraina, E. Laratta, M. Riccio, N. Comi, and G. Fuiano, "Cool temperature hemodialysis and biocompatibility in chronic hemodialysis patients: A preliminary study," *J. Nephrol.*, vol. 22, no. 6, pp. 760–765, 2009.
- [23] N. M. Selby and C. W. McIntyre, "A systematic review of the clinical effects of reducing dialysate fluid temperature," *Nephrol. Dial. Transplant.*, vol. 21, no. 7, pp. 1883–1898, 2006.
- [24] D. Schneditz and N. W. Levin, "Keep your temper: how to avoid heat accumulation in haemodialysis.," *Nephrol Dial Transpl.*, vol. 16, no. 1, pp. 7–9, 2001.
- [25] V. Maheshwari, T. Lau, L. Samavedham, and G. P. Rangaiah, "Effect of cool vs. warm dialysate on toxin removal: rationale and study design.," *BMC Nephrol.*, vol. 16, no. 25, p. 1-5, 2015.
- [26] J. P. Kooman, K. Katzarski, F. M. Sande, K. M. Leunissen, and P. Kotanko, "Hemodialysis: A model for extreme physiology in a vulnerable patient population," *Semin. Dial.*, vol. 31, no. 5, pp. 500–506, 2018.
- [27] L. A. Usvyat, P. Kotanko, F. M. van der Sande, J. P. Kooman, M. Carter, K. M. L. Leunissen, and N. W. Levin, "Circadian variations in body temperature during dialysis," *Nephrol. Dial. Transplant.*, vol. 27, no. 3, pp. 1139–1144, 2012.
- [28] F. M. Van Der Sande, G. Wystrychowski, J. P. Kooman, L. Rosales, J. Raimann, P. Kotanko, M. Carter, C. T. Chan, K. M. L. Leunissen, and N. W. Levin, "Control of core temperature and blood pressure stability during hemodialysis," *Clin. J. Am. Soc. Nephrol.*, vol. 4, no. 1, pp. 93–98, 2009.
- [29] G. Ozkan and S. Ulusoy, "Acute complications of hemodialysis," *Tech. Probl.*

Patients Hemodial., pp. 251–294, 2011.

- [30] Q. Maggiore, F. Pizzarelli, S. Sisca, C. Zoccali, S. Parlongo, F. Nicolo, and G. Creazzo, “Blood temperature and vascular stability during hemodialysis and hemofiltration,” *Trans. Am. Soc. Artif. Intern. Organs*, vol. 28, no. 1, pp. 523–527, 1982.
- [31] A. Ghasemi, M. Shafiee, and K. Rowghani, “Stabilizing effects of cool dialysate temperature on hemodynamic parameters in diabetic patients undergoing hemodialysis,” *Saudi J. Kidney Dis. Transplant.*, vol. 19, no. 3, pp. 378–383, 2008.
- [32] G. K. Sakkas, A. A. Krase, C. D. Giannaki, and C. Karatzaferi, “Cold dialysis and its impact on renal patients’ health: An evidence-based mini review,” *World J. Nephrol.*, vol. 6, no. 3, pp. 119–122, 2017.
- [33] P. E. Pergola, N. M. Habiba, and J. M. Johnson, “Body temperature regulation during hemodialysis in long-term patients: Is it time to change dialysate temperature prescription?,” *Am. J. Kidney Dis.*, vol. 44, no. 1, pp. 155–165, 2004.
- [34] M. J. Damasiewicz and K. R. Polkinghorne, “Intra-dialytic hypotension and blood volume and blood temperature monitoring,” *Nephrology*, vol. 16, no. 1, pp. 13–18, 2011.
- [35] L. J. Chesterton, N. M. Selby, J. O. Burton, and C. W. McIntyre, “Cool dialysate reduces asymptomatic intradialytic hypotension and increases baroreflex variability,” *Hemodial. Int.*, vol. 13, no. 2, pp. 189–196, 2009.
- [36] A. T. Azar, “Effect of dialysate temperature on hemodynamic stability among hemodialysis patients.,” *Saudi J. Kidney Dis. Transplant.*, vol. 20, no. 4, pp. 596–603, 2009.
- [37] H. Ebrahimi, M. Safavi, M. H. Saeidi, and M. H. Emamian, “Effects of sodium concentration and dialysate temperature changes on blood pressure in hemodialysis patients: A randomized, triple-blind crossover clinical trial,” *Ther. Apher. Dial.*, vol. 21, no. 2, pp. 117–125, 2017.
- [38] R. A. Mustafa, F. Bdair, E. A. Akl, A. X. Garg, H. Thiessen-Philbrook, H. Salameh, S. Kisra, G. Nesrallah, A. Al-Jaishi, P. Patel, P. Patel, A. A. Mustafa, and H. J.

- Schünemann, “Effect of lowering the dialysate temperature in chronic hemodialysis: A systematic review and meta-analysis,” *Clin. J. Am. Soc. Nephrol.*, vol. 11, no. 3, p. 442-457, 2016.
- [39] A. Ayoub and M. Finlayson, “Effect of cool temperature dialysate on the quality and patients’ perception of haemodialysis,” *Nephrol. Dial. Transplant.*, vol. 19, no. 1, pp. 190–194, 2004.
- [40] A. B. Korkor, C. M. Bretzmann, and D. Eastwood, “Effect of dialysate temperature on intradialytic hypotension,” *Dial. Transplant.*, vol. 39, no. 9, pp. 377–385, 2010.
- [41] K. P. Parker, J. L. Bailey, D. B. Rye, D. L. Bliwise, and E. J. W. Van Someren, “Lowering dialysate temperature improves sleep and alters nocturnal skin temperature in patients on chronic hemodialysis,” *J. Sleep Res.*, vol. 16, no. 1, pp. 42–50, 2007.
- [42] G. K. Sakkas, E. Tsaknaki, C. S. Rosa, C. D. Giannaki, A. A. Krase, E. Lavdas, G. M. Hadjigeorgiou, I. Stefanidis, and C. Karatzaferi, “The effect of cold dialysis in motor and sensory symptoms of RLS/WED occurring during hemodialysis: A double-blind study,” *ASAIO J.*, vol. 64, no. 1, 2018.
- [43] K. S. Gray, D. E. Cohen, and S. M. Brunelli, “Dialysate temperature of 36 °C: association with clinical outcomes,” *J. Nephrol.*, vol. 31, no. 1, pp. 129–136, 2018.
- [44] F. M. van der Sande, J. P. Kooman, J. H. Burema, P. Hameleers, a M. Kerkhofs, J. M. Barendregt, and K. M. Leunissen, “Effect of dialysate temperature on energy balance during hemodialysis: quantification of extracorporeal energy transfer.,” *Am J Kidney Dis*, vol. 33, no. 6, pp. 1115–1121, 1999.
- [45] J. W. Larkin, M. M. Reviriego-Mendoza, L. A. Usvyat, P. Kotanko, and F. W. Maddux, “To cool, or too cool: Is reducing dialysate temperature the optimal approach to preventing intradialytic hypotension?,” *Semin. Dial.*, vol. 30, no. 6, pp. 501–508, 2017.
- [46] A. Bullen, D. Rifkin, and D. Trzebinska, “Individualized cool dialysate as an effective therapy for intradialytic hypotension and hemodialysis patients’ perception,” *Ther. Apher. Dial.*, vol. 23, no. 2, pp. 145-152, 2018.
- [47] H. J. Jefferies, J. O. Burton, and C. W. McIntyre, “Individualised dialysate

temperature improves intradialytic haemodynamics and abrogates haemodialysis-induced myocardial stunning, without compromising tolerability," *Blood Purif.*, vol. 32, no. 1, pp. 63–68, 2011.

- [48] L.-F. Xu, C.-L. Wu, H.-M. Sun, and T.-Q. Liu, "Exploration of a reasonable dialysate temperature setting in hemodialysis for patients with hypertension," *Chinese Nurs. Res.*, vol. 3, no. 3, pp. 133–136, 2016.
- [49] A. Odudu, M. T. Eldehni, G. P. McCann, and C. W. McIntyre, "Randomized controlled trial of individualized dialysate cooling for cardiac protection in hemodialysis patients," *Clin. J. Am. Soc. Nephrol.*, vol. 10, no. 8, pp. 1408–1417, 2015.
- [50] M. T. Eldehni, A. Odudu, and C. W. McIntyre, "Randomized clinical trial of dialysate cooling and effects on brain white matter," *J Am Soc Nephrol*, vol. 26, pp. 957–965, 2015.
- [51] A. Davenport, "Can advances in hemodialysis machine technology prevent intradialytic hypotension?," *Semin. Dial.*, vol. 22, no. 3, pp. 231–236, 2009.
- [52] I. Chapdelaine, C. Déziel, and F. Madore, "Automated blood volume regulation during hemodialysis," *Prog. Hemodial. - From Emergent Biotechnol. to Clin. Pract.*, 2011.
- [53] F. Javed, A. V Savkin, G. S. H. Chan, J. D. Mackie, and N. H. Lovell, "Recent advances in the monitoring and control of haemodynamic variables during haemodialysis: a review," *Physiol. Meas.*, vol. 33, no. 1, pp. 1–31, 2011.
- [54] H.-W. Gil, K. Bang, S. Y. Lee, B. G. Han, J. K. Kim, Y. O. Kim, H. C. Song, Y. J. Kwon, and Y.-S. Kim, "Efficacy of hemocontrol biofeedback system in intradialytic hypotension-prone hemodialysis patients," *J. Korean Med. Sci.*, vol. 29, no. 6, pp. 805–810, 2014.
- [55] N. M. Selby, S. H. Lambie, P. G. Camici, C. S. Baker, and C. W. McIntyre, "Occurrence of regional left ventricular dysfunction in patients undergoing standard and biofeedback dialysis," *Am. J. Kidney Dis.*, vol. 47, no. 5, pp. 830–841, 2006.
- [56] G. E. Nesrallah, R. S. Suri, H. Thiessen-Philbrook, P. Heidenheim, and R. M. Lindsay,

- “Can extracellular fluid volume expansion in hemodialysis patients be safely reduced using the hemocontrol biofeedback algorithm? A randomized trial,” *ASAIO J.*, vol. 54, no. 3, pp. 270-274, 2008.
- [57] A. T. Azar, “Biofeedback systems and adaptive control hemodialysis treatment,” *Saudi J. Kidney Dis. Transplant.*, vol. 19, no. 6, pp. 895–903, 2008.
- [58] C. Johner, P. W. Chamney, D. Schneditz, and M. Krämer, “Evaluation of an ultrasonic blood volume monitor.,” *Nephrol. Dial. Transplant.*, vol. 13, no. 8, pp. 2098–2103, 1998.
- [59] N. Lameire, W. Van Biesen, and R. Vanholder, “Did 20 years of technological innovations in hemodialysis contribute to better patient outcomes?,” *Clin. J. Am. Soc. Nephrol.*, vol. 4, no. SUPPL. 1, pp. 30–40, 2009.
- [60] K. C. W. Leung, R. R. Quinn, P. Ravani, and J. M. MacRae, “Ultrafiltration biofeedback guided by blood volume monitoring to reduce intradialytic hypotensive episodes in hemodialysis: study protocol for a randomized controlled trial,” *Trials*, vol. 15, no. 1, p. 483, 2014.
- [61] F. Javed, A. V. Savkin, G. S. H. Chan, J. D. MacKie, and N. H. Lovell, “Identification and control for automated regulation of hemodynamic variables during hemodialysis,” *IEEE Trans. Biomed. Eng.*, vol. 58, no. 6, pp. 1686–1697, 2011.
- [62] E. Mancini, E. Mambelli, M. Irpinia, D. Gabrielli, C. Cascone, F. Conte, G. Meneghel, F. Cavatorta, A. Antonelli, G. Villa, A. D. Canton, L. Cagnoli, F. Aucella, F. Fiorini, E. Gaggiotti, G. Triolo, V. Nuzzo, and A. Santoro, “Prevention of dialysis hypotension episodes using fuzzy logic control system,” *Nephrol. Dial. Transplant.*, vol. 22, no. 5, pp. 1420–1427, 2007.
- [63] K. Moret, J. Aalten, W. van den Wall Bake, P. Gerlag, C. Beerenhout, F. van der Sande, K. Leunissen, and J. Kooman, “The effect of sodium profiling and feedback technologies on plasma conductivity and ionic mass balance: A study in hypotension-prone dialysis patients,” *Nephrol. Dial. Transplant.*, vol. 21, no. 1, pp. 138–144, 2006.
- [64] L. Col, G. La Manna, G. Comai, M. Ursino, D. Ricci, M. Piccari, F. Locatelli, S. Di

- Filippo, L. Cristinelli, M. Bacchi, A. Balducci, F. Aucella, V. Panichi, F. P. Ferrandello, R. Tarchini, D. Lambertini, C. Mura, G. Marinangeli, E. Di Loreto, F. Quarello, G. Forneris, M. Tancredi, M. Morosetti, G. Palombo, M. Di Luca, M. Martello, G. Emiliani, R. Bellazzi, and S. Stefoni, "Automatic adaptive system dialysis for hemodialysis-associated hypotension and intolerance: A noncontrolled multicenter trial," *Am. J. Kidney Dis.*, vol. 58, no. 1, pp. 93–100, 2011.
- [65] Fresenius, "BTM – Blood Temperature Monitor," 2005.
- [66] Q. Maggiore, F. Pizzarelli, A. Santoro, G. Panzetta, G. Bonforte, T. Hannedouche, M. A. A. De Lara, I. Tsouras, A. Loureiro, P. Ponce, S. Sulková, G. Van Roost, H. Brink, and J. T. C. Kwan, "The effects of control of thermal balance on vascular stability in hemodialysis patients: Results of the European randomized clinical trial," *Am. J. Kidney Dis.*, vol. 40, no. 2, pp. 280–290, 2002.
- [67] A. Saxena, R. K. Sharma, A. Gupta, and M. M. John, "Non- invasive Method for Preventing Intradialytic Hypotension : A Pilot Study," *Saudi J. Kidney Dis. Transplant.*, vol. 26, no. 5, pp. 896–905, 2015.
- [68] J. Horáček, S. D. Sulková, M. Fořtová, F. Lopot, M. Kalousová, L. Sobotka, J. Chaloupka, V. Tesař, A. Žák, and T. Zima, "Resting energy expenditure and thermal balance during isothermic and thermoneutral haemodialysis - Heat production does not explain increased body temperature during haemodialysis," *Nephrol. Dial. Transplant.*, vol. 22, no. 12, pp. 3553–3560, 2007.
- [69] D. Schneditz, L. Rosales, A. M. Kaufman, G. Kaysen, and N. W. Levin, "Heat accumulation with relative blood volume decrease," *Am. J. Kidney Dis.*, vol. 40, no. 4, pp. 777–782, 2002.
- [70] R. Ramos, C. Soto, R. Mestres, J. Jara, H. Zequera, J. I. Merello, and F. Moreso, "How can symptomatic hypotension be improved in hemodialysis patients: cold dialysis vs isothermal dialysis," *NEFROLOGÍA*, vol. 27, no. 6, pp. 737–741, 2007.
- [71] A. Dhondt, S. Eloot, F. Verbeke, and R. Vanholder, "Dialysate and blood temperature during hemodialysis: Comparing isothermic dialysis with a single-pass batch system," *Artif. Organs*, vol. 34, no. 12, pp. 1132–1137, 2010.

- [72] D. du Cheyron, N. Terzi, A. Seguin, X. Valette, F. Prevost, M. Ramakers, C. Daubin, P. Charbonneau, and J.-J. Parienti, "Use of online blood volume and blood temperature monitoring during haemodialysis in critically ill patients with acute kidney injury: a single-centre randomized controlled trial.," *Nephrol. Dial. Transplant*, vol. 28, no. 2, pp. 430–437, 2013.
- [73] F. Pizzarelli, "From cold dialysis to isothermic dialysis: A twenty-five year voyage," *Nephrol. Dial. Transplant.*, vol. 22, no. 4, pp. 1007–1012, 2007.
- [74] F. M. van der Sande, J. P. Kooman, C. J. Konings, and K. M. L. Leunissen, "Thermal effects and blood pressure response during postdilution hemodiafiltration and hemodialysis: The effect of amount of replacement fluid and dialysate temperature," *J. Am. Soc. Nephrol.*, vol. 12, no. 9, p. 1916-1920, 2001.
- [75] A. Zeraati, S. S. Beladi Mousavi, and M. Beladi Mousavi, "A review article: access recirculation among end stage renal disease patients undergoing maintenance hemodialysis," *Nephrourol. Mon.*, vol. 5, no. 2, pp. 728–732, 2013.
- [76] D. Schneditz, E. Wang, and N. W. Levin, "Validation of haemodialysis recirculation and access blood flow measured by thermodilution," *Nephrol. Dial. Transplant.*, vol. 14, no. 2, pp. 376–383, 1999.
- [77] S. Lan, E. Li, Z. Liang, L. Sheng, L. En, and L. Zize, "Research on the Temperature Control Methods to a Hemodialysis System with Large Inertia and Hysteresis," in *35th Chinese Control Conference*, pp. 9400–9405, 2016.
- [78] P. Busono, A. Fitrianto, T. Handoyo, A. Barkah, Y. Suryana, and R. Febryarto, "Development of Fuzzy Logic Based Temperature Controller for Dialysate Preparation System," in *International Conference on Electrical Engineering, Computer Science and Informatics (EECSI 2015)*, 2015.
- [79] C. De Capua, L. Fabbiano, R. Morello, and G. Vacca, "Optimized procedure to evaluate the thermal energy transfer in hemodialysis treatment," *Instrum. Sci. Technol.*, vol. 42, no. 4, pp. 458–468, 2014.
- [80] L. a. Zadeh, "Fuzzy sets," *Inf. Control*, vol. 8, no. 3, pp. 338–353, 1965.
- [81] S. Padmanaban, F. Blaabjerg, L. Martirano, P. Siano, Z. Leonowicz, and K. P. Maroti,

- “PI and fuzzy control strategies for high voltage output DC-DC boost power converter — Hardware implementation and analysis,” in *2016 IEEE 16th International Conference on Environment and Electrical Engineering (EEEIC)*, pp. 1–6, 2016.
- [82] N. Allahverdi, “Some applications of fuzzy logic in medical area,” *2009 Int. Conf. Appl. Inf. Commun. Technol. AICT 2009*, no. 1, 2009.
- [83] N. Allahverdi, “Design of fuzzy expert systems and its applications in some medical areas,” *Int. J. Appl. Math. Electron. Comput.*, vol. 2, no. 1, pp. 1–8, 2014.
- [84] N. Mishra and P. Jha, “Fuzzy expert system and its utility in various field,” vol. 6, no. 1, pp. 41–45, 2014.
- [85] Y. Hata, K. Kuramoto, S. Kobashi, and H. Nakajima, “A survey of fuzzy logic in medical and health technology,” *World Autom. Congr.*, pp. 1–6, 2012.
- [86] S. Guo, Q. Chen, N. Xiao, and Y. Wang, “A fuzzy PID control algorithm for the interventional surgical robot with guide wire feedback force,” in *2016 IEEE International Conference on Mechatronics and Automation*, pp. 426–430, 2016.
- [87] M. S. Qureshi, P. Swarnkar, and S. Gupta, “A supervisory on-line tuned fuzzy logic based sliding mode control for robotics: An application to surgical robots,” *Rob. Auton. Syst.*, vol. 109, pp. 68–85, 2018.
- [88] R. Precup, T. Haidegger, and L. Kovács, “Stable hybrid fuzzy controller-based architecture for robotic telesurgery systems,” *Int. J. Comput. Intell. Patt. Recogn.*, vol. 1, no. 1, pp. 61–76, 2014.
- [89] P. Qi, C. Liu, L. Zhang, S. Wang, H. Lam, and K. Althoefer, “Fuzzy logic control of a continuum manipulator for surgical applications,” in *2014 IEEE International Conference on Robotics and Biomimetics (ROBIO 2014)*, pp. 413–418, 2014.
- [90] A. Gölcük and İ. Güler, “The use of stepper motor-controlled proportional valve for fio₂ calculation in the ventilator and its control with fuzzy logic,” *J. Med. Syst.*, vol. 41, no. 1, p. 1, 2016.
- [91] M. R. Yousefi, N. D. Samani, H. Hashemi, and F. Shahlaei, “Controlling the depth of anesthesia during operation by vital parameters of the patient’s body using a fuzzy

- controller,” in *2018 IEEE International Symposium on Medical Measurements and Applications (MeMeA)*, pp. 1–6, 2018.
- [92] B. Hamed and A. A. K. A. Ras, “Fuzzy controller for dual sensors cardiac pacemaker system in patients with bradycardias at rest,” *Intell. Cont. Automation*, vol. 6, no. 3, pp. 159–167, 2015.
- [93] J. B. Awotunde, O. E. Matiluko, and O. W. Fatai, “Medical diagnosis system using fuzzy logic,” *African J. Comput. ICT*, vol. 7, no. 2, pp. 99–106, 2014.
- [94] S. Das, D. Guha, and B. Dutta, “Medical diagnosis with the aid of using fuzzy logic and intuitionistic fuzzy logic,” *Appl. Intell.*, vol. 45, no. 3, pp. 850–867, 2016.
- [95] M. Lagzian, M. Shirazian, A. V. Kamyad, M. Layeghian, and R. Hekmat, “A new fuzzy control model for kidney patients,” *Appl. Math.*, vol. 03, no. 09, pp. 1097–1101, 2012.
- [96] W. Chen, C. Kan, C. Lin, and T. Chen, “A rule-based decision-making diagnosis system to evaluate arteriovenous shunt stenosis for hemodialysis treatment of patients using fuzzy petri nets,” *IEEE J. Biomed. Heal. Informatics*, vol. 18, no. 2, pp. 703–713, 2014.
- [97] J. Klespitz and L. Kovacs, “Multivariable control structures of hemodialysis machines for patient fluid balance maintenance,” in *2018 IEEE 12th International Symposium on Applied Computational Intelligence and Informatics (SACI)*, pp. 415–418, 2018.
- [98] J. Klespitz and L. Kovács, “Identification and control of peristaltic pumps in hemodialysis machines,” in *2013 IEEE 14th International Symposium on Computational Intelligence and Informatics (CINTI)*, pp. 83–87, 2013.
- [99] J. Klespitz, M. Takács, I. Rudas, and L. Kovács, “Performance of soft computing controllers in hemodialysis machines,” *Int. J. Fuzzy Syst.*, vol. 17, no. 3, pp. 414–422, 2015.
- [100] V. R. Nafisi, M. Eghbal, M. R. J. Motlagh, and F. Yavari, “Fuzzy logic controller for hemodialysis machine based on human body model,” *J. Med. Signals Sens.*, vol. 1, no. 1, pp. 36–48, 2011.

- [101] W. Li, S. Sun, G. Zhao, D. Gao, and W. Ding, "Simulation of velocity and concentration fields in artificial kidneys," in *ASME 2013 Summer Bioengineering Conference SBC2013*, pp. 2–3, 2016.
- [102] D. Donato, A. Boschetti-de-Fierro, C. Zweigart, M. Kolb, S. Eloit, M. Storr, B. Krause, K. Leypoldt, and P. Segers, "Optimization of dialyzer design to maximize solute removal with a two-dimensional transport model," *J. Memb. Sci.*, vol. 541, pp. 519–528, 2017.
- [103] M. Fukuda, K. Namekawa, and K. Sakai, "Identical dependence of dialysate-side mass transfer coefficient on reynolds number using dimensionless correlation based on the mass transfer model in newly developed dialyzers and a downsized dialyzer," *Adv. Biomed. Eng.*, vol. 5, pp. 118–123, 2016.
- [104] Gambro, "Polyflux™ 210H," 2012.
- [105] A. Hedayat, J. Szpunar, N. A. P. K. Kumar, R. Peace, H. Elmoselhi, and A. Shoker, "Morphological characterization of the Polyflux 210H hemodialysis filter pores," *Int. J. Nephrol.*, vol. 2012, pp. 1–6, 2012.
- [106] R. Morello, C. De Capua, L. Fabbiano, and G. Vacca, "A thermal energy balance model for hypotension prevention in hemodialysis," in *2013 IEEE International Instrumentation and Measurement Technology Conference (I2MTC), Minneapolis*, pp. 1078–1082, 2013.
- [107] J. Ali and R. Syahputra, "Heat exchanger control based on artificial intelligence approach," *Int. J. Appl. Eng. Res.*, vol. 11, no. 16, pp. 9063–9069, 2016.
- [108] G. M. Sarabeevi and M. L. Beebi, "Temperature control of shell and tube heat exchanger system using internal model controllers," in *2016 International Conference on Next Generation Intelligent Systems (ICNGIS)*, pp. 1–6, 2016.
- [109] G. Oltean and L. Ivanciu, "Implementation of a Fuzzy Logic-Based Embedded System for Temperature Control," in *40th International Spring Seminar on Electronics Technology (ISSE)*, pp. 1–6, 2017.
- [110] R. G. J. Anduray and S. M. Z. Irigoyen, "Development of a fuzzy controller for liquid level by using Raspberry pi and Internet of Things," in *2017 IEEE Central America*

and Panama Student Conference (CONESCAPAN), pp. 1–5, 2017.

- [111] V. Higuti, H. Borrero Guerrero, A. Velasquez, R. Moreira, L. Tinelli, D. Magalhães, M. Becker, J. Fajardo Barrero, and D. Milori, “Low-cost embedded computer for mobile robot platform based on Raspberry board,” in *23rd ABCM International Congress of Mechanical Engineering*. 2015.
- [112] J. Klespitz, M. Takács, and L. Kovács, “Application of fuzzy logic in hemodialysis equipment,” in *IEEE 18th International Conference on Intelligent Engineering Systems INES*, pp. 169–173, 2014.
- [113] Z. Dong, Y. Li, S. Zhang, and F. Shang, “Fuzzy temperature control of induction cooker,” in *IECON 2017 - 43rd Annual Conference of the IEEE Industrial Electronics Society*, pp. 3051–3056, 2017.
- [114] Number Eight Innovation Limited, “Overview of Megunolink,” <https://www.megunolink.com/documentation/overview/>, 2018.
- [115] N. Aphiratsakun and N. Otaryan, “Ball on the plate model based on PID tuning methods,” in *2016 13th International Conference on Electrical Engineering/Electronics, Computer, Telecommunications and Information Technology (ECTI-CON)*, pp. 1–4, 2016.
- [116] M. S. Islam and J. Szpunar, “Study of dialyzer membrane (Polyflux 210H) and effects of different parameters on dialysis performance,” *Open J. Nephrol.*, vol. 3, no. 3, pp. 161–167, 2013.
- [117] J. Saliba, J. Charara, and M. H. Hassan, “Nanostructured Porous Silicon Membrane for Hemodialysis,” in *2nd International Conference on Advances in Biomedical Engineering*, 2013, pp. 145–147.
- [118] S. Eloit, Y. D’Asseler, P. De Bondt, and P. Verdonck, “Combining SPECT Medical Imaging and Computational Fluid Dynamics for Analyzing Blood and Dialysate Flow in Hemodialyzers,” *Int. J. Artif. Organs*, vol. 28, no. 7, pp. 739–749, 2005.
- [119] W. Ding, W. Li, S. Sun, X. Zhou, P. A. Hardy, S. Ahmad, and D. Gao, “Three-dimensional simulation of mass transfer in artificial kidneys,” *Artif. Organs*, vol. 39, no. 6, pp. 79–89, 2015.

- [120] J. Günther, P. Schmitz, C. Albasi, and C. Lafforgue, "A numerical approach to study the impact of packing density on fluid flow distribution in hollow fiber module," *J. Memb. Sci.*, vol. 348, no. 1–2, pp. 277–286, 2010.
- [121] S. Albert, J. S. Rossmann, and R. Balaban, "Numerical simulation of blood flow in the renal arteris: influence of the ostium flow diverter," in *ASME 2013 Summer Bioengineering Conference*, pp. 3–4, 2013.
- [122] I. dos Santos, D. Haemmerich, C. D. S. Pinheiro, and A. F. da Rocha, "Effect of variable heat transfer coefficient on tissue temperature next to a large vessel during radiofrequency tumor ablation.," *Biomed. Eng. Online*, vol. 7, no. 21, pp. 1–11, 2008.
- [123] K.-H. Grote and E. K. Antonsson, *Springer Handbook of Mechanical Engineering*. 2009.
- [124] R. Bird, W. Stewart, and E. Lightfoot, *Transport Phenomena*. 1960.
- [125] Y. Sano and A. Nakayama, "A porous media approach for analyzing a countercurrent dialyzer system," *ASME, J. Heat Transfer*, vol. 134, no. 7, pp. 072602-11, 2012.
- [126] P. Powell and A. J. Ingen Housz, *Engineering with Polymers, 2nd Edition*. 1998.
- [127] A. Ram, *Fundamentals of Polymer Engineering*. 1997.
- [128] L. Maryanne, L. Poladian, G. Barton, and M. A. van Eijkelenborg, *Microstructured Polymer Optical Fibres*. 2008.
- [129] T. A. Hussein and A. S. Malik, "Effect of dialysate temperature on hemodynamic stability among hemodialysis patients among hemodialysis patients," *Iraqi J. Med. Sci.*, vol. 12, no. 2, pp. 173–179, 2014.
- [130] P. Ahrenholz, R. E. Winkler, and D. Zende-Zartochti, "The role of the dialysate flow rate in haemodialysis," in *Updates in Hemodialysis*, R. E. Winkler, Ed. Rijeka: IntechOpen, p. Ch. 11, 2015.
- [131] D. R. M. Hassell, F. M. van der Sande, J. P. Kooman, J. P. Tordoir, and K. M. L. Leunissen, "Optimizing dialysis dose by increasing blood flow rate in patients with reduced vascular-access flow rate," *Am. J. Kidney Dis.*, vol. 38, no. 5, pp. 948–955,

2001.

- [132] F. Locatelli, U. Buoncristiani, B. Canaud, H. Köhler, T. Petitclerc, and P. Zucchelli, "Haemodialysis with on-line monitoring equipment: Tools or toys?," *Nephrol. Dial. Transplant.*, vol. 20, no. 1, pp. 22–33, 2005.
- [133] K. Matthias and P. Hans-Dietrich, "Control of blood temperature and thermal energy balance during hemodialysis," in *Engineering in Medicine and Biology Society, 1992 14th Annual International Conference of the IEEE*, pp. 2299–2300, 1992.
- [134] Y. Arya, "Automatic generation control of two-area electrical power systems via optimal fuzzy classical controller," *J. Franklin Inst.*, vol. 355, no. 5, pp. 2662–2688, 2018.
- [135] Y. Bai and D. Wang, "Fundamentals of fuzzy logic control — fuzzy sets, fuzzy rules and defuzzifications BT - Advanced fuzzy logic technologies in industrial applications," Y. Bai, H. Zhuang, and D. Wang, Eds. London: Springer London, pp. 17–36, 2006.
- [136] Q. Sun, D. Xing, Q. Yang, H. Zhang, and J. Patel, "A new design of fuzzy logic control for smes and battery hybrid storage system," *Energy Procedia*, vol. 105, pp. 4575–4580, 2017.
- [137] M. Dhimish, V. Holmes, B. Mehrdadi, and M. Dales, "Comparing Mamdani Sugeno fuzzy logic and RBF ANN network for PV fault detection," *Renew. Energy*, vol. 117, pp. 257–274, 2018.
- [138] A. Bakdi, A. Hentout, H. Boutami, A. Maoudj, O. Hachour, and B. Bouzouia, "Optimal path planning and execution for mobile robots using genetic algorithm and adaptive fuzzy-logic control," *Rob. Auton. Syst.*, vol. 89, pp. 95–109, 2017.
- [139] P.-C. Cheng, B.-R. Peng, Y.-H. Liu, Y.-S. Cheng, and J.-W. Huang, "Optimization of a fuzzy-logic-control-based MPPT algorithm using the particle swarm optimization technique," *Energies*, vol. 8, no. 6, 2015.
- [140] C. Song, C. Yu, Y. Xiao, and J. Zhang, "Fuzzy logic control based on genetic algorithm for a multi-source excitations floating raft active vibration isolation system," *Adv.*

Mech. Eng., vol. 9, no. 6, 2017.

- [141] H. H. Choi, H. M. Yun, and Y. Kim, "Implementation of evolutionary fuzzy PID speed controller for PM synchronous motor," *IEEE Trans. Ind. Informatics*, vol. 11, no. 2, pp. 540–547, 2015.
- [142] S. F. Ahmed, K. Kushsairy, M. I. A. Bakar, D. Hazry, and M. K. Joyo, "Attitude stabilization of quad-rotor (UAV) system using fuzzy PID controller (an experimental test)," in *2015 Second International Conference on Computing Technology and Information Management (ICCTIM)*, pp. 99–104, 2015.
- [143] O. N. Almasi, V. Fereshtehpoor, M. H. Khooban, and F. Blaabjerg, "Analysis, control and design of a non-inverting buck-boost converter: A bump-less two-level T–S fuzzy PI control," *ISA Trans.*, vol. 67, pp. 515–527, 2017.
- [144] S. Gdaim, A. Mtibaa, and M. F. Mimouni, "Design and experimental implementation of DTC of an induction machine based on fuzzy logic control on FPGA," *IEEE Trans. Fuzzy Syst.*, vol. 23, no. 3, pp. 644–655, 2015.
- [145] A. Jemaa, O. Zarrad, M. A. Hajjaji, and M. N. Mansouri, "Hardware implementation of a fuzzy logic controller for a hybrid wind-solar system in an isolated site," *Int. J. Photoenergy*, vol. 2018, pp. 1–16, 2018.
- [146] M. A. Hannan, Z. A. Ghani, A. Mohamed, S. Member, M. N. Uddin, and S. Member, "Real-time testing of a fuzzy-logic-controller based grid-connected photovoltaic inverter system," *IEEE Trans. Ind. Appl.*, vol. 51, no. 6, pp. 4775–4784, 2015.
- [147] H. G. Nguyen, A. D. Hoang, V. S. Nguyen, and V. D. Nguyen, "Fuzzy-based treadmill speed control for lower extremity rehabilitation of patient after stroke," in *2016 International Conference on Advanced Technologies for Communications (ATC)*, pp. 307–311, 2016.
- [148] G. S. Nhivekar, S. S. Nirmale, and R. R. Mudholker, "Implementation of fuzzy logic control algorithm in embedded microcomputers for dedicated application," *Int. J. Eng. Sci. Technol.*, vol. 3, no. 4, pp. 276–283, 2011.
- [149] F. Chabni, R. Taleb, A. Benbouali, and M. A. Bouthiba, "The application of fuzzy control in water tank level using Arduino," in *International Journal of Advanced*

Computer Science and Applications (IJACSA), vol. 7, no. 4, pp. 261–265, 2016.

- [150] P. Bhatkhande and T. C. Havens, “Real time fuzzy controller for quadrotor stability control,” in *IEEE International Conference on Fuzzy Systems (FUZZ-IEEE)*, pp. 913–919, 2014.
- [151] H. R. Jayetileke, W. R. de Mei, and H. U. W. Ratnayake, “Real-time fuzzy logic speed tracking controller for a DC motor using Arduino Due,” in *7th International Conference on Information and Automation for Sustainability*, pp. 1–6, 2014.
- [152] M. Sajjad, M. Nasir, K. Muhammad, S. Khan, Z. Jan, A. K. Sangaiah, M. Elhoseny, and S. W. Baik, “Raspberry Pi assisted face recognition framework for enhanced law-enforcement services in smart cities,” *Futur. Gener. Comput. Syst.*, 2017.
- [153] S. Fahim and R. Tarif Ryad, “A fuzzy based low-cost monitoring module built with Raspberry Pi-Python-Java architecture,” in *International Conference on Smart Sensors and Application (ICSSA)*, pp. 127–132, 2015.
- [154] V. Vujović and M. Maksimović, “Raspberry Pi as a Sensor Web node for home automation,” *Comput. Electr. Eng.*, vol. 44, pp. 153–171, 2015.
- [155] A. Uroidhi, R. Mardiyanto, and D. Purwanto, “Automatic navigation for a mobile robot with real time depth kinect sensor and map database,” *JAVA - Int. J. Electr. Electron. Eng.*, vol. 14, no. 1, pp. 33–37, 2016.
- [156] W. Kao, C. Hsu, and T. Lee, “Intelligent control for a dynamically stable two-wheel mobile manipulator,” in *2017 Joint 17th World Congress of International Fuzzy Systems Association and 9th International Conference on Soft Computing and Intelligent Systems (IFSA-SCIS)*, pp. 1–5, 2017.
- [157] A. Velasquez, V. Higuti, H. Borrero Guerrero, D. Milori, D. Magalhães, and M. Becker, “Helvis - a small-scale agricultural mobile robot prototype for precision agriculture,” in *13th International Conference on Precision Agriculture*, pp. 2–17, 2016.
- [158] M. H. A. Jabbar, S. Anandan Shanmugam, and P. S. Khiew, “Design and implementation of dialysate temperature control system for hemodialysis: A pilot study,” in *Intelligent Embedded Systems*, pp. 1–10, 2018.

- [159] M. Pilatásig, J. Buele, J. Espinoza, F. Silva, P. Pilatásig, A. Mullo, and E. Pruna, "Implementation of fuzzy controller in low cost embedded boards for a flow system," in *2017 CHILEAN Conference on Electrical, Electronics Engineering, Information and Communication Technologies (CHILECON)*, pp. 1–7, 2017.
- [160] I. H. Altas and A. M. Sharaf, "A generalized direct approach for designing fuzzy logic controllers in matlab/simulink gui environment," *Int. J. Inf. Technol. Intell. Comput. Int. J. IT&IC*, vol. 1, no. 4, 2007.
- [161] W. Chang and F.-L. Hsu, "Mamdani and Takagi-Sugeno fuzzy controller design for ship fin stabilizing systems," in *2015 12th International Conference on Fuzzy Systems and Knowledge Discovery (FSKD)*, pp. 345–350, 2015.
- [162] U. M. Arief, F. Nugroho, S. Purbawanto, D. N. Setyaningsih, and Suryono, "Analysis of maizena drying system using temperature control based fuzzy logic method," *AIP Conf. Proc.*, vol. 1941, no. 1, p. 20005, 2018.
- [163] A. Kaur and A. Kaur, "Comparison of Mamdani-type and Sugeno-type fuzzy inference systems for air conditioning System," *Int. J. Soft Comput. Eng.*, vol. 2, no. 2, pp. 323–325, 2012.
- [164] N. Saad and M. Arrofiq, "A PLC-based modified-fuzzy controller for PWM-driven induction motor drive with constant V/Hz ratio control," *Robot. Comput. Integr. Manuf.*, vol. 28, no. 2, pp. 95–112, 2012.
- [165] Y. Wang and Y. Chen, "A Comparison of Mamdani and Sugeno fuzzy inference systems for traffic flow prediction," *J. Comput.*, vol. 9, no. 1, pp. 12–21, 2014.
- [166] E. Lacson and S. M. Brunelli, "Hemodialysis treatment time: a fresh perspective," *Clin. J. Am. Soc. Nephrol.*, vol. 6, no. 10, p. 2522-2530, 2011.
- [167] D. Schneditz, K. Martin, M. Kramer, T. Kenner, and F. Skrabal, "Effect of controlled extracorporeal blood cooling on ultrafiltration-induced blood volume changes during hemodialysis," *J. Am. Soc. Nephrol.*, vol. 8, no. 6, pp. 956–964, 1997.
- [168] J. M. G. Keijman, F. M. van der Sande, J. P. Kooman, and K. M. L. Leunissen, "Thermal energy balance and body temperature: comparison between isolated ultrafiltration and haemodialysis at different dialysate temperatures," *Nephrol.*

Dial. Transplant., vol. 14, no. 9, pp. 2196–2200, 1999.

- [169] A. M. Kaufman, A. T. Morris, V. A. Lavarias, Y. Wang, J. F. Leung, M. B. Glabman, S. A. Yusuf, A. L. Levoci, H. D. Polaschegg, and N. W. Levin, “Effects of controlled blood cooling on hemodynamic stability and urea kinetics during high-efficiency hemodialysis,” *J. Am. Soc. Nephrol.*, vol. 9, no. 5, p. 877-883, 1998.
- [170] Q. Maggiore, “Isothermic dialysis for hypotension-prone patients,” *Semin. Dial.*, vol. 15, no. 3, pp. 187–190, 2002.
- [171] M. Albalade, R. Pérez-García, P. de Sequera, E. Corchete, R. Alcazar, M. Ortega, and M. Puerta, “Is it useful to increase dialysate flow rate to improve the delivered Kt?,” *BMC Nephrol.*, vol. 16, no. 20, pp. 1–6, 2015.
- [172] Y. o. Kim, W. j. Song, S. a. Yoon, M. j. Shin, H. c. Song, Y. s. Kim, S. . Kim, Y. s. Chang, and B. k. Bang, “The effect of increasing blood flow rate on dialysis adequacy in hemodialysis patients with low Kt/V,” *Hemodial. Int.*, vol. 8, no. 1, p. 85, 2004.
- [173] O. R. Reyes II, “Effects of arterial needle placement in arteriovenous fistula on dialysis adequacy of end-stage renal disease patients undergoing maintenance hemodialysis,” *J. Nurs. Healthc.*, volsq. 1, no. 2, pp. 1–10, 2016.

9.1 Appendix A - DTCM Simulink model

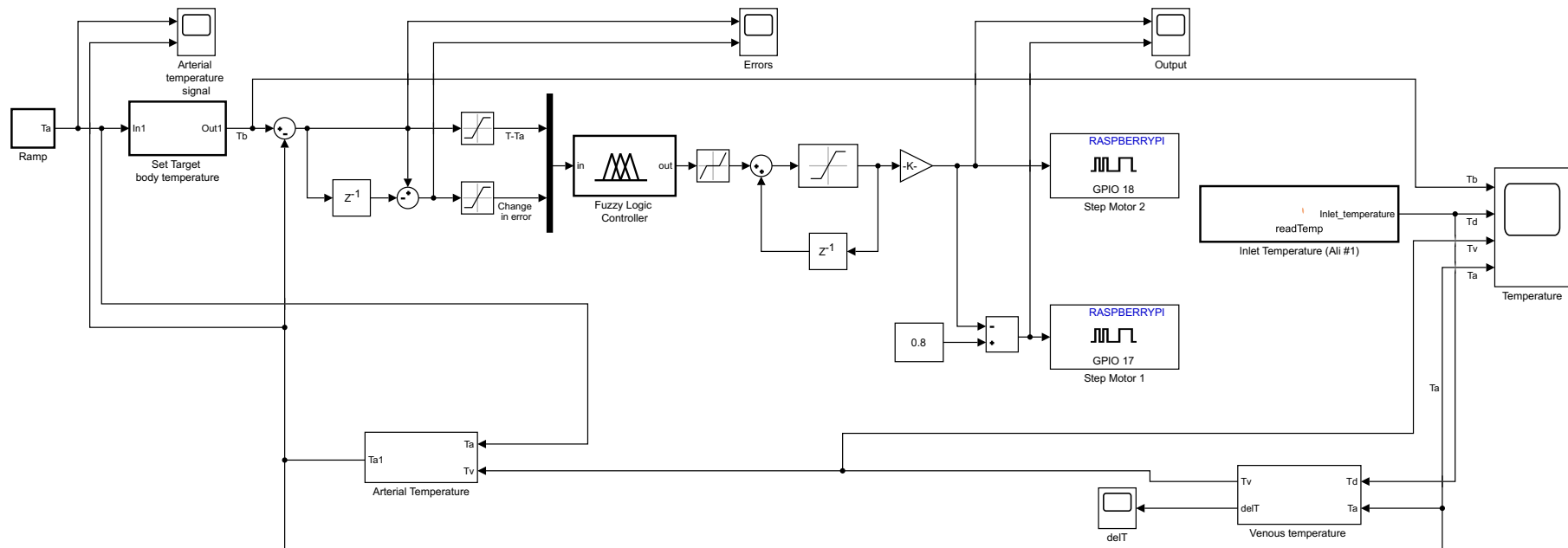


Figure A 1 – Overall Simulink model of DTCM prototype.

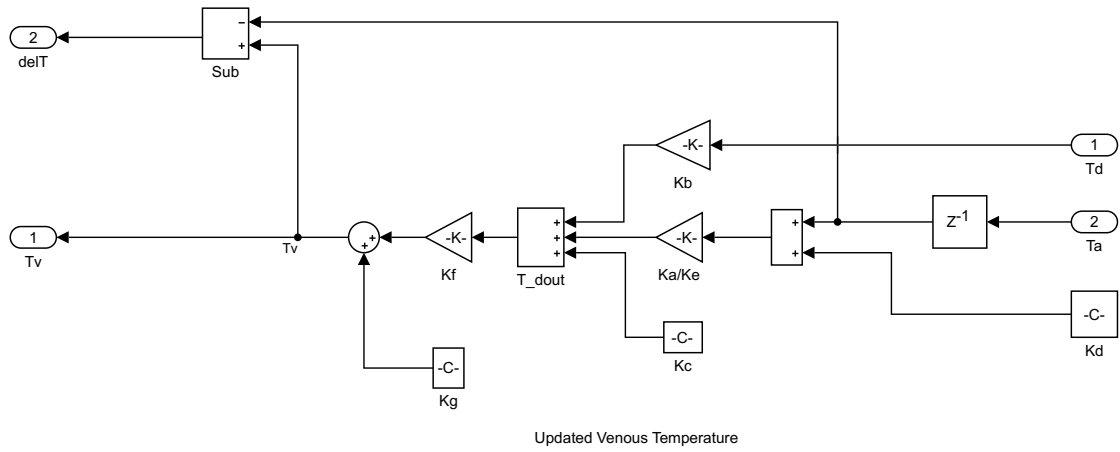


Figure A 2 - Estimation of venous temperature model of DTCM prototype.

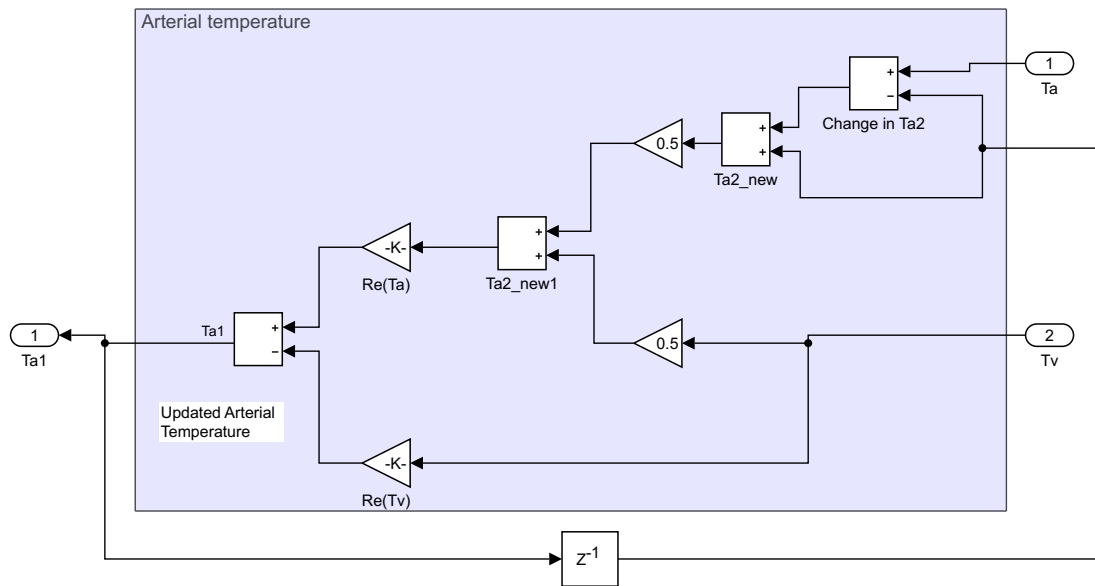


Figure A 3 - Estimation of arterial temperature model of DTCM prototype.

9.2 Appendix B - Temperature and output response of DTCM

under various conditions

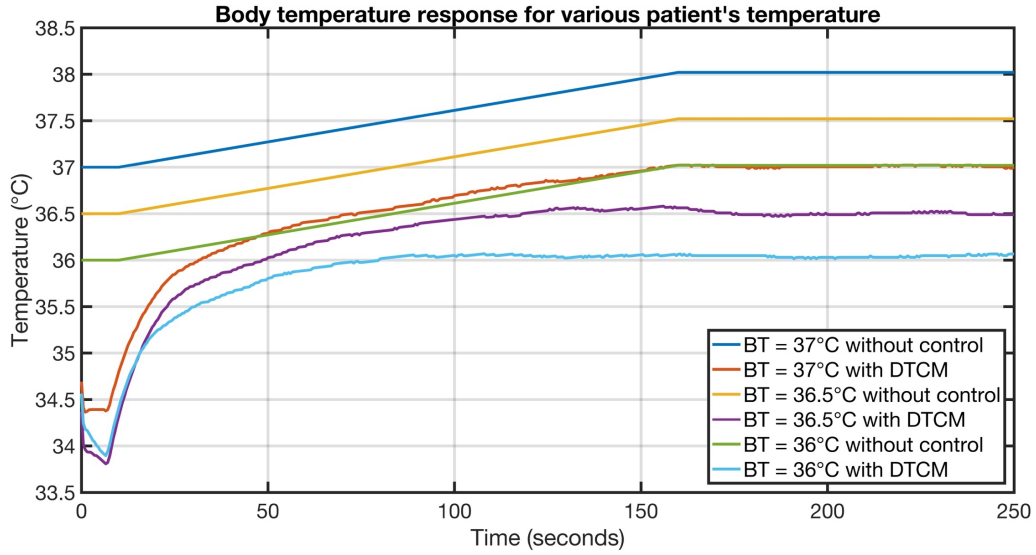


Figure B 1 – Temperature response of DTCM under various patient's temperature.

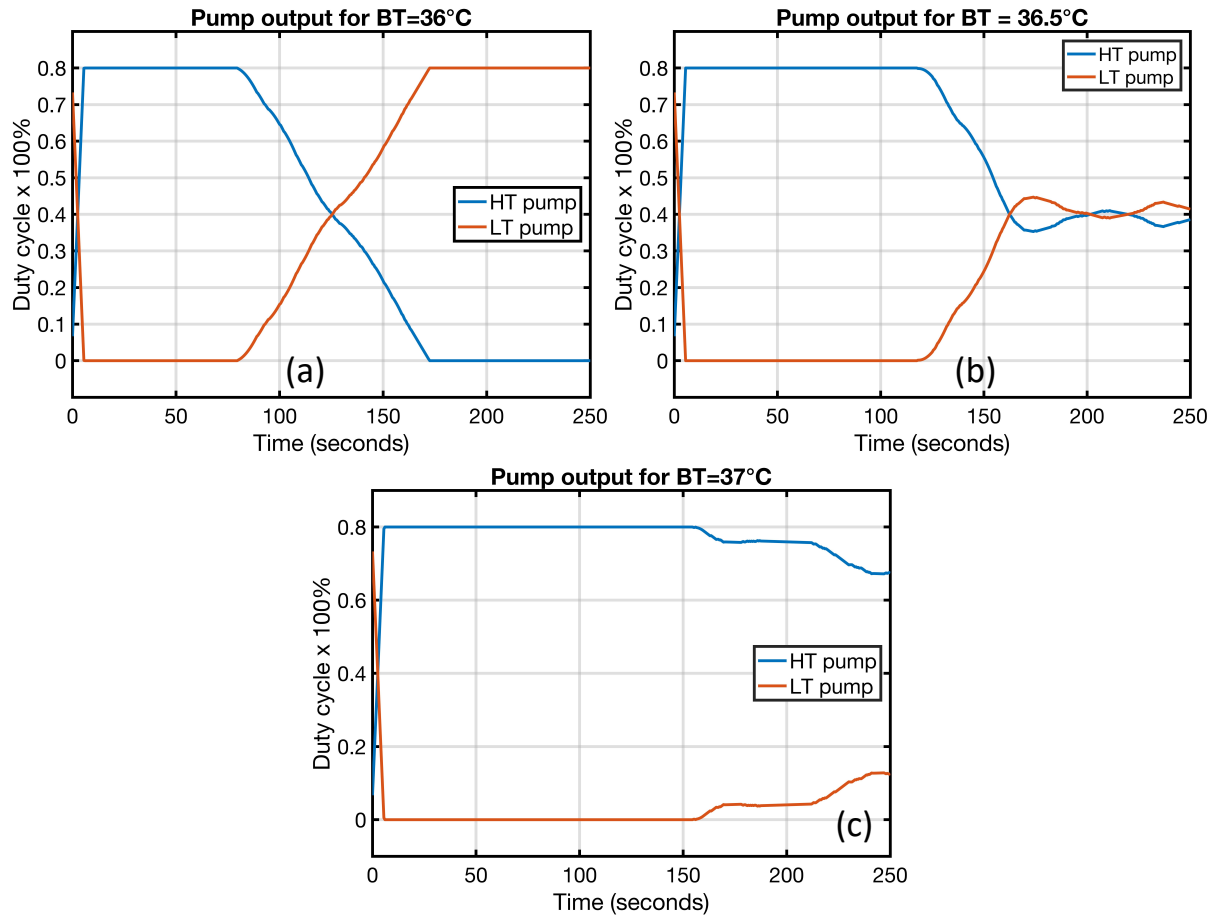


Figure B 2 - Output response of DTCM under various patient's temperature.

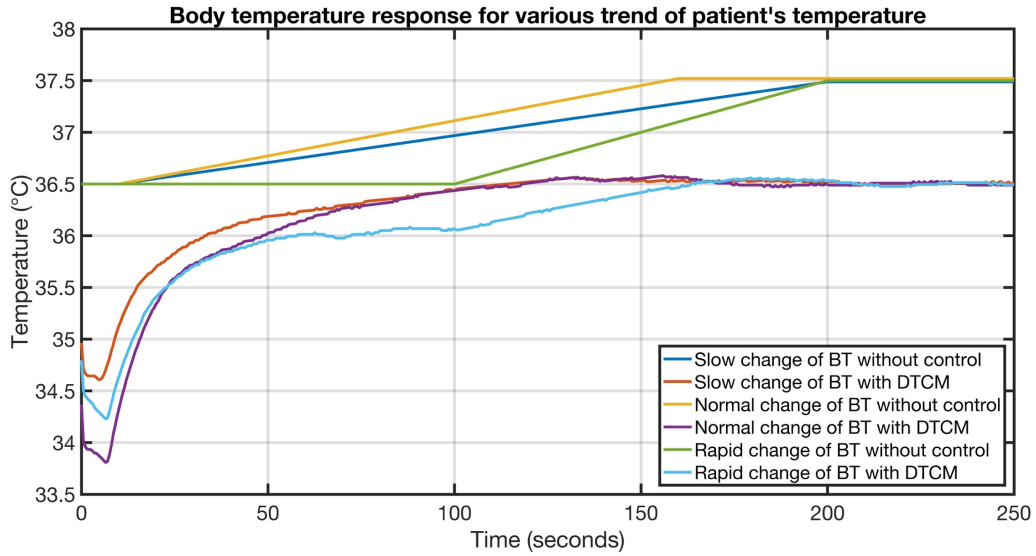


Figure B 3- Temperature response of DTCM under various trend of patient's temperature.

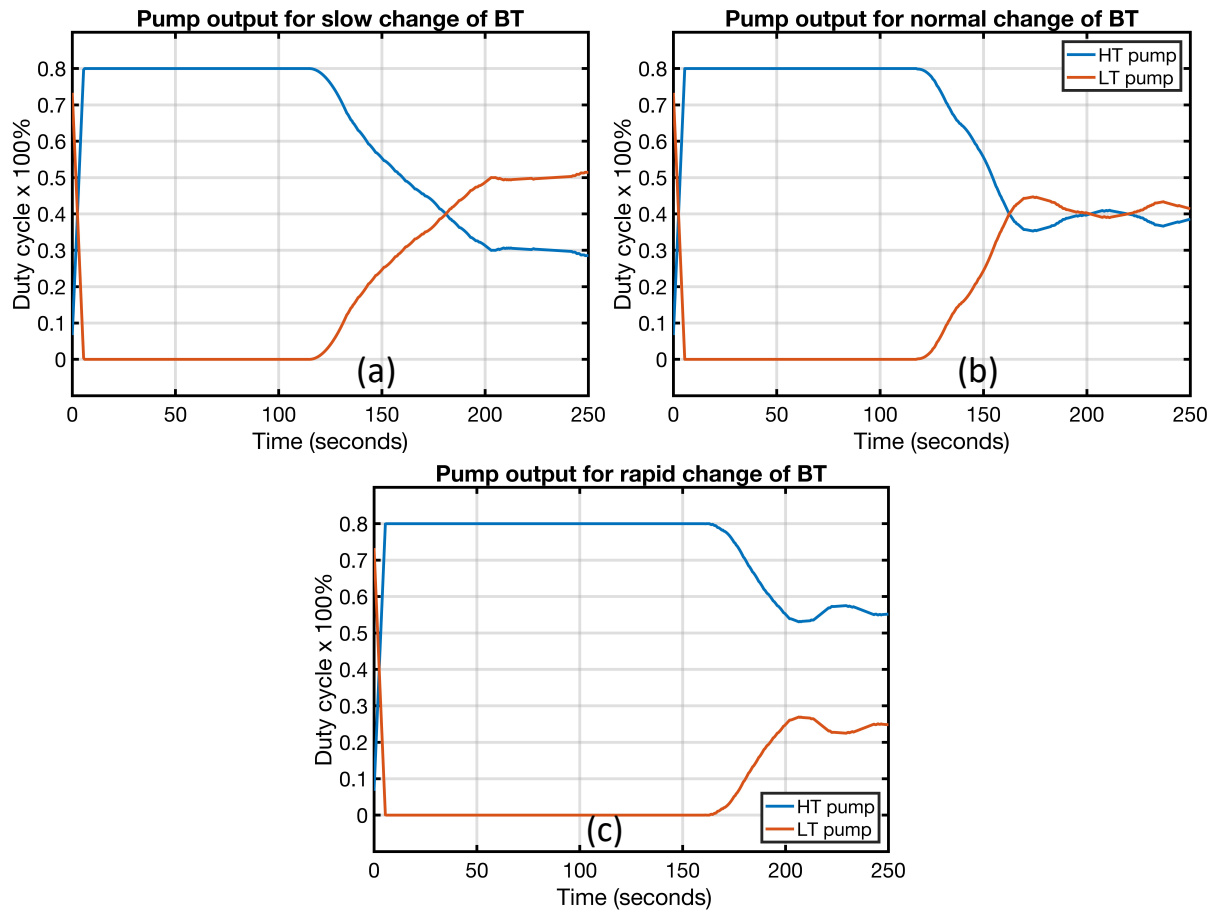


Figure B 4 – Output response of DTCM under various trend of patient's temperature.

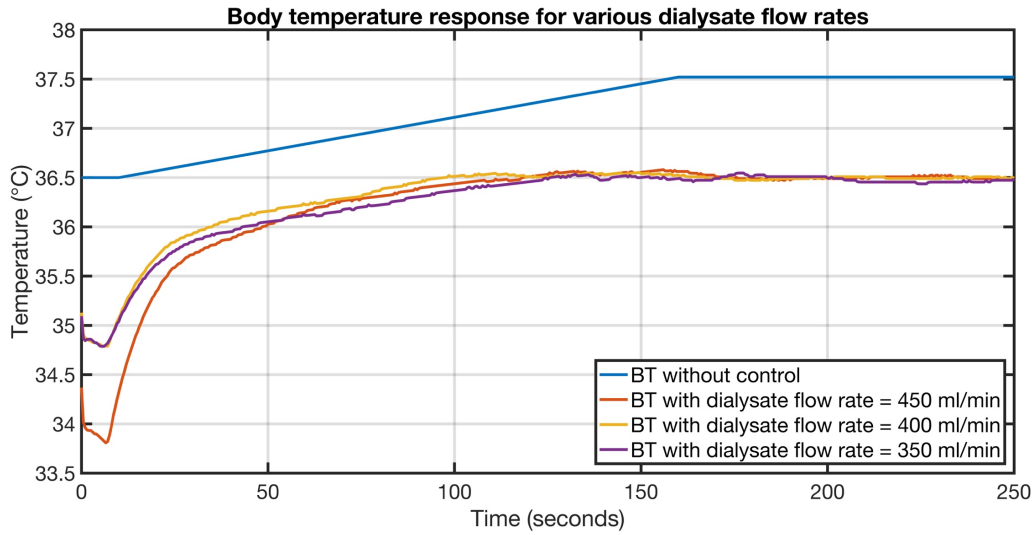


Figure B 5 - Temperature response of DTCM under various dialysate flow rates.

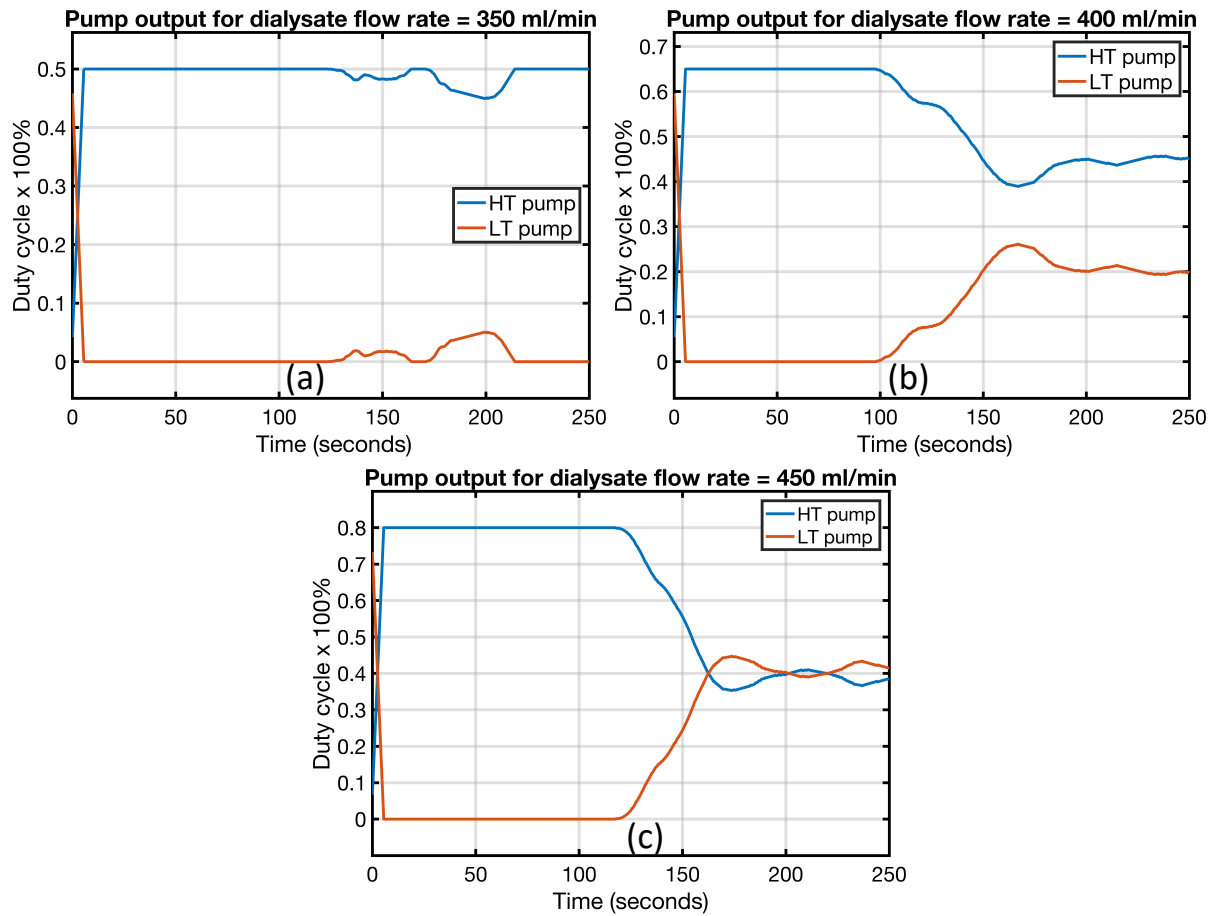


Figure B 6 - Output response of DTCM under various dialysate flow rates.

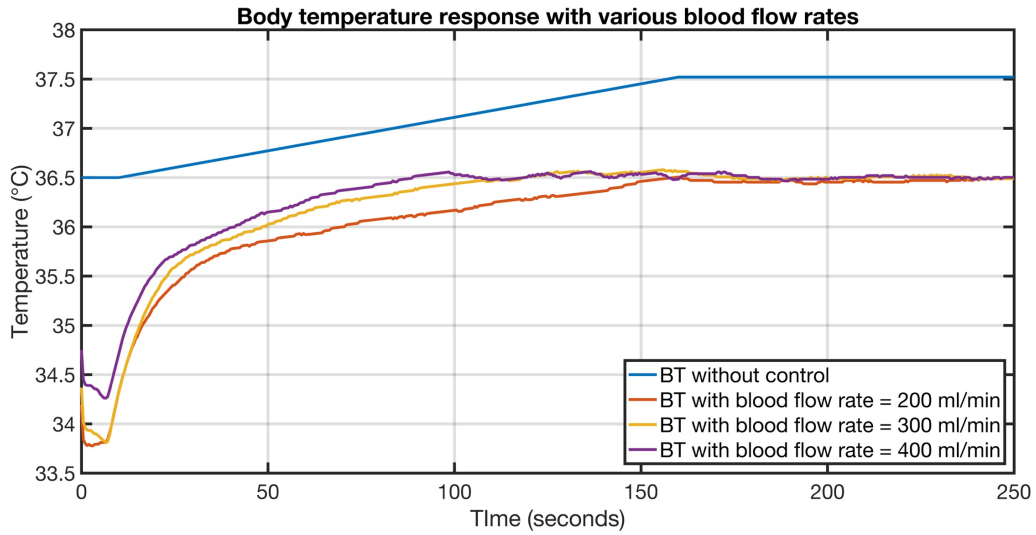


Figure B 7 - Temperature response of DTCM under various blood flow rates.

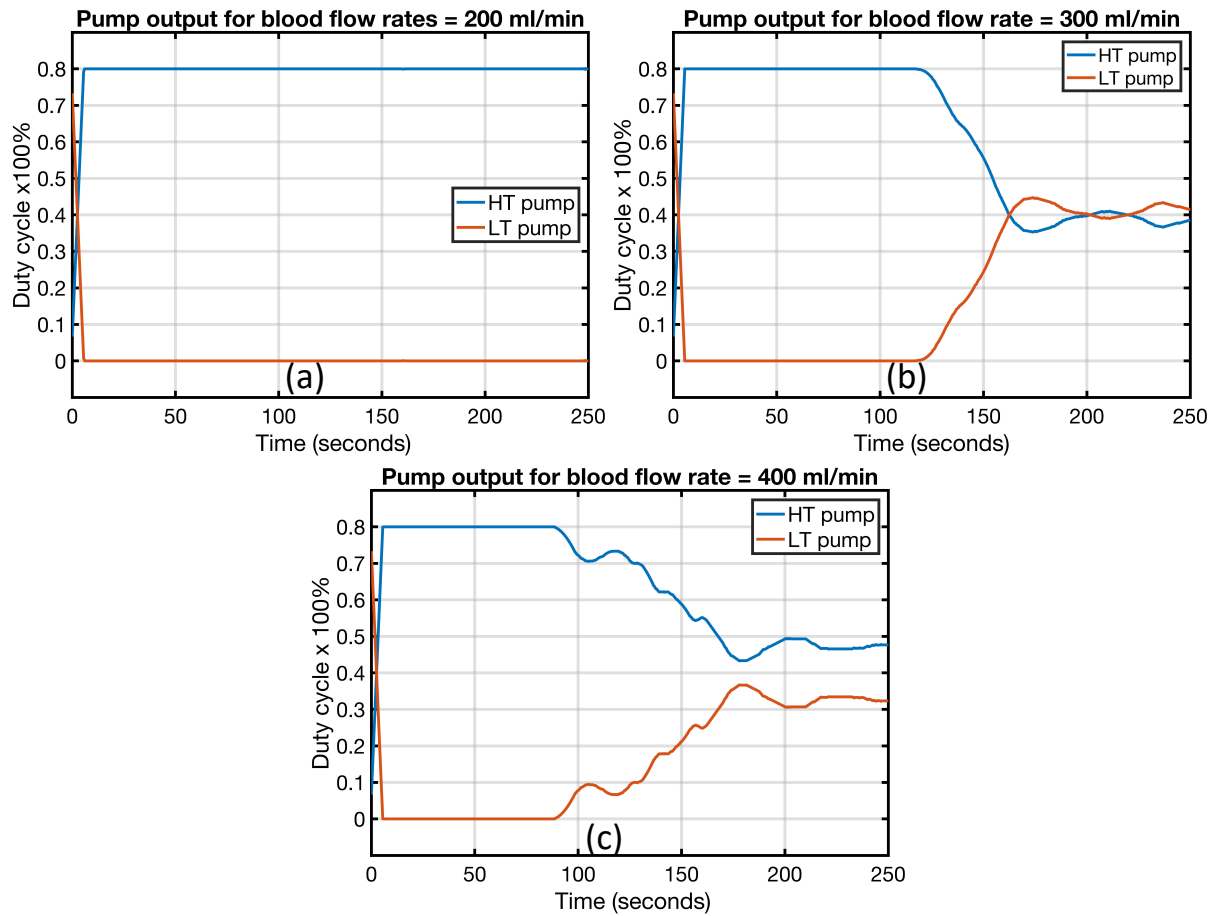


Figure B 8 – Output response of DTCM under various blood flow rates.

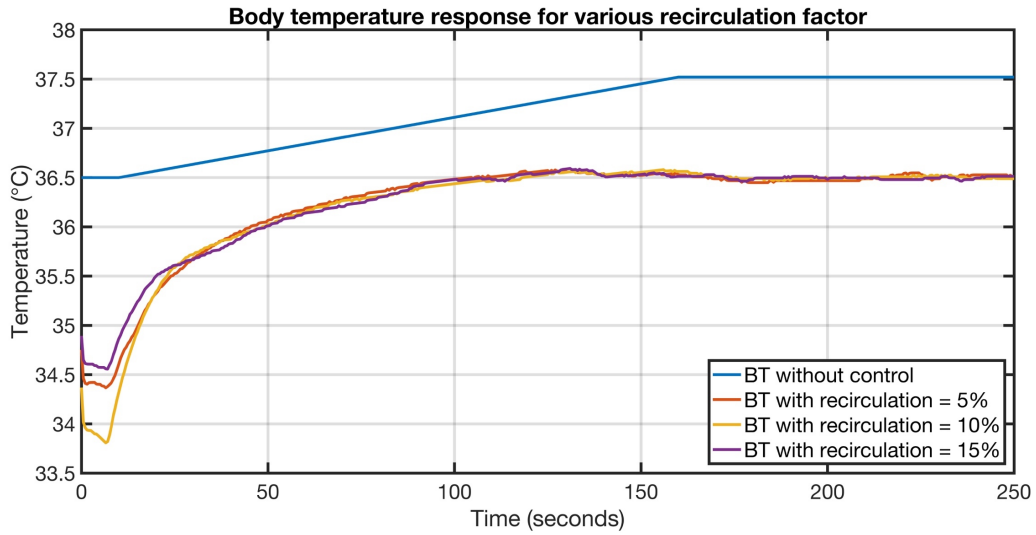


Figure B 9 - Temperature response of DTCM under various recirculation factor.

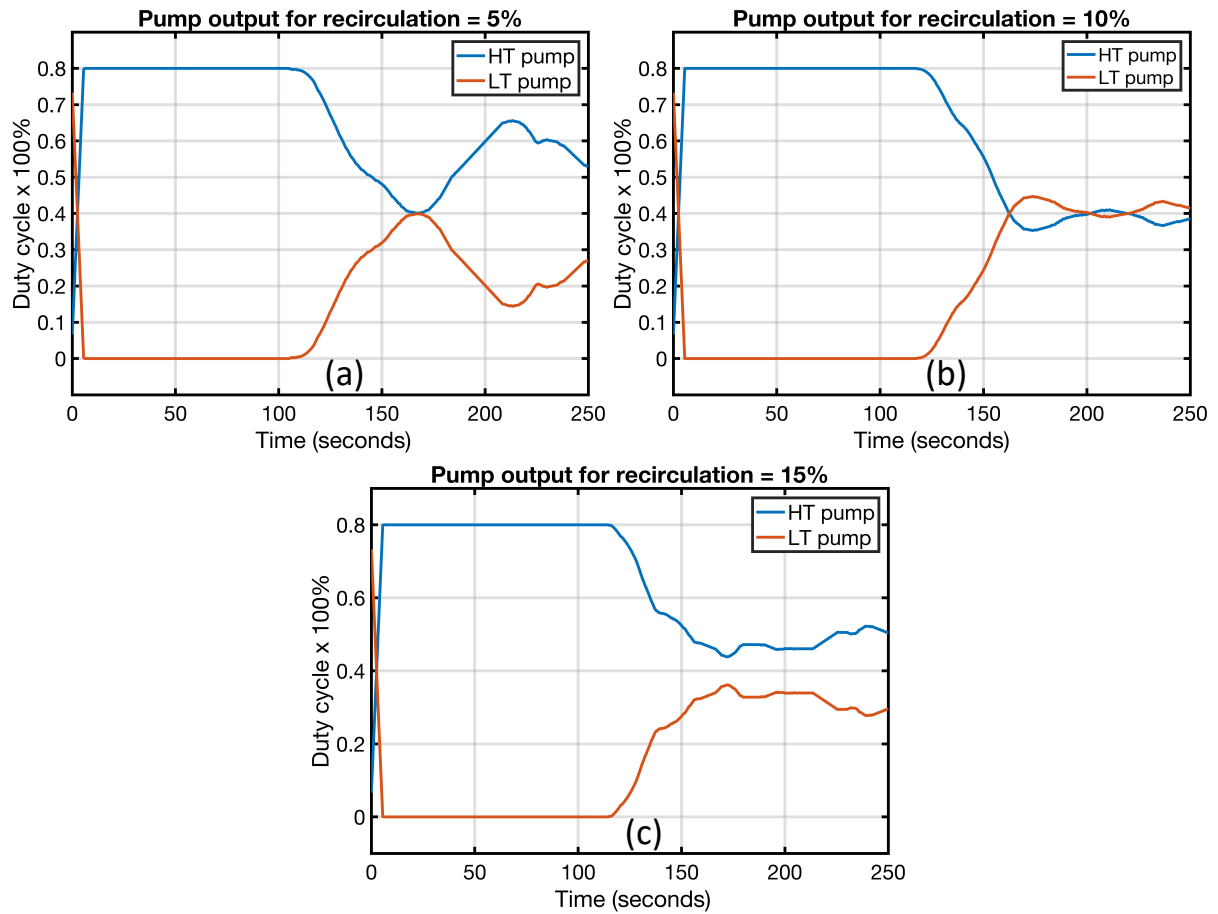


Figure B 10 - Output response of DTCM under various recirculation factor.

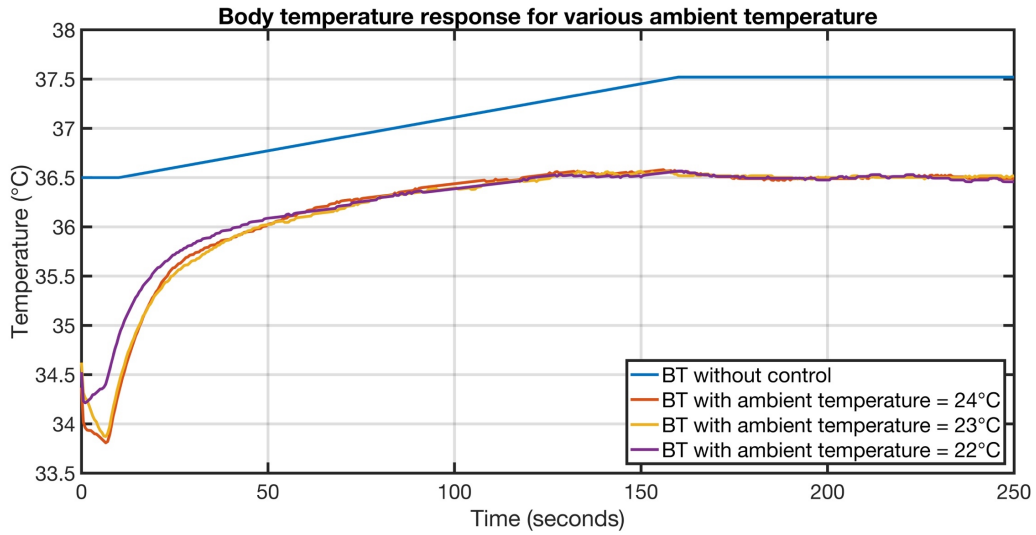


Figure B 11 - Temperature response of DTCM under various ambient temperature.

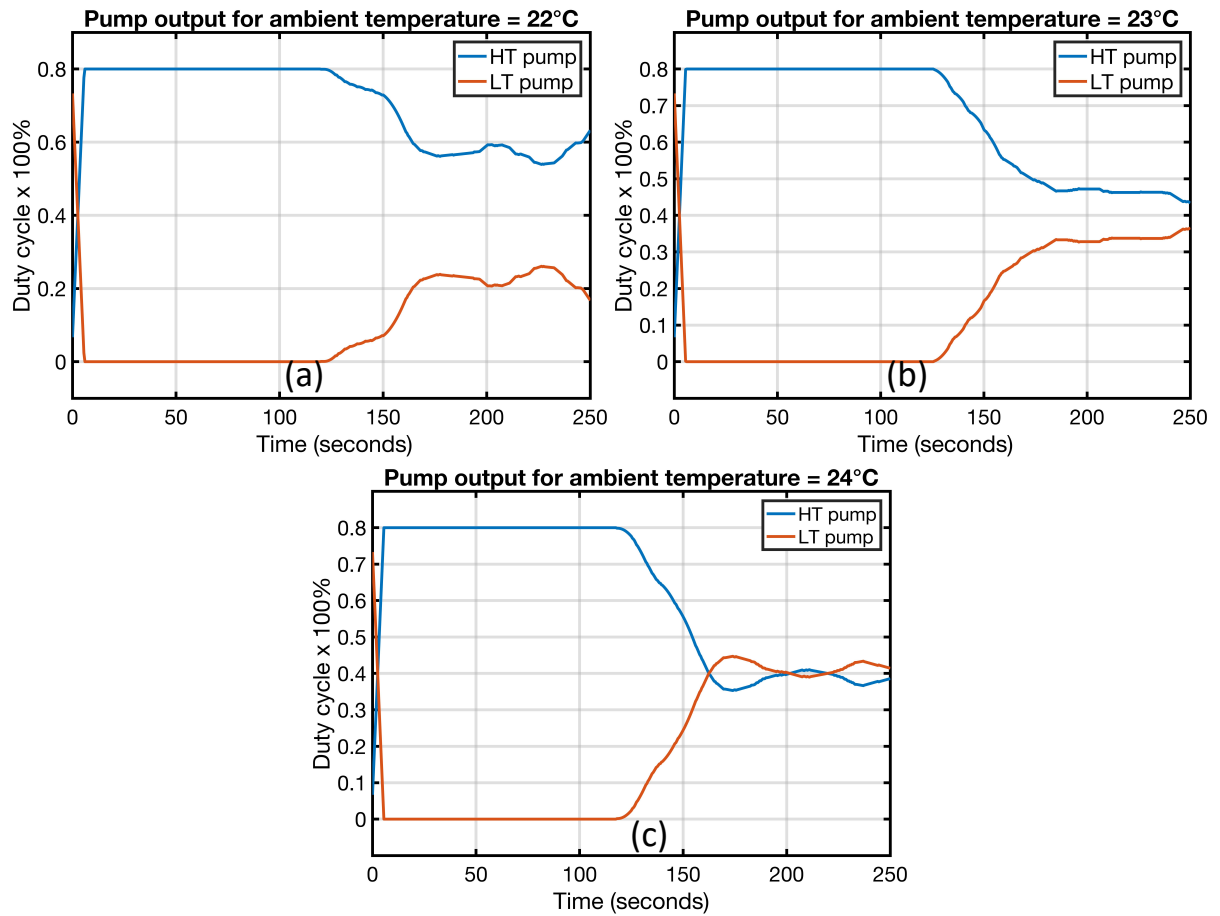


Figure B 12 - Output response of DTCM under various ambient temperature.

9.3 Appendix C - Calibration of peristaltic pump

Calibration of peristaltic pump

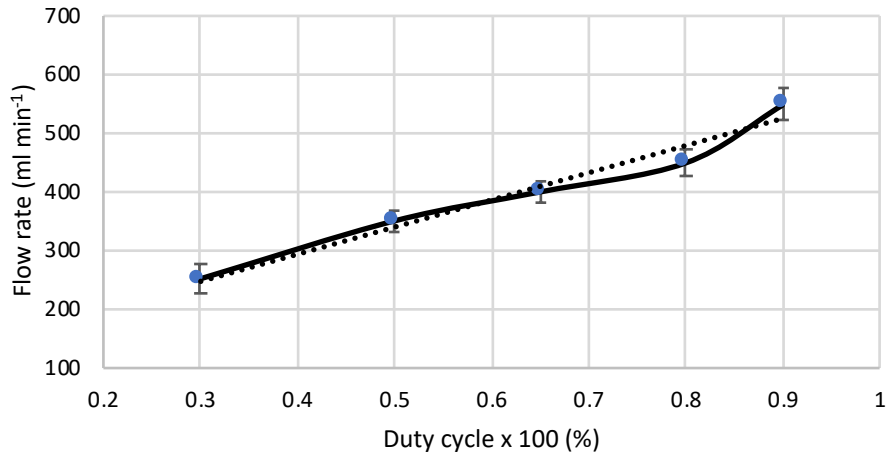


Figure C 1 – Graph of peristaltic pump calibration with duty cycle via Simulink.



Figure C 2 - Rotameter readings for Qd450, Qd400 and Qd350 showing the flow rate in ml min⁻¹.